ANALYSES IN SUPPORT OF EXCEPTIONAL EVENT FLAGGING AND EXCLUSION FROM MODELING FOR THE WEIGHT OF EVIDENCE ANALYSIS

Supporting the
Utah State Implementation Plan
for the 2017 MD8A Ozone
National Ambient Air Quality Standard

March 2023

Table of Contents

Figures

Tables

Acronyms

AERONET – Aerosol Robotic Network
AOD – Aerosol Optical Depth
AQS – Air Quality System
BC – Brown Carbon
BDV – Baseline Design Value
BrC – Brown Carbon
BV – Bountiful Viewmount
CAA – Clean Air Act
CAMS – Copernicus Atmosphere Monitoring Service
CO – Carbon Monoxide
CONUS – Continental United States
DV – Design Value
ECMWF – European Centre for Medium-Range Weather Forecast
FA – Free Atmosphere
FDV – Future Design Value
FRP – Fire Radiative Power
GDAS – Global Data Assimilation System
GFS – Global Forecasting System
GMAO – Global Modeling and Assimilation Offic
GOES – Geostationary Operational Environment Satellite
GSL – Great Salt Lake
H3 – Herriman #3
HMS – Hazard Mapping System
HRRR – High Resolution Rapid Refresh
HW – Hawthorne
HYPSPLIT – Hybrid Single-Particle Lagrangian Integrated Trajectory model
KSLC – Salt Lake City International Airport
MAIAC – Multi-Angle Implementation of Atmospheric Correction
MD8A – Max Daily 8-hour Average
MERRA-2 – Modern-Era Retrospective analysis for Research and Applications, Version 2
ML – Mixed Layer
MODIS – Moderate Resolution Imaging Spectroradiometer
MST – Mountain Standard Tim
NAAQS – National Ambient Air Quality Standard
NCEP – National Center for Environmental Predictions
NEDIS - National Environmental Satellite Data and Information Service
NEON_ONAQ – National Ecological Observatory Network - Onaqui-Ault
NOAA – National Oceanic and Atmospheric Administration
OC – Organic Carbon

OMPS – Ozone Mapping and Profiler Suite
PBL – Planetary Boundary Layer
PNW – Pacific Northwest
SIP – State Implementation Plan
UDAQ – Utah Division of Air Quality
UTC – Coordinated Universal Time
VIIRS – Visible Infrared Imaging Radiometer Suite
VOCs – Volatile Organic Compounds
WPC – Weather Prediction Center
Z – Zulu

Analysis in Support of Exceptional Event Flagging and Exclusion from Modeling for the Weight of Evidence Analysis

1.0 Introduction

The Utah Division of Air Quality (UDAQ) has determined that ozone concentrations exceeding the NAAQS on August 4, 2016 and September 2, 5 and 6, 2017 qualify as wildfire smoke impacted ozone exceedances. The purpose of this document is to provide technical documentation supporting a concurrence and petition to the Regional Administrator for Region 8 of the U.S. Environmental Protection Agency (EPA) for the exceptional event flagging, proceeding data modification, and exclusion of the aforementioned wildfire smoke impacted ozone exceedances (8/4/16, 9/2/17, 9/5/17, and 9/6/17) from the 2017 baseline design value (BDV). A summary of the high-concentration events excluded from base year design value calculation as a part of Weight of Evidence analysis for the Ozone SIP is presented in **Table 1**. In the following subsection, a brief overview of the wildfire smoke impacted high-concentration events is given.

Table 1 - Event MD8A ozone and PM2.5

Date	HW			BV			H3			Event Type	
	PM2.5 24hr (ppb)	Monthly Avg. PM2.5 (ppb)	MD8A O3 (ppb)	PM2.5 24hr (ppb)	Monthly Avg. PM2.5 (ppb)	MD8A O3 (ppb)	PM2.5 24hr (ppb)	Monthly Avg. PM2.5 (ppb)	MD8A O3 (ppb)	Regional	Local
8/4/2016	20.8	9.33	81	24.7	10.91	80	35.3	7.77	83	✔	✔
9/2/2017	14.5	6.98	83	15.9	8.33	78	12.1	5.68	83	✔	✔
9/5/2017	25.7	6.98	79	32.6	8.33	72	24.9	5.68	83	✔	✔
9/6/2017	35.2	6.98	76	43.4	8.33	81	32.4	5.68	82	✔	✔

Table 1. MD8A ozone and 24hr PM2.5 observed at the controlling monitors Hawthorne (HW), Bountiful (BV), and Herriman (H3). The MD8A ozone data is flagged as Exceptional Events and excluded Base Year Design Value (BDV) calculation.

1.1 Overview of Events

On August 4, 2016, September 2, 5, and 6, 2017, high ozone concentrations were observed across the Northern Wasatch Front Nonattainment area, with four ozone MD8A exceedances of the 2015 NAAQS (> 70 ppb) measured at each of the controlling monitors of Hawthorne (HW), Bountiful (BV), and Herriman (H3) as shown in **Table 1**. These ozone exceedances were due to the presence of wildfire smoke transported over the Wasatch Front from fires located in Box Elder, Co Utah on August 4, 2016 and fire complexes in California, Oregon, Washington, Idaho, and Montana on September 2, 5, and 6, 2017. The presence of wildfire smoke from each of these high O3 events was flagged due to observed elevated tracer concentrations of PM2.5, CO, and black/brown carbon, which will be detailed further in the following sections. The wildfire smoke contained a mixture of particulate matter (PM2.5) and attendant emissions,

including O3 itself -formed from photochemical reactions within the aged smoke plumes- and O3 precursors. These O3 precursors include nitrogen oxides (NOx) and volatile organic compounds (VOCs), which were both major contributors to O3 formation during the specified high O3 events.

1.2 Regulatory Significance and Justification

The EPA states in the "Additional Methods, Determinations, and Analyses to Modify Air Quality Data Beyond Exceptional Events (Clarification Memo on Data Modification)" [1] memorandum there are determinations and analyses not covered by the Exceptional Events Rule (i.e., not included in the list of covered regulatory actions) that also rely on ambient air quality monitoring data that may have been influenced by atypical, extreme, or unrepresentative events. In such events, independent determinations and analyses covered by other regulatory programs (not exceptional events) are allowed to be made when regarding mechanisms for possible monitoring data exclusion, selection, or adjustment. Specifically, monitoring data exclusion, selection, or adjustment may qualify for determinations and analyses by meeting two main requirements:

1. Ambient air data are not representative per other applicable EPA rules/guidance (i.e., 40 CFR Part 58 requirements and relevant guidance).
2. Ambient data are not representative to characterize background concentrations or base period concentrations in accordance with the EPA Guideline, which may impact a determinative value in a past or projected time period. Situations could include removal of air quality monitoring data that apply to characterizing background contributions for NAAQS compliance demonstrations under PSD and transportation conformity, and to developing alternative current and future year design values for SIP modeling in attainment demonstrations.

The four flagged wildfire smoke impacted O3 exceedances of the NAAQS at HW, BV, and H3 (**Table 1**) are not representative of O3 background or base period concentrations, and without exclusion impact base and projected future design values within the SIP modeling for attainment demonstration. UDAQ's flagged wildfire smoke impacted O3 exceedances meet the qualifying requirements to progress with a monitoring data modification and exclusion analysis. Therefore, as promulgated by EPA's Guideline on Air Quality Models ("*Guideline*"; see 40 CFR Part 51, Appendix W)[2], the appropriate types of determination or analysis to justify a monitoring data modification and exclusion includes:

1. Estimating base and future year design values for ozone and PM2.5 SIP attainment demonstration.
2. Determining whether a SIP satisfies CAA 110(a)(2)(D)(i)(I).

[1] Additional Methods, Determinations, and Analyses to Modify Air Quality Data Beyond Exceptional Events (Clarification Memo on Data Modification). Available on EPA's web page at: https://www.epa.gov/sites/default/files/2019-04/documents/clarification_memo_on_data_modification_methods.pdf

[2] 40 CFR Part 51, Appendix W is available online at https://www.epa.gov/sites/default/files/2020-09/documents/appw_17.pdf

The procedure for monitoring data exclusion, selection, or adjustment, given the two above types of determination and analysis, involves following EPA's recommendations detailed in Section 8.3.2 c.ii. and d., and Section 8.3.3 d. of the *Guideline*. UDAQ follows the suggested EPA analysis and procedures in support monitor data modification and exclusion, by presenting air quality along with meteorological analysis, trajectory-dispersion modeling, satellite analysis, and wildfire smoke products in the sections below. We utilize the Hybrid Single-Particle Lagrangian Integrated Trajectory model (HYSPLIT), developed by NOAA's Air Resources Laboratory, as the trajectory-dispersion model[3]. HYSPLIT is one of the most widely used models for atmospheric trajectory and dispersion calculations and is often applied for identifying the origin of smoke from wildfires (Stein et al., 2015). The analysis demonstrates the impact of wildfire smoke on high O3 concentrations and provides justification for data exclusion at the HW, BV, and H3 monitoring stations. In order to estimate the base and future year design values for the SIP attainment demonstration, the 2017 BDV and SIP modeled 2023 future year design value (FDV) are recalculated by excluding the flagged MD8A O3 exceedances. The preceding analysis and estimates of the adjusted BDV and FDV are revealed in more detail in Section 3.

2.0 Conceptual Overview

2.1 Region Description

2.1.1 Monitor Overview

In this document, the analysis focuses on the monitor data modification and exclusion from HW, BV, and H3 monitors on the selected dates in **Table 1**. The rationale behind focusing on the three monitoring sites is three-fold: 1) these monitors were deemed significantly impacted by wildfire smoke on the selected flagged dates, 2) historically, the controlling monitor for the Northern Wasatch Front Nonattainment area has always been one of these three UDAQ monitoring sites, and 3) HW, BV, and H3 collectively represent the types of airsheds (urban, suburban, and industrial) that comprise the Wasatch Front Nonattainment area. The monitors of Hawthorne (HW) and Herriman (H3) are located within the Salt Lake Valley, with HW being representative of an urban environment and H3 being representative of a suburban/residential area. The Bountiful (BV) monitoring site is situated just to the north of Salt Lake Valley within Davis Co and is characterized as industrial/suburban. The location and description of these sites is shown in **Table 2** and **Figure 1**, respectively.

[3] Hybrid Single-Particle Lagrangian Integrated Trajectory model (HYSPLIT) *NOAA Air Resources Laboratory (ARL)* https://www.ready.noaa.gov/HYSPLIT_traj.php

Table 2 - Select UDAQ Monitor Details

AIRS Code	Site Code	Site Name	Start Year	End Year	O3	CO	PM2.5	Brown Carbon	Latitude	Longitude
490353006	HW	Hawthorne	1997	present	X	X	X		40.73	-111.87
490110004	BV	Bountiful	2003	present	X		X	X	40.90	-111.88
490353013	H3	Herriman # 3	2014	present	X		X		40.49	-112.03

Table 2. Hawthorne (HW), Bountiful (BV), Herriman (H3) UDAQ monitor details.

Figure 1 - Map of UDAQ Monitor Locations

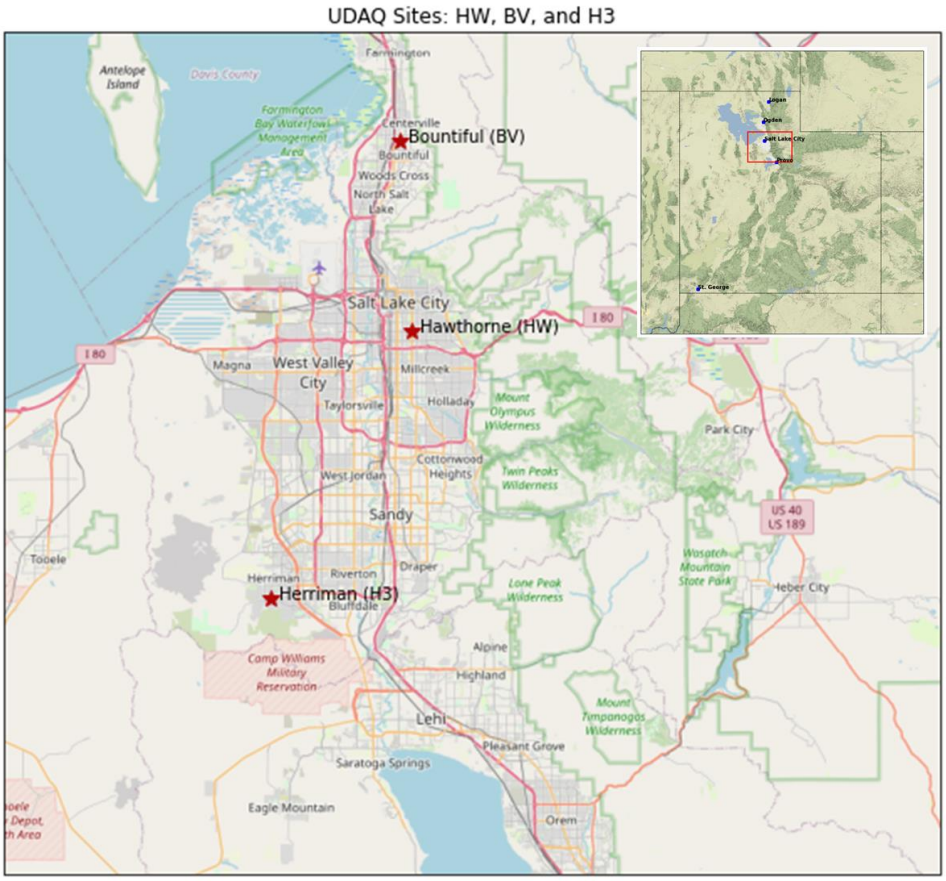

Figure 1. Location of Hawthorne (HW), Viewmount Bountiful (BV), and Herriman #3 (H3) UDAQ monitoring sites

2.1.2 Summertime Climatology and Geography

During the summer, the large-scale weather (synoptic) pattern over Utah is dominated by upper-level ridging or high pressure as seen in **Figure 2**. This synoptic pattern creates relatively benign and quiescent conditions across the Wasatch Front, with deep planetary boundary layer mixed layers, hot temperatures, weak surface and mid-level winds, and dry conditions. In **Table 3**, the average daily high

temperatures and precipitation are given for Salt Lake City, which is deemed a representative location for summertime climate along the Wasatch Front. Generally, most precipitation during the summer is attributed to late spring (June) mid-latitude cyclones or afternoon thunderstorms during the monsoon season (July-August).

Figure 2 - Summertime Mean 1000-500 mb Composites

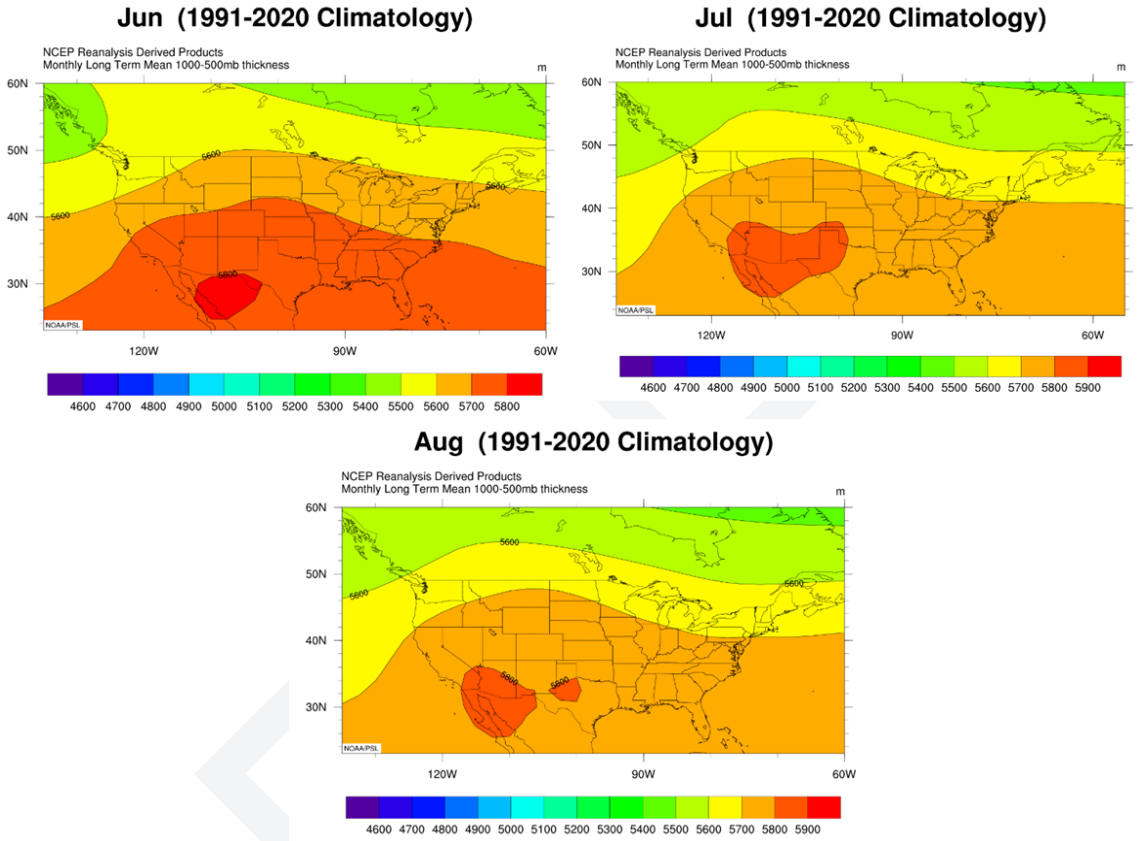

Figure 2. Mean 1000-500 mb thickness composites for Jun, Jul, and Aug (1991-2020 Climatology). Warmer colors indicate higher thicknesses and higher pressure on average, with a relatively persistent upper-level ridge axis evident across western CONUS for the months Jun-Aug.

Table 3 - KSLC Climatology

Month	Normal Low (F)	Normal High (F)	Normal Precipitation (inches)
June	59.1	84.2	Total: 0.95
July	68.3	94	Total: 0.49
August	66.6	91.8	Total: 0.58
September	56.3	80.7	Total: 1.06

Table 3. Average high, low, and normal precipitation between the months June-September at Salt Lake City International Airport (KSLC).

Besides creating hot and dry conditions, the characteristic summertime upper-level pattern forms a conducive environment for the transport of wildfire smoke from local and distant sources into Utah. This is due to the clockwise and relatively weak winds around a ridge of high pressure, which tend to accumulate and swirl wildfire smoke from across the western United States into Utah. The pattern frequently creates periods of diffuse and dense wildfire smoke being advected over the Wasatch Front, with elevated smoke layers often mixed down to the surface due to the characteristic deep mixed layers and subsidence under an upper level ridge.

The geography of the Wasatch Front is characterized as complex topography, with the valley areas of highest population density bounded by the Great Salt Lake on the north and west and the Wasatch Mountains on the east. This geographical setup creates a unique and complex lake-valley-mountain climate and weather system. Mesoscale and thermally driven winds, including mountain, canyon, and valley-lake breezes, dominate the summertime wind climatology. Often, these types of complex topographical winds occur on a diurnal periodicity, and are fairly consistent under calm and quiescent synoptic weather conditions. A wind climatology summary is given in **Figure 3** in the form of wind rose from Salt Lake City International Airport (KSLC). The wind rose in **Figure 3** demonstrates the consistent nature of the diurnal lake (daytime N-NW winds) and valley breeze (nighttime S-SE winds) in the Salt Lake Valley during the summer months. Only under strong synoptic forcing does the lake breeze not occur, which is rarer given the typical benign summer climate. An example of the thermally driven daytime (lake) and nighttime (valley) breeze is given in **Figure 4**.

Figure 3 - KSLC Wind Rose Climatology (Jun-Aug)

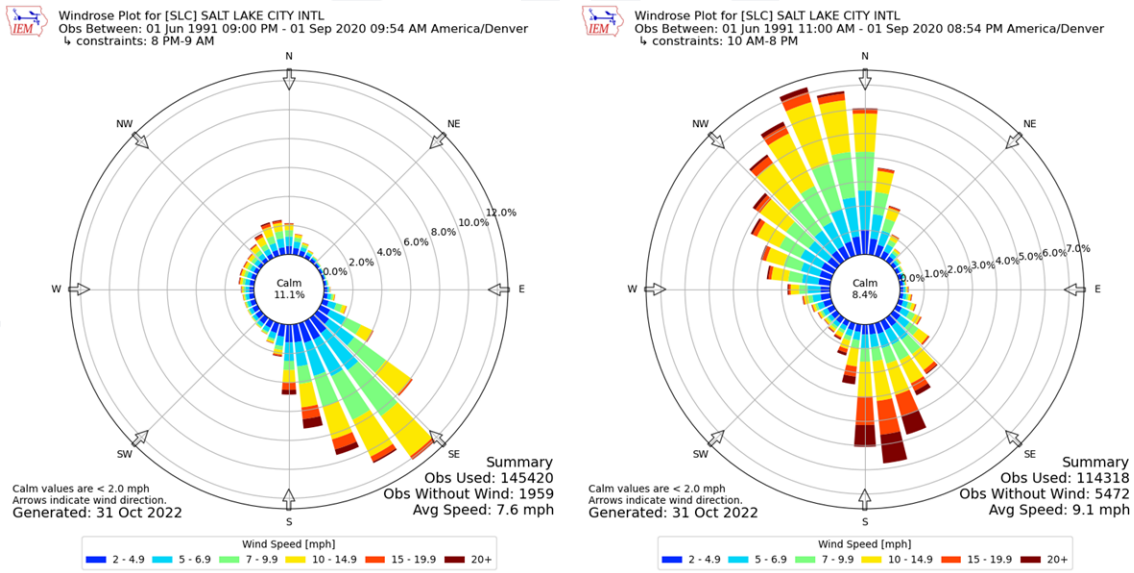

Figure 3. KSLC Jun-Sept wind rose composite (1991-2020 Climatology) broken down by day and night periods. **Left:** Wind during the period 2100-1000 MDT, representing the nighttime valley winds (S-SE). **Right:** Wind during the period 1000-2100 MDT, representing the daytime lake breeze (N-NW).

Figure 4 - Conceptual Diagram of Lake/Valley Breeze

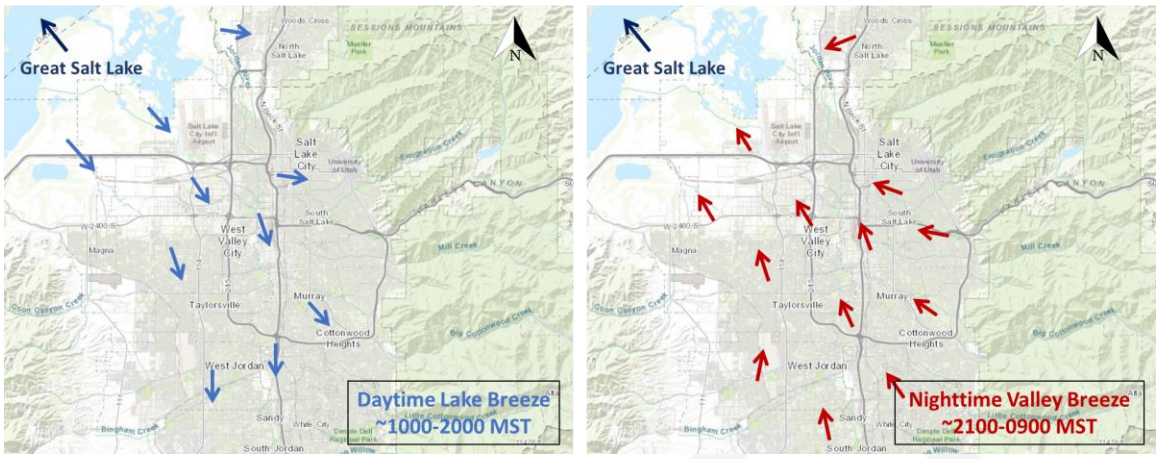

Figure 4. Conceptual diagram of the **left:** daytime N-NW lake breeze (1000-2000 MST) and **right:** nighttime S-SE valley breeze (2100-0900 MST).

2.2 Ozone Climatology and Conceptual Model

2.2.1 Characteristics of Non-Flagged High Ozone Events

The typical summertime high O3 season for the Wasatch Front area is marked between June and September when increased incident solar radiation along with clear skies and hot temperatures aid in O3 formation **Figure 5**. In particular, the meteorological conditions favoring elevated O3 concentrations along the Wasatch Front are known to occur under upper-level ridges/domes of high pressure, which create a stagnant environment with decreased emission dispersion, deep vertical mixed layers, weak surface and mid-level winds, and increased surface temperatures. These conditions allow the buildup of O3 precursors (NOx and VOCs) and create the optimal environment for O3 photochemistry. Additionally, thermally driven circulations arising from the Great Salt Lake (GSL) and nearby mountains are noted to impact the formation of summertime O3 (Doran et al., 2002; Zumpfe and Horel, 2007).

Figure 5 - Wasatch Front O3 AQI Climatology

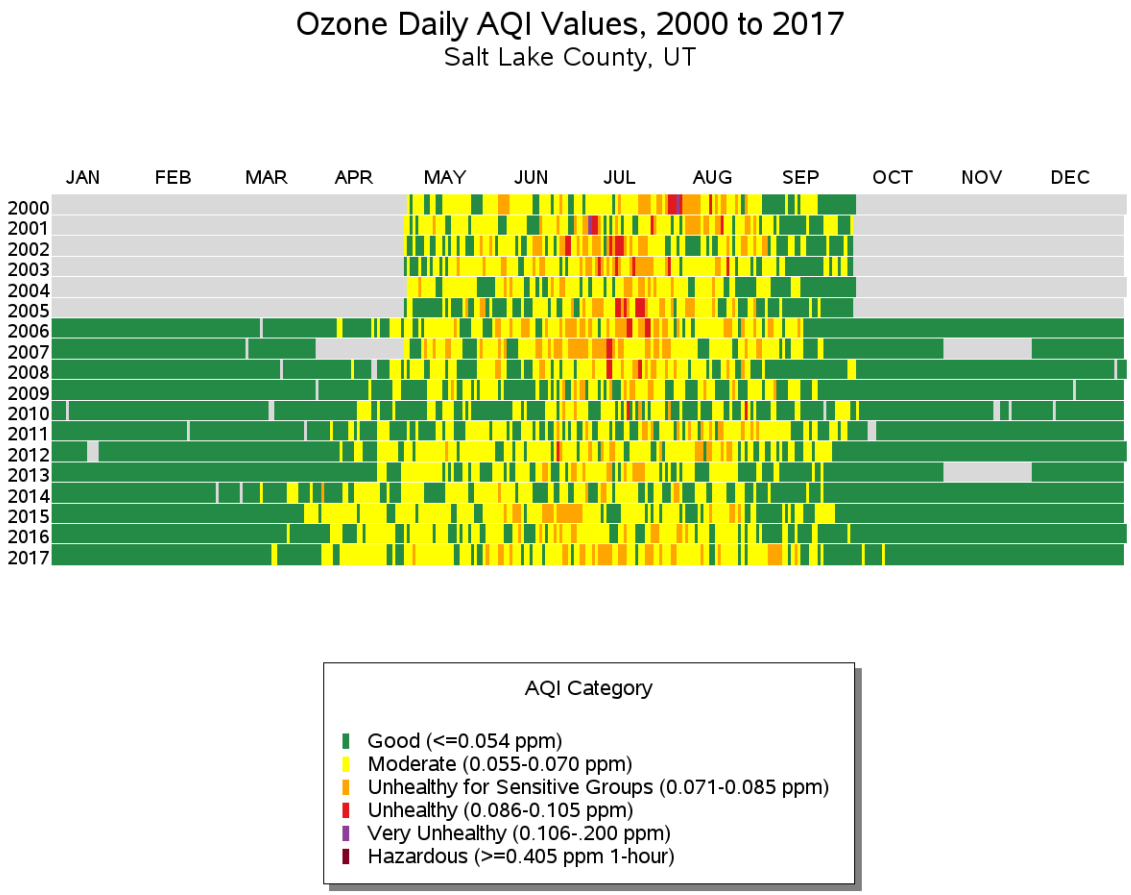

Source: U.S. EPA AirData <https://www.epa.gov/air-data>
Generated: December 8, 2022

Figure 5. Ozone daily AQI values for the 2000-2017. The focus of elevated AQI values extends Jun-Sep, which is considered ozone season for the Wasatch Front.

Past research has attempted to outline the most common meteorological factors contributing to high surface O3 concentrations across the western U.S. The presence of increased 500 hPa heights or upper level ridging has been linked to increased O3, particularly for areas of elevated terrain near urban sources with high emissions of NO2 and other O3 precursors (Reddy and Pfister, 2016). Salt Lake City was included in this study as one of the urban areas in elevated terrain, with high O3 events linked to upper-level ridging and deep vertical mixing. The study concluded that "upper level ridges in the west reduce westerlies at the surface and aloft and allow cyclic terrain-driven circulations to reduce transport away from sources. Upper level ridges can also increase background concentrations within the ridge. O3 and NO2 concentrations build locally, and deeper vertical mixing in this region provides a potential mechanism for recapture of O3 in layers aloft including urban plume residual layers, O3 from thunderstorms, and O3 and precursors from smoke. O3 precursors and reservoir species in large-scale basin drainage flows can be brought back to source areas and nearby mountains by daytime, thermally driven upslope flows. In addition, recirculation and local accumulation can allow precursors with lower reactivities more time to contribute to local O3" (Reddy and Pfister, 2016).

As mentioned in the previous studies (Doran et al., 2002; Reddy and Pfister, 2016; Zumpfe and Horel, 2007) the formation of O3 across the western U.S. is not only impacted by upper level ridging, but also by complex topographical and thermally wind systems. In particular, the diurnal lake-valley breeze is noted as being a potential contributing factor to high O3 concentrations in Salt Lake City during upper level ridging. Past research has attempted to explore the relationship between summertime O3 concentrations along the Wasatch Front and complex topographical wind systems. Specifically, UDAQ initiated the Great Salt Lake Summer Ozone Study (GSLSO3S) in 2015 to explore how summer O3 concentrations are influenced by the diurnal lake-valley breeze. The study showed the Great Salt Lake can impact O3 concentrations along the Wasatch Front through several mechanisms: 1) Lake-induced wind systems modulate the transport and exchange of background ozone and ozone precursors between the lake and urban environments, with nocturnal land breezes from the Wasatch Front towards the Lake transporting ozone precursors towards the Lake; and afternoon lake breezes transporting at times air with higher ozone and precursor concentrations towards the Wasatch Front while at other times advecting cleaner air into the urban corridor, and 2) Lake-modulated boundary-layer depth affecting pollutant vertical mixing over the Lake and along the Wasatch Front (Horel et al., 2016; Long, 2017). A conceptual schematic of the daytime W-NW lake breeze advecting accumulated emissions from over the GSL back into the urban valleys can be seen in **Figure**. The interaction of the lake breeze and O3 formation is revealed to be a fairly common phenomena between June-August, with the N-NW lake breeze from the GSL observed at KSLC nearly 75-80% of dry days for the POR 1948-2003 (Zumpfe and Horel, 2007). The climatology of the GSL lake-valley breeze occurrence, for dry and synoptically benign days, is shown in **Figure 4**. As exhibited by Zumpfe and Horel (2007), the nearly consistent nature of the lake-valley breeze during the summer makes it an integrated component of the general meteorology and therefore the air quality climatology of the Wasatch Front. This persistent occurrence of the lake-valley breeze and associated transport is noted to impact O3 formation on a frequent basis as described by Horel et al. (2016).

Considering the above criteria, the main ingredients for a non-flagged high surface O3 concentration event along the Wasatch Front include:

1. The presence of an upper-level ridge/high pressure system situated over western CONUS, creating stagnant conditions
2. Weak surface and mid-level winds
3. Topographic and thermally driven wind systems such as the GSL lake-valley breeze. The diurnal nature of these winds recirculates emissions back into source areas cyclically, which enhances the accumulation and residence time of O3 precursor emissions.

2.2.2 Characteristics of Wildfire Impacted High O3 Concentration Events

High O3 concentration events flagged for wildfire smoke impacts over the Wasatch Front contain many overlapping meteorological characteristics as non-flagged events. Findings from previous research, investigating the link between high O3 and meteorology in Salt Lake City and across western CONUS, make it evident that the meteorological conditions favorable for high O3 concentrations (e.g. upper lever

ridging, weak surface and mid-level winds, and occurrence of diurnal thermally driven winds) are also favorable for the transport of wildfire smoke and subsequent impacts on surface O3 formation (Reddy and Pfister, 2016; Zumpfe and Horel et al., 2016). Therefore, the common meteorological conditions that influence non-flagged high O3 concentrations and those that contribute to flagged wildfire impacts on O3 are often the same and not necessarily independent from one another.

Wildfire season across the western U.S typically ranges between Jun-Oct when hot and dry conditions and upper level ridging persist. These conditions create dry fuels and favorable fire weather for wildfire formation. The clockwise winds around the upper level ridge allows the long-range transport and accumulation of wildfire smoke from numerous fires across the western region. This type of transport around an upper level ridge creates large areas of dense and diffuse smoke over the west and sometimes the entire CONUS. As noted in previous works, under an upper level ridge a few factors can contribute to wildfire smoke impacts on O3 formation. These factors can include the development of a deep vertical mixed layer and subsidence under a ridge, that can provide a mechanism for the capture of elevated O3 and precursors from wildfire smoke, and the stagnation and accumulation of O3 precursor emissions at the surface (Reddy and Pfister, 2016; Horel et al., 2016). Other studies across the west have also concluded that upper level ridging, leading to higher temperatures and less synoptic ventilation, was the dominant meteorological setup during high O3 wildfire impacted days (Pan and Faloona, 2022).

Wildfires emit large amounts of primary pollutants including PM2.5, black/brown carbon, carbon monoxide (CO) and O3 precursors, including NOx and large amounts of VOCs. The O3 precursors are transported within the wildfire smoke plume downwind of the source and undergo various photochemical reactions as the plume ages (Lindass et al., 2017). When the VOC rich wildfire smoke plume is transported across urban areas and mixes with NOx rich urban air, O3 formation is enhanced and high O3 concentrations can develop (Lu Xu et al., 2021). A number of observational studies have indicated the link between increased surface O3 concentrations and arrival of wildfire smoke emissions across urban areas. (e.g. Jaffe et al., 2008, Lu et al., 2016). During periods of upper level ridging, wildfire smoke is frequently transported over the Wasatch Front from both in state and out of state sources. Observational evidence from relatively recent studies (e.g. Horel et al., 2016; Long, 2017) has shown that elevated O3 concentrations along the Wasatch Front coincide with large-scale ridging and the presence of wildfire smoke. For example, Horel et al. (2016) observed high O3 concentrations that exceeded the NAAQS in the Salt Lake Valley during the latter half of August 2015 as a result of both strong ridging aloft and regional transport of wildfire smoke.

The magnitude of surface O3 enhancement by wildfire smoke is non-trivial and has significant ramifications for air quality monitoring data. Studies that have quantified the impact of wildfire smoke on surface O3 concentrations across the western U.S. have shown wildfire smoke can increase O3 by up to 5-10 ppb (Pan and Faloona, 2022, Lindaas et al., 2017). The increase of O3 commonly leads to situations that would have been in compliance with the NAAQs if not for the contributing wildfire emissions (Lindaas et al., 2017). Interestingly, Lindaas et al. (2017) revealed that enhancement of O3 concentrations by wildfire smoke can occur independent of warmer temperatures or anomalous meteorological conditions, meaning the influence of transport emissions from wildfire smoke has a profound effect on surface O3 formation.

Considering the above criteria, the main ingredients for a flagged wildfire smoke impacted high surface O3 concentration event along the Wasatch Front include:

1. The presence of an upper-level ridge/high pressure system situated over western CONUS, aiding in the transport of wildfire smoke from source areas to the Wasatch Front.
2. Weak surface and mid-level winds, creating stagnant conditions
3. Topographic and thermally driven winds, transporting smoke via canyon, valley, or lake-valley flows.
4. A deep PBL mixed layer, mixing wildfire smoke emissions from PBL residual layers or other elevated layers to the surface
5. Enhanced surface concentrations of wildfire smoke tracers, including PM2.5, CO, and brown carbon, marking the presence of smoke

2.3 Flagging Methodology: Wildfire Smoke Event Criteria

To identify the influence of wildfire smoke at surface monitoring sites, UDAQ employs air quality monitoring observations of PM2.5, CO, and brown carbon concentrations (BV site) at an hourly frequency. Additionally, we utilize the National Oceanic and Atmospheric Administration (NOAA) National Environmental Satellite, Data, and Information Service (NESDIS) Hazard Mapping System (HMS) smoke product, as well as GOES Satellite imagery and products to distinguish the residence of wildfire smoke over the Wasatch Front. Historical observations of PM2.5 along the Wasatch Front date back through 2016 and 2017 for all three sites, with brown carbon extending back to 2017 at the Bountiful (BV) site and CO at Hawthorne (HW) for 2016 and 2017.

Numerous studies have shown observations of tracer concentrations are related to the influence of wildfire smoke on surface O3. In particular, brown carbon, which coexists with black carbon, has been shown to be extremely useful for identifying biomass burning emissions. Any observational value (> 0 ng/m^-3) of brown carbon signals the presence of smoke from some biomass burning. UDAQ has continuous aethalometer observations of brown carbon dating back to July 18, 2017 at the BV site. An aethalometer is an instrument that measures the concentration of optically absorbing black carbon particles in ambient air. The brown carbon observations (delta) are derived by finding the separation between the absorption of two channels of different wavelengths. Other tracers, such as PM2.5 and CO, are relatively ubiquitous measurements taken at air quality monitoring stations, with many sites having observations over an extended historical timeframe. The commonality and typical long period of record (POR) of PM2.5 observations make it a useful tool for distinguishing abnormal levels of particulate matter in the context of historical concentrations. Therefore, PM2.5 historical average concentrations are often used as threshold criteria to filter wildfire smoke events from non-smoke events. PM2.5 is also used to indicate the potential magnitude of O3 enhancement by wildfire smoke. Empirical relationships between PM2.5 and O3 concentrations reveal that surface O3 increases at low to moderate PM2.5 concentrations up to 30-50 ppb before decreasing at higher PM2.5 levels (Ninneman and Jaffe, 2021). The negative relationship between high PM2.5 concentrations and O3 suggests that O3 production can be suppressed due to backscattering/attenuation of solar radiation in dense smoke (high PM2.5), leading to reduced O3 photochemistry near the surface.

Following the established use of PM2.5 as a tracer for wildfire smoke, PM2.5 concentrations from the UDAQ monitors Hawthorne (HW), Bountiful Viewmont (BV), and Herriman #3 (H3) are analyzed to flag days impacted by wildfire smoke. Flagged smoke days are delineated where the daily 24-hour average PM2.5 concentration ($\overline{PM2.5}_{24hr}$) exceeds one standard deviation above the monthly mean PM2.5 concentration ($\overline{PM2.5}_{24hr} > \overline{PM2.5}_{month} + \sigma$). Using the above PM2.5 criteria to detect the presence of wildfire smoke at surface UDAQ monitors, days are flagged for further investigation. The HMS smoke tool as well as satellite data are then analyzed to corroborate the occurrence of wildfire smoke on days flagged using the above PM2.5 criteria.

3.0 Analysis of Wildfire Smoke Events

In this section, we review the meteorological conditions that characterize each flagged wildfire smoke impacted O3 event (August 4, 2016 and September. 2, 5, and 6, 2017) in conjunction with the analysis of surface PM2.5, CO, and brown carbon trends, satellite data, HRRR Smoke, assimilated observed and modeled smoke aerosol transport, the HMS smoke product, and forward and backwards HYSPLIT trajectories to identify the source areas of smoke and transport. The aforementioned tools and analysis will provide the evidence and support the case for the presence of wildfire smoke and subsequent impact on surface O3 enhancement above the 2015 NAAQS of 70 ppb for the flagged dates Aug. 4, 2016 and Sept. 2, 5, and 6, 2017.

3.1 August 4, 2016 Flagged Event

3.1.1 Meteorological Conditions

A moderately progressive pattern characterized August 4, 2016, with a weak upper level ridge and marginal synoptic forcing present (**Figure 6**). However, on the preceding day August 3, 2016 at 00Z, a short wave 500 mb trough and attendant jet streak pushed into the PNW and progressed eastward along the U.S.-Canadian border (**Figure 7**). Over the course of 18 hours, the trough moved east-northeast bringing lower heights and a trailing weak dry cold front across northern Utah by August 3, 18Z. Mid-level winds, heights, isotherms, and surface analysis (**Figure 8 and 9**) and observations exhibit the cold frontal passage on the afternoon of August 3 at 21Z, with winds shifting W-NW from the surface up to 500 mb (**Figures 7-12**). Across Utah and the western U.S, the 700 mb level is representative of the top of the PBL or mixed layer and therefore smoke from wildfires is mixed, like other scalar quantities, from the surface to top of the PBL. Therefore, the 700 mb winds are frequently considered to represent the mean steering flow and the flow responsible for wildfire smoke transport. As seen in **Figure 11**, 700 mb winds shifted N-NW across northern Utah between 21Z August 3 and 00Z August 4. This N-NW shift in winds was also evident at the surface as illustrated in **Figure 12**.

By August 4 at 00Z, the trough ejected northeastward into the Canadian provinces of Manitoba and Saskatchewan (**Figure 7c**), allowing a modest 500 mb ridge to build over Utah through August 4 at 12Z (Figure). Due to marginal cold air advection from the preceding day, surface temperatures remained slightly below average on August 4 only topping out in the upper 80s/near 90F for the northern Wasatch Front (**Table 4**). The orientation of the 500 mb ridge axis centered along the UT-NV border and extended along a SE to NW axis into Idaho, allowing the surface to 500 mb winds to remain W-NW through August 4 (**Figure 7d**). Radiosonde data from KSLC at 12Z August 4 and 00Z August 5 shows winds W-NW from the surface to near 480 mb and winds W-NW from the surface to 640 mb, respectively (**Figure 13**).

Figure 6 - NCEP Composite Mean 500 mb Heights Aug. 4

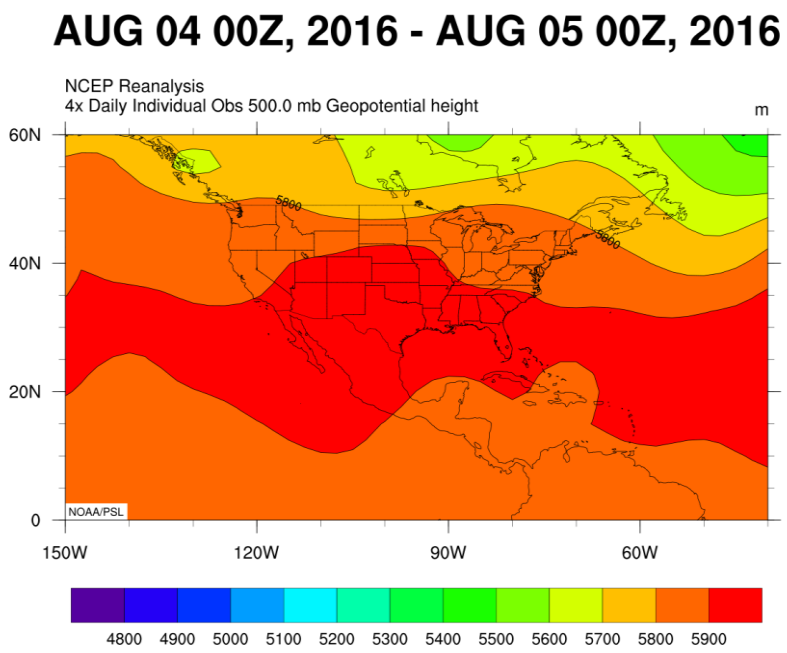

Figure 6. NCEP Reanalysis composite mean 500 mb heights August 4-5, 2016.

Figure 7 - Aug. 3-4 GFS 0.25 Analyzed 500 mb Heights and Winds

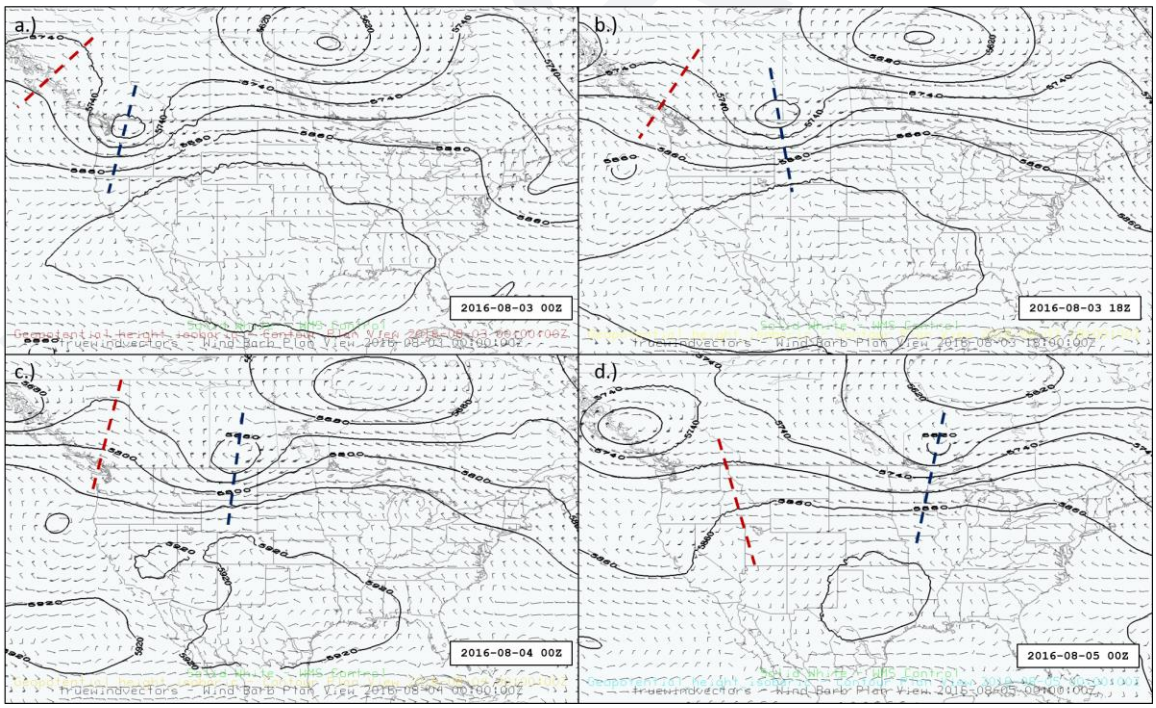

Figure 7. GFS 0.25 degrees analyzed 500 mb heights and winds for **a.)** 2016-08-03 00Z, **b.)** 2016-08-03 18Z**, c.)** 2016-08-04 00Z, and **d.)** 2016-08-04 00Z. The red dashed line represents the 500 mb ridge axis and blue dashed line represents the 500 mb trough axis.

Figure 8 - Surface Analysis Aug. 3 at 21Z

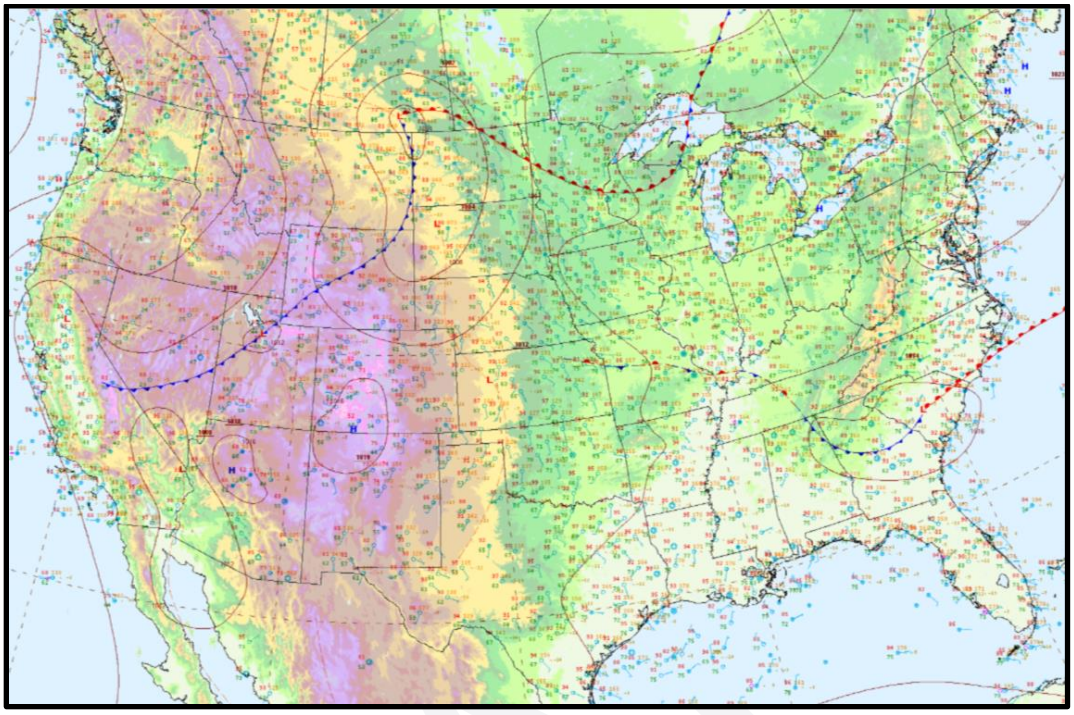

Figure 8. Surface analysis on August 3, 2016 at 21Z. A cold front is draped SW to NE across the Wasatch Front.

Figure 9 - Surface Analysis and Observations Aug. 3

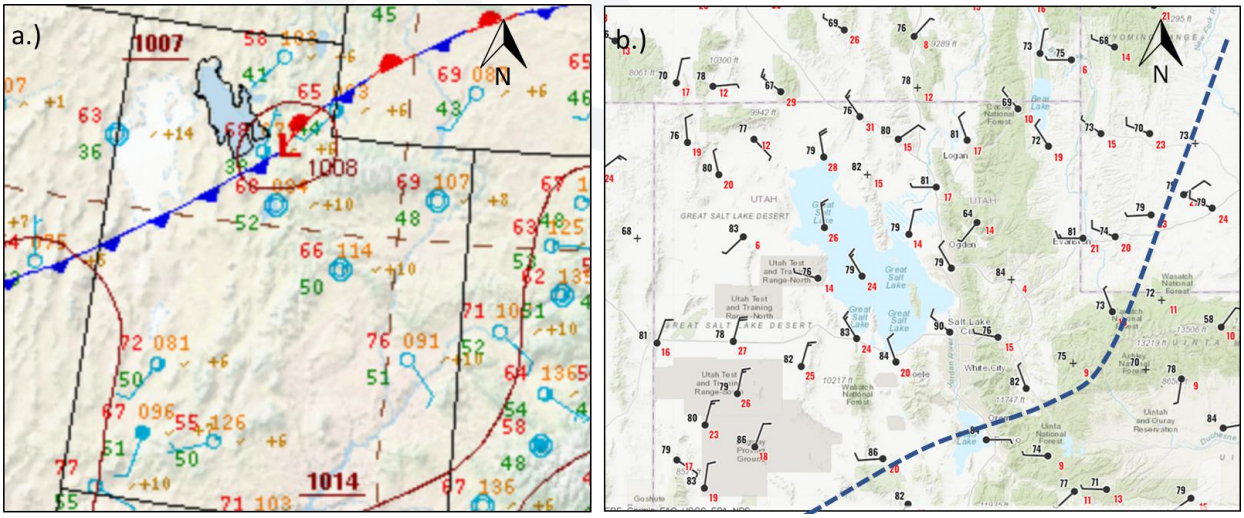

Figure 9. Left: Analyzed surface chart with location of surface cold frontal boundary across northern Utah on August 3, 2016 at 21Z; **Right:** Surface observations on August 3, 2016 at 21Z zoomed in across northern Utah. Winds are N-NW across the Wasatch Front signifying the passage of the cold front to the E-SE of the area. The blue dashed line represents the approximate location of the surface front at 21Z.
(Source: https://www.wrh.noaa.gov/map/)

Figure 10 - Surface Met Observations KSLC

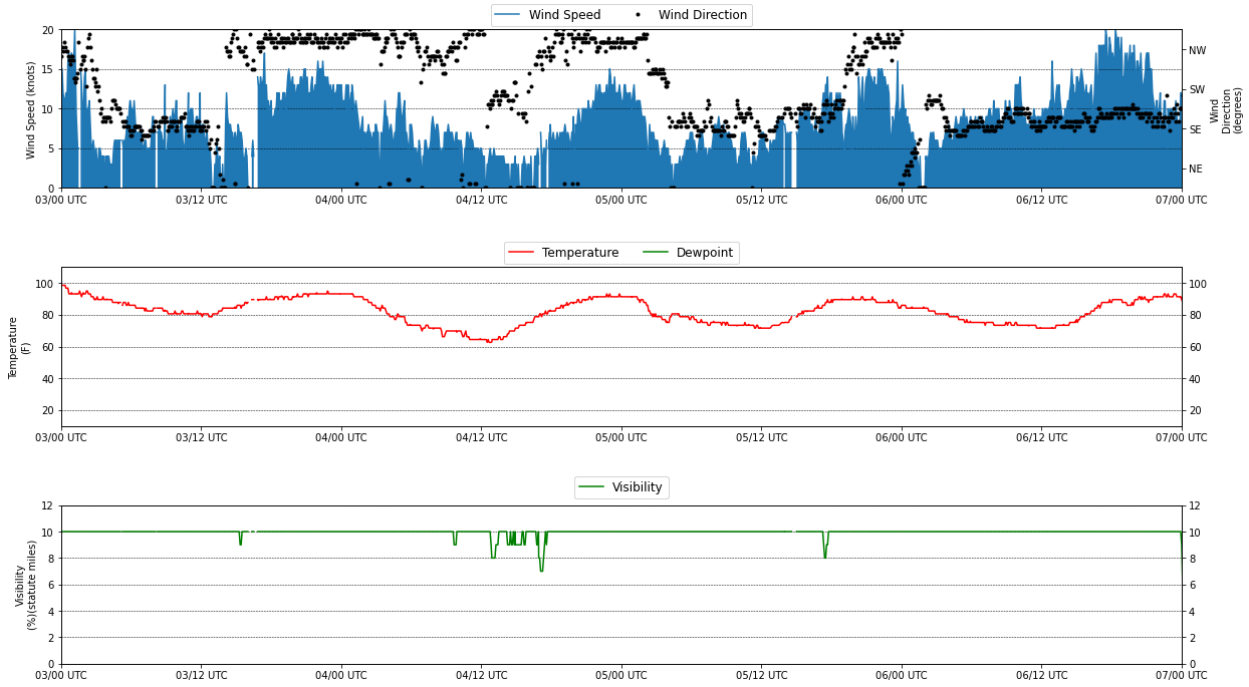

Figure 10. Surface wind observations at KSLC from August 3 00Z to August 5 00Z. Shift in wind direction to the N-NW at 08-03 15Z marks the surface cold frontal passage.

Figure 11 - 700 mb Winds and Heights Aug. 3-4

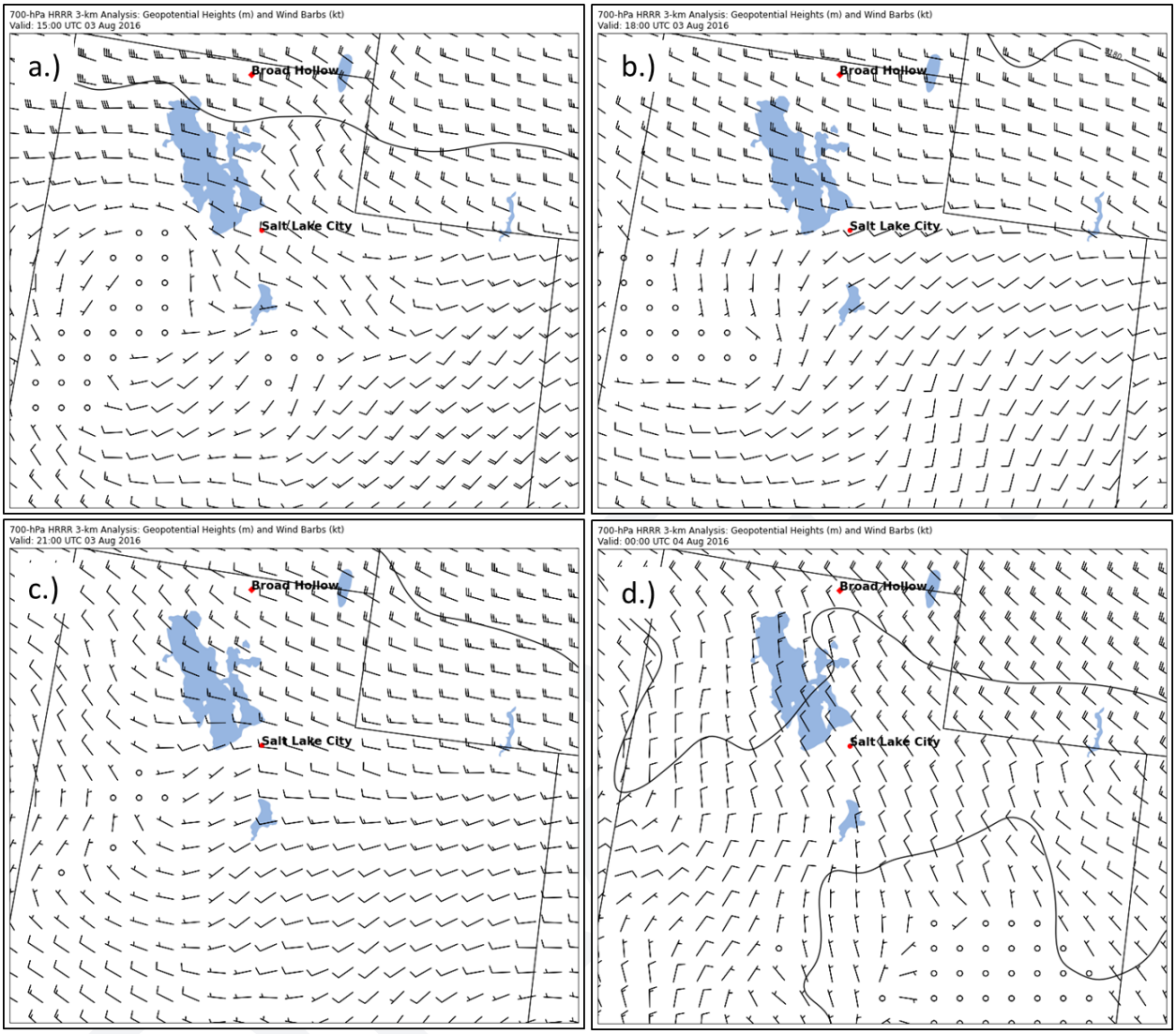

Figure 11. HRRRv1 3 km analyzed 700 mb winds and heights over northern Utah on **a.)** 2016-08-03 15Z, **b.)** 2016-08-03 18Z, **c.)** 2016-08-03 21Z, and **d.)** 2016-08-04 00Z. The location of the Box Elder wildfire (Broad Hollow Fire) is marked by a red diamond.

Figure 12 - 10m Winds Aug. 3-4

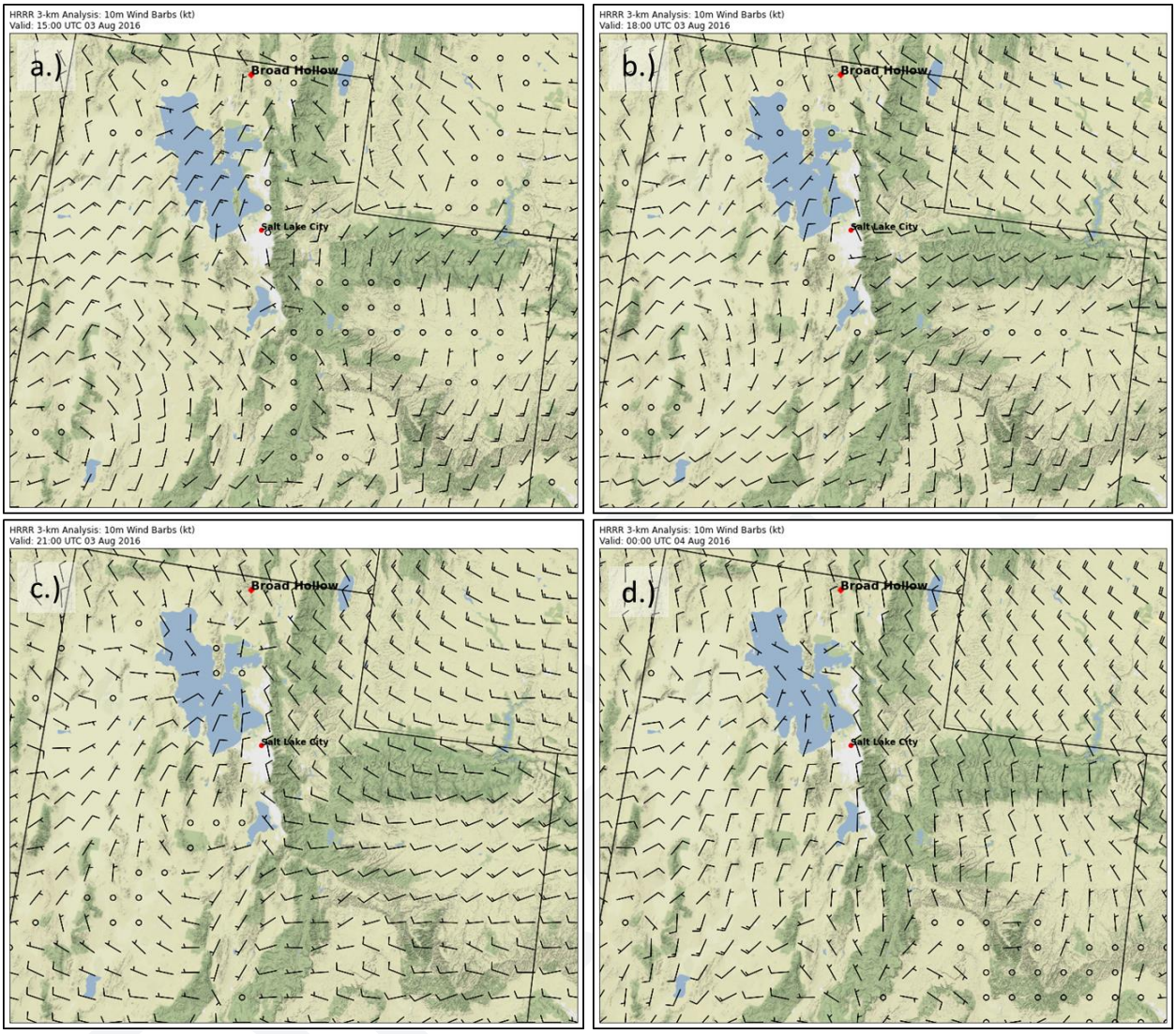

Figure 12. HRRRv1 3 km analyzed 10m winds over northern Utah on **a.)** 2016-08-03 15Z, **b.)** 2016-08-03 18Z, **c.)** 2016-08-03 21Z, and **d.)** 2016-08-04 00Z. The location of the Box Elder wildfire (Broad Hollow Fire) is marked by a red diamond.

Figure 13 - KSLC Radiosonde Skew-T's Aug. 3-4

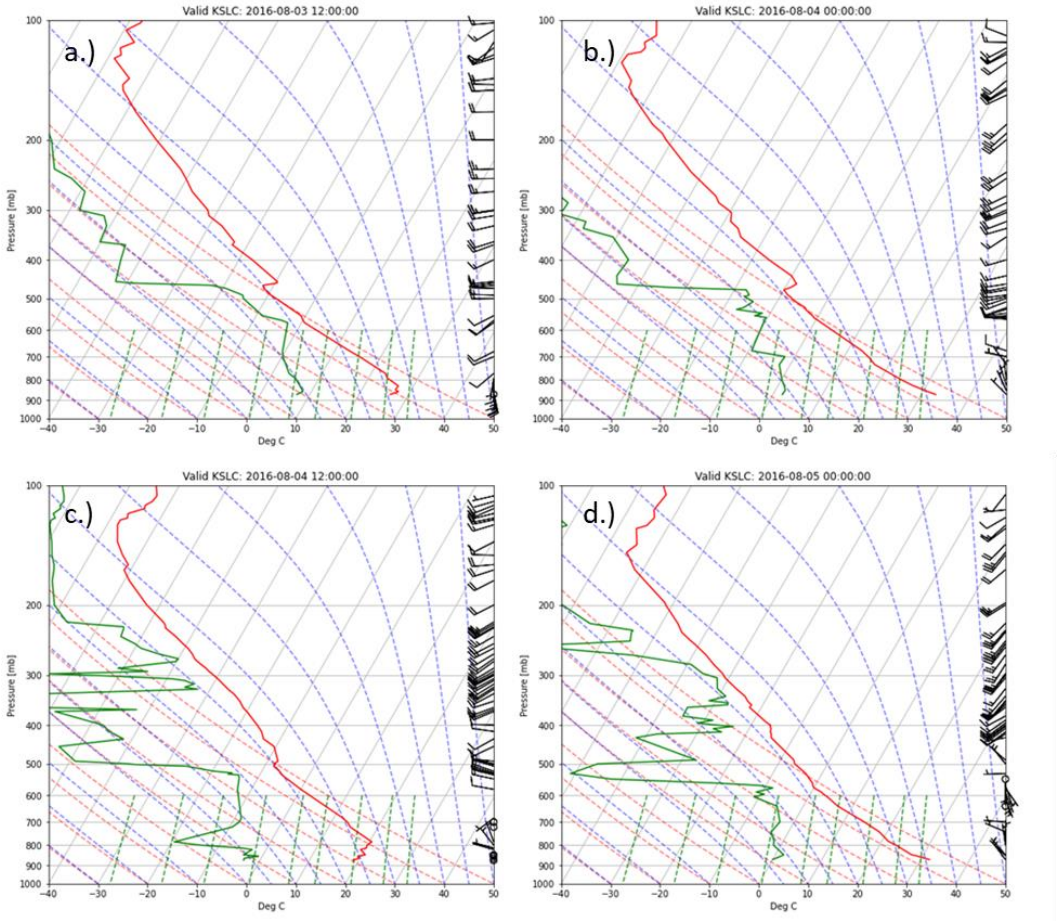

Figure 13. Radiosonde observations from KSLC on **a.)** 2016-08-03 12Z, **b.)** 2016-08-04 00Z, **c.)** 2016-08-04 12Z, and **d.)** 2016-08-05 00Z. Dew point (**green solid line**), temperature (**red solid line**), and wind barbs (**right vertical axis**) are plotted to 100 mb. (Source: Integrated Global Radiosonde Archive (IGRA) - https://www.ncei.noaa.gov/access/metadata/landing-page/bin/iso?id=gov.noaa.ncdc:C00975)

Table 4 - KSLC Observed and Climate Normals Aug. 2-6

Date	Observed Low (F)	Observed High (F)	Normal Low (F)	Normal High (F)	Observed Precipitation (inches)	Normal Precipitation (inches)	Record Precipitation (inches)
8/2/2016	73	101	66	94	0	0.02	1.72
8/3/2016	69	95	66	93	0	0.02	1.22
8/4/2016	**62**	**93**	**66**	**93**	**0**	**0.02**	**1.62**
8/5/2016	71	92	66	93	T	0.02	0.48
8/6/2016	71	94	66	93	0.03	0.02	0.4

Table 4. Observed and normal high/low temperatures and precipitation accumulations for KSLC for the period August 2 - August 6, 2016. The event date August 4 is bolded.
(Source: NWS SLC https://www.weather.gov/slc/CliPlot)

3.1.3 Wildfire Conditions

On August 4, 2016, a number of active wildfires located in Utah and across western CONUS contributed to the transport of wildfire smoke over the Wasatch Front. The locations of these wildfires are revealed in **Figure 14** by the MODIS wildfire hotspot thermal sensor and visible imagery in Utah, Idaho, California. Due to the presence of a 500 mb ridge axis centered across Utah, the lower to upper level winds and August 4 were characterized by W-NW flow. This pattern allowed the transport of wildfire smoke from the previously mentioned wildfires into northern Utah.

Figure 14 MODIS Terra/Aqua True Color Image-West CONUS on Aug. 4

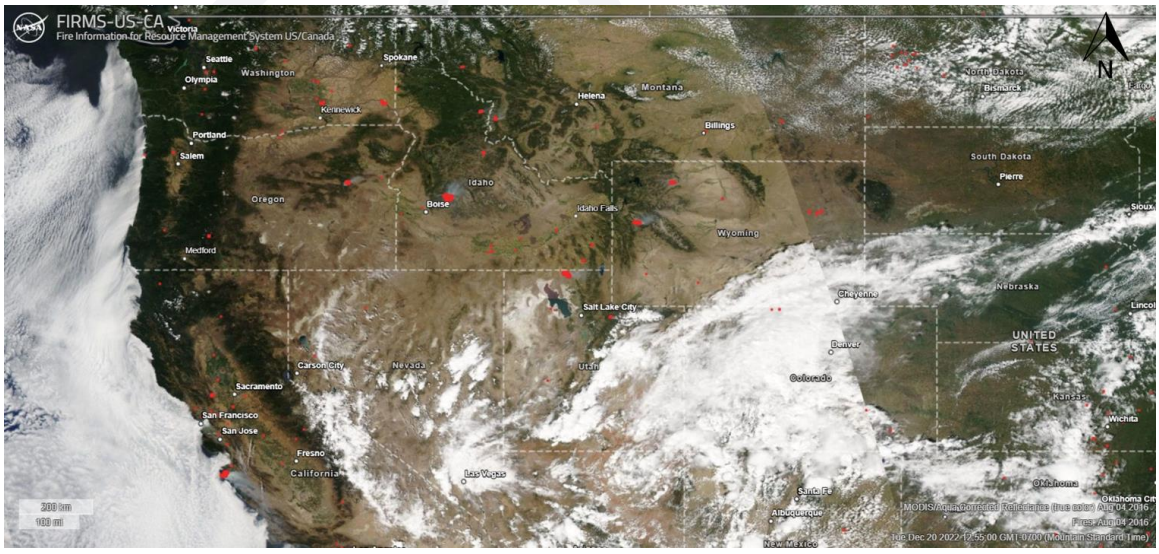

Figure 14. MODIS Terra/Aqua True Color image on August 4, 2016. Red markers indicate VIIRS/MODIS active fire detections and thermal anomalies (hot spot detection).
(Source: https://firms.modaps.eosdis.nasa.gov/usfs/map/)

The immediate source of smoke originated from a large wildfire complex (Broad Fork Fire) in Box Elder Co, UT in the north, while more distant fires in Idaho also potentially contributed to the smoke across the Wasatch (**Figure 16**). In **Figures 16 and 17**, the HMS smoke tool reveals the southern extent of light to moderate wildfire smoke reaching down across the northern Wasatch Front but does not analyze a smoke field over BV, HW, and H3. However, other observations and analysis indicate the presence of wildfire smoke over the Wasatch. This discrepancy largely has to do with some HMS smoke detection inaccuracies that arise when wildfires/smoke plumes are relatively localized or increase at a rapid rate (Hu et al., 2016). Although HMS smoke does not exhibit a smoke plume extending across the southern Wasatch Front, the presence of wildfire smoke is substantiated by visible True Color imagery from the MODIS Terra/Aqua satellite, exhibiting dense and diffuse smoke plumes residing over northern Utah (**Figure 18**). Additionally, MODIS Terra/Aqua MAIAC and ECMWF/CAMS Aerosol Optical Depth (AOD) at 550 nm show increased AOD's over the northern Wasatch Front (**Figure 19**).

Figure 15 - MODIS Terra/Aqua True Color Image-Utah Aug. 4

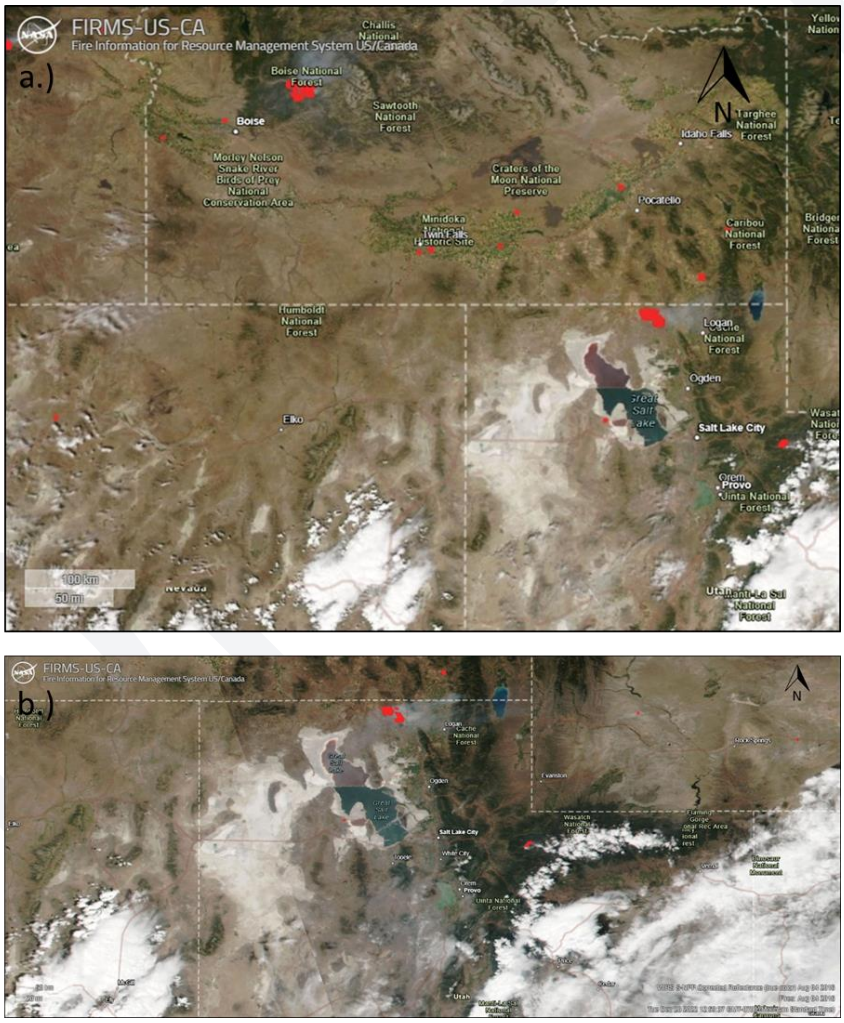

Figure 15. MODIS Terra/Aqua True Color image on August 4, 2016. Red markers indicate VIIRS/MODIS active fire detections and thermal anomalies (hot spot detection). The Box Elder fire complex is located in the area of the highest concentration of thermal hot spots in far northern Utah.
(Source: https://firms.modaps.eosdis.nasa.gov/usfs/map/)

Figure 16 - HMS Smoke Detection-CONUS Aug. 4

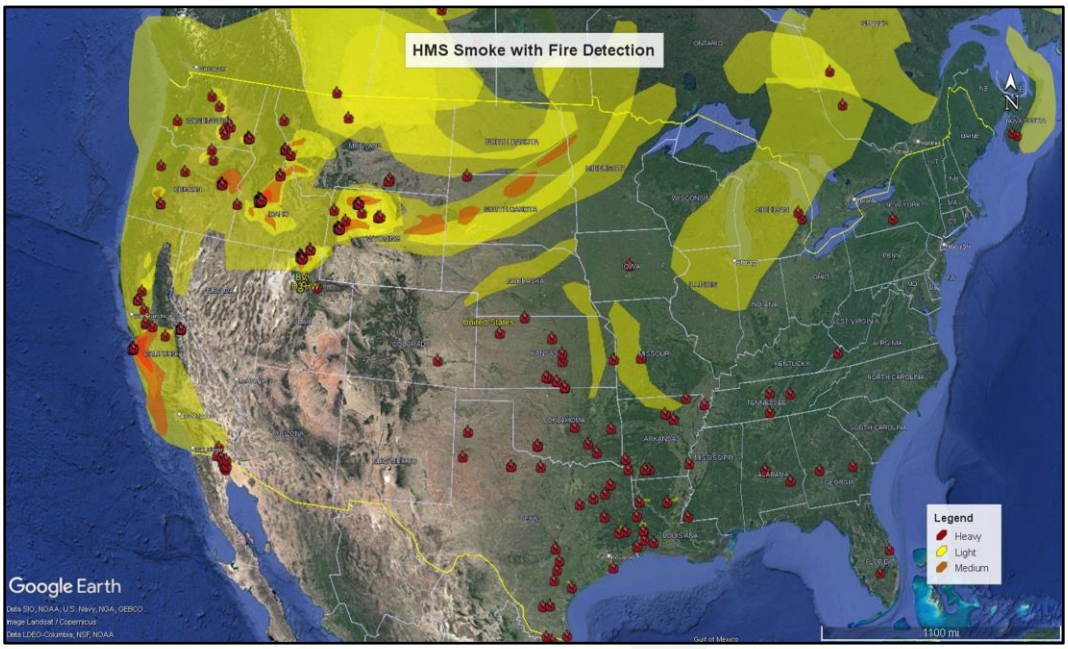

Figure 16. HMS smoke detection (yellow: light smoke, orange: moderate smoke, and dark brown: heavy smoke) and VIIRS/MODIS active fire detections and thermal anomalies (**red flames**) on August 4, 2016. (Source: https://globalfires.earthengine.app/view/hms-smoke)

Figure 17 - HMS Smoke Detection Aug. 4 - Utah

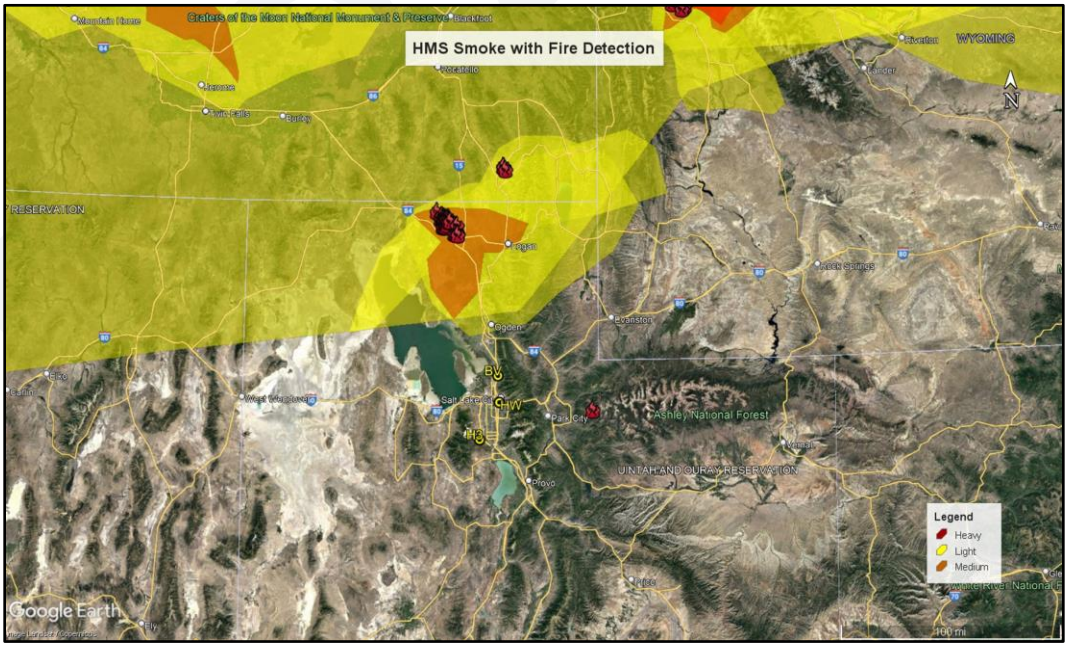

Figure 17. HMS smoke detection (yellow: light smoke, orange: moderate smoke, and dark brown: heavy smoke) and VIIRS/MODIS active fire detections and thermal anomalies (**red flames**) on August 4, 2016. (Source: https://globalfires.earthengine.app/view/hms-smoke)

The presence of wildfire smoke as noted by satellite imagery across the Wasatch Front is corroborated by surface observations of the aerosol optical depth (AOD) from the Aerosol Robotic Network (AERONET) (**Figure 20**). A larger or thicker AOD signifies more attenuation/scattering of incident solar radiation through the column of the atmosphere and can be correlated with the presence of wildfire smoke. We utilize AERONET AOD observations from the NEON_ONAQ site, which is located approximately 48 miles due SW (40.17759 N, 112.45244 W) of the HW monitor. **Figure 19** shows AOD ranging from < 0.2 on August 3 to 0.6-0.9 on August 4. The increase in AOD from August 3 to August 4 is due to the increased transport of wildfire smoke across the area. For reference on clear days with no smoke, AOD's are < 0.1.

Figure 18 - MODIS Terra/Aqua MAIAC Optical Depth Aug. 4

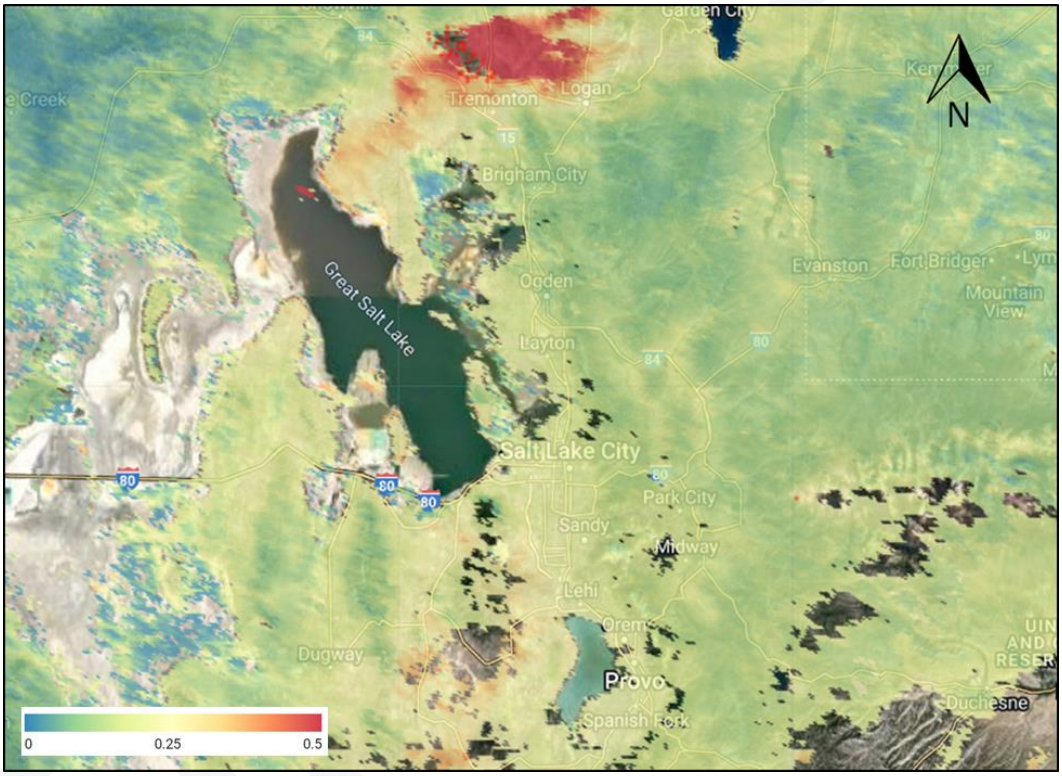

Figure 18. MODIS Terra/Aqua MAIAC Optical Depth (AOD) at 550 nm on August 4, 2016. Red markers indicate VIIRS/MODIS active fire detections and thermal anomalies (hot spot detection).
(Source: https://globalfires.earthengine.app/view/hms-smoke)

Figure 19 - OMPS Aerosol Index Aug. 4

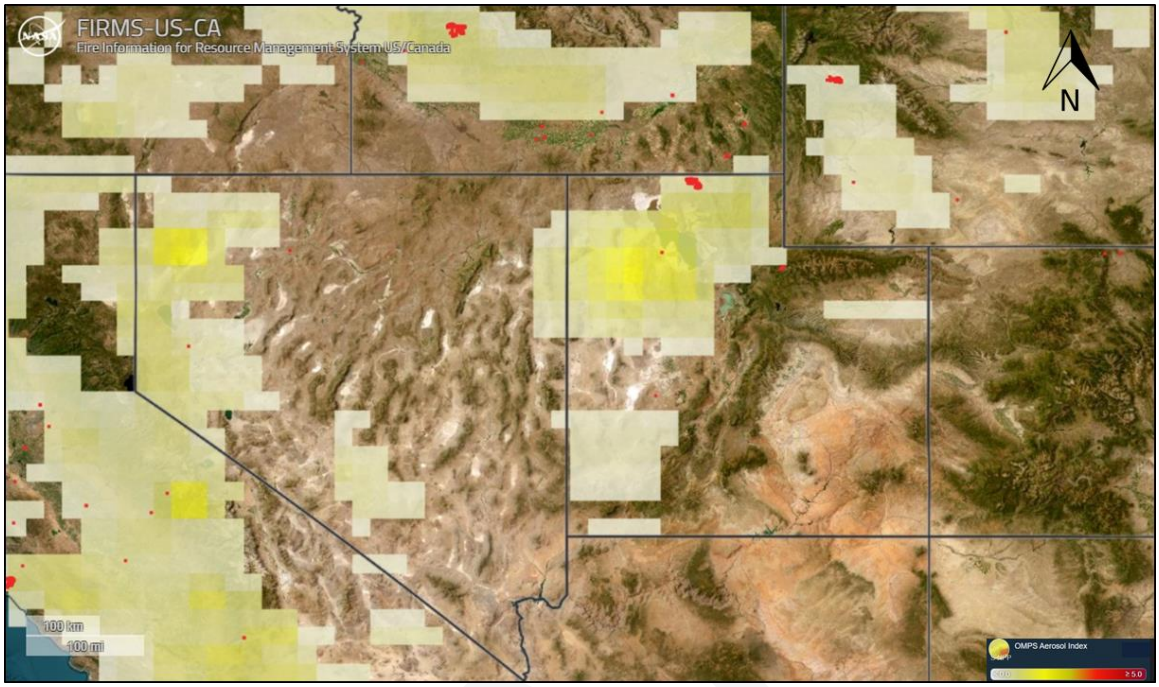

Figure 19. The OMPS Aerosol Index layer on August 4, 2016, which indicates the presence of ultraviolet (UV)-absorbing particles in the air (aerosols) such as soot particles in the atmosphere; it is related to both the thickness of the aerosol layer located in the atmosphere and to the height of the layer. The Aerosol Index is a unitless range from < 0 to >= 5, where 5 indicates heavy concentrations of aerosols related to biomass burning smoke located in the lower troposphere (1-3 km). Red markers indicate VIIRS/MODIS active fire detections and thermal anomalies (hot spot detection).
(Source: https://disc.gsfc.nasa.gov/datasets/OMPS_NPP_NMMIEAI_L2_2/summary)

Figure 20 - AERONET AOD Aug. 4

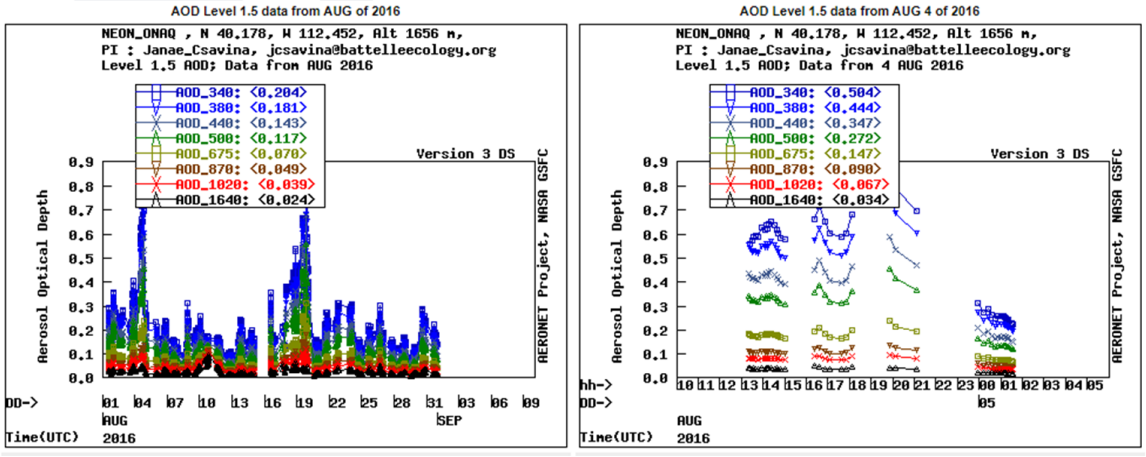

Figure 20. Time series of Aerosol Optical Depth (AOD) measured by the AERONET observation network at NEON_ONAQ site (40.17759 N, 112.45244 W) for **left:** August 1-31, 2016 and **right:** August 4 12Z - August 5 06Z. (Source: https://aeronet.gsfc.nasa.gov)

In addition to satellite imagery and derived products, we utilize analysis of HRRR Smoke fields to investigate the spatial and temporal variability of near surface and vertically integrated concentrations of wildfire smoke across the Wasatch Front during the flagged event. The locations of numerous fires in the western U.S. along with the Box Elder Fire complex are shown in **Figures 21a** and **21b**, respectively. Specifically, the fire radiative power (FRP) analyzed from the VIIRS satellite shows high values at the Box Elder fire and a fire just to the north in Idaho. These high FRP values signify that the fire in Box Elder County was burning hot. In **Figure 22**, the progression of near surface and vertically integrated smoke is shown through the course of August 4, with high concentrations of smoke noted across northern Utah and the Wasatch Front. This swath of dense smoke corresponds in large part to the N to S transport of wildfire smoke from the Box Elder County fire complex along with regional transport of wildfire smoke from other wildfires in Idaho, Wyoming, and Nevada. Captured images from the Salt Lake Valley on August 3 and 4 illustrate how wildfire smoke emissions increased across the Wasatch Front on August 4 (**Figure 23**). On August 3, visibility was relatively good, with the Wasatch Mountains visible (**Figure 23a**). However, by August 4 wildfire smoke had been transported across the Wasatch Front and was dense enough to completely obscure the Wasatch Range (**Figure 21b**).

Figure 21 - Fire Radiative Power Aug. 4

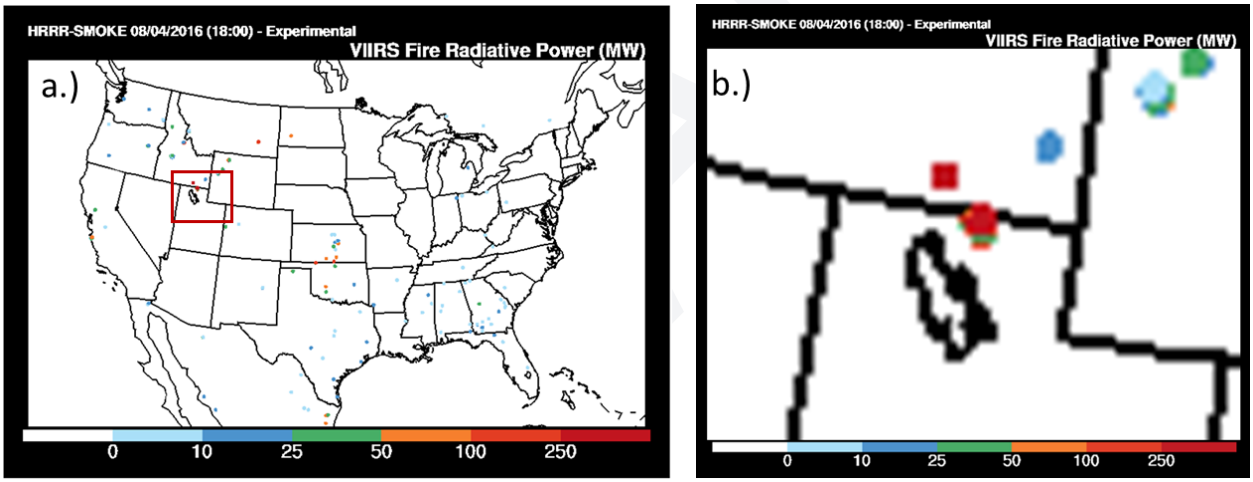

Figure 21. Fire Radiative Power (FRP) in megawatts (MW) derived from the VIIRS satellite **a.)** CONUS view and **b.)** zoomed into northern Utah (red box). Highest FRP (>250 MW) noted over the Box Elder Fire complex.

Figure 22 - HRRR Smoke Near-Surface and Vertically Integrated Smoke Aug. 4

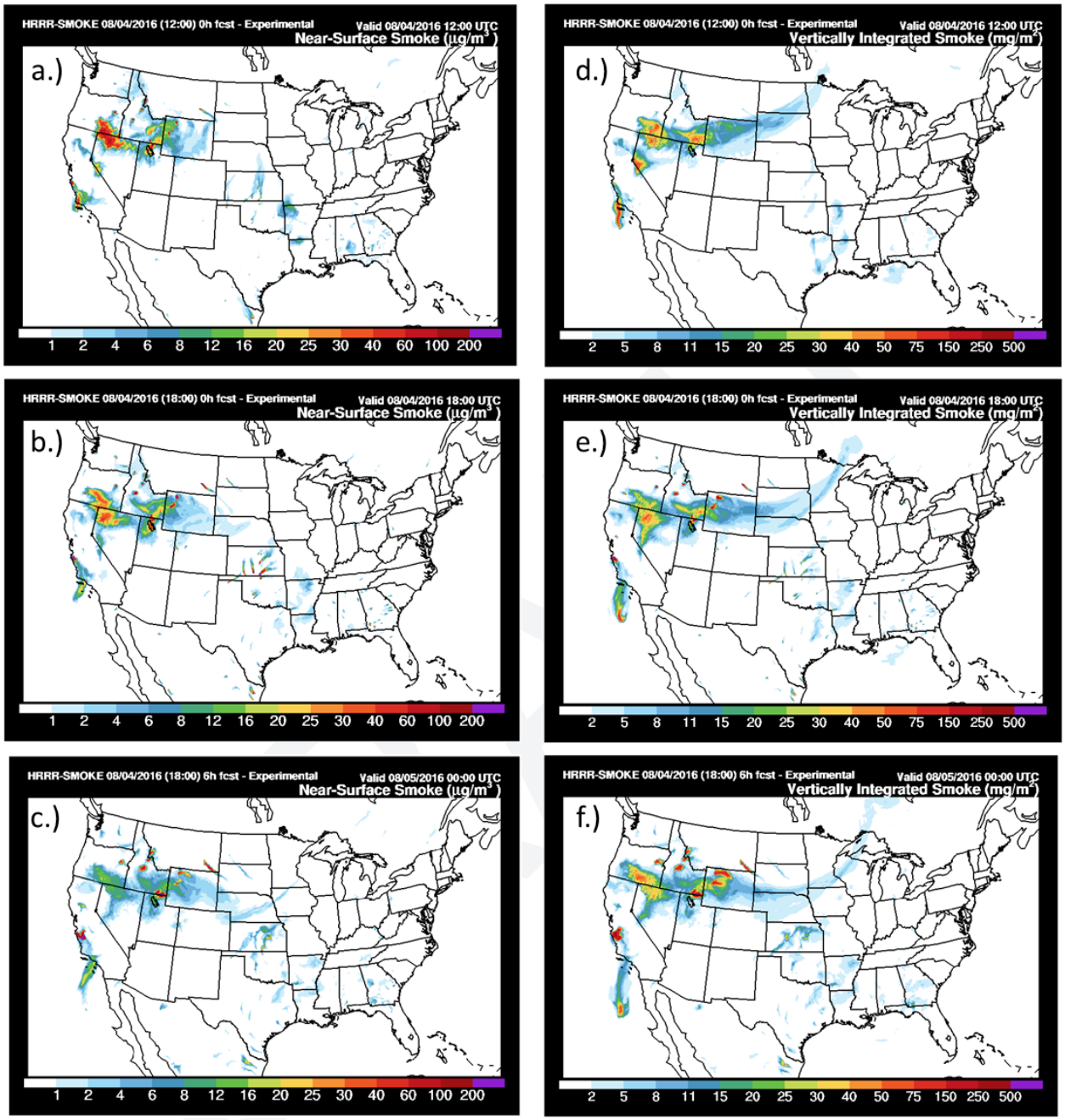

Figure 22. HRRR Smoke forecast valid for Near-Surface Smoke at **a.)** 2016-08-04 12Z, **b.)** 2016-08-04 18Z, and **c.)** 2016-08-04 00Z and for Vertically Integrated Smoke at **d.)** 2016-08-04 12Z, **e.)** 2016-08-04 18Z, and **f.)** 2016-08-04 21Z.

Figure 23 - Camera Images Salt Lake Valley Aug. 3-4

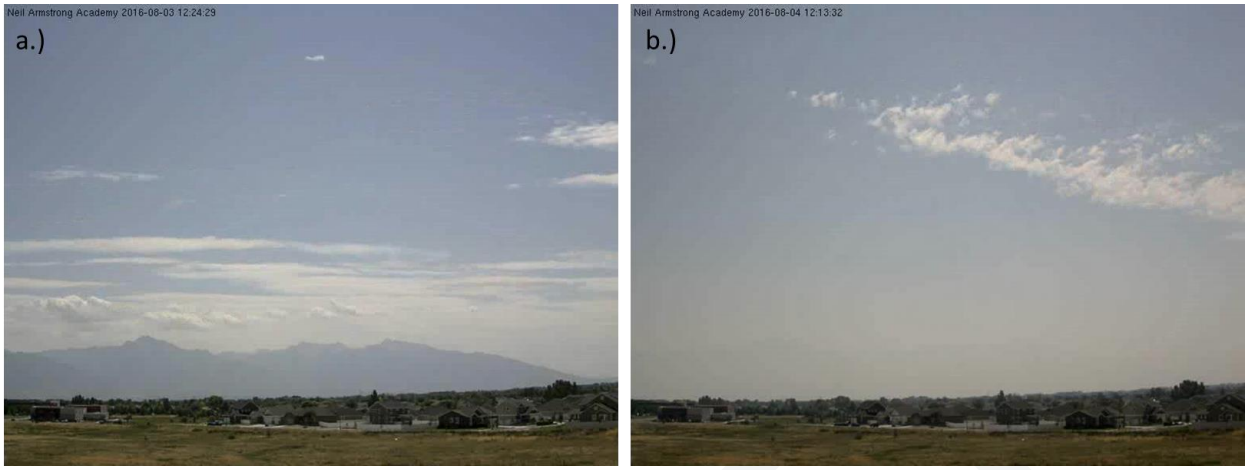

Figure 23. Snapshots from the Neil Armstrong Academy-MesoWest camera on **a.)** 2016-08-03, and **b.)** 2016-08-04. (Perspective: westside of Salt Lake Valley facing east towards the Wasatch Mountains)

3.1.4 Event Analysis August 4, 2016

The accumulated mass of smoke from the Box Elder County fire complex along with Idaho, Wyoming, and Nevada was advected over the UDAQ monitors HW, BV, and H3, leading to the concurrence of enhanced surface PM2.5 and elevated O3 concentrations on August 4. **Figures 24-26** exhibits the time series analysis of PM2.5 and MD8A for HW, BV, and H3 monitors over the period August 1-6, 2016, revealing a distinct spike in hourly PM2.5, 24hrly average PM2.5, and MD8A O3 on August 4, 2016. The spike in PM2.5 concentrations marks the transport of wildfire smoke across all three UDAQ sites and corresponds temporally to enhanced O3 concentrations. In order to distinguish if the increased PM2.5 and O3 levels are potentially linked, we show the MD8A O3 and PM2.5 observations for the days preceding and proceeding August 4 (**Figures 24-26**).

Figure 24 - HW: MD8A and PM2.5 Aug. 1-6

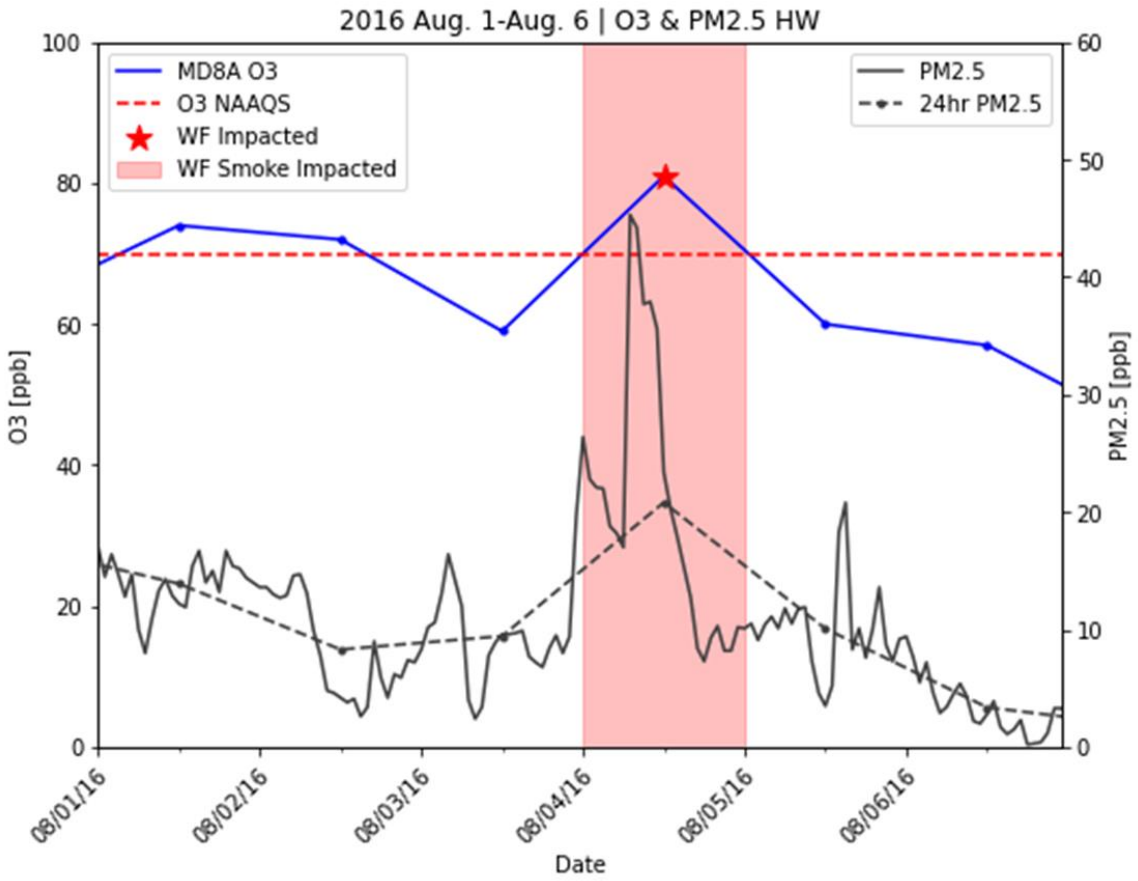

Figure 24. Observed concentrations at the HW monitor of MD8A O3 concentrations **(blue solid line)**, PM2.5 (**black solid line**), 24hr averaged PM2.5 (**dashed black line**). The 2015 MD8A O3 NAAQS is overlaid (**red dashed line**) and the red shaded area represents the event period. Red star marks the MD8A O3 value impacted by wildfire smoke.

Figure 25 - BV: MD8A and PM2.5 Aug. 1-6

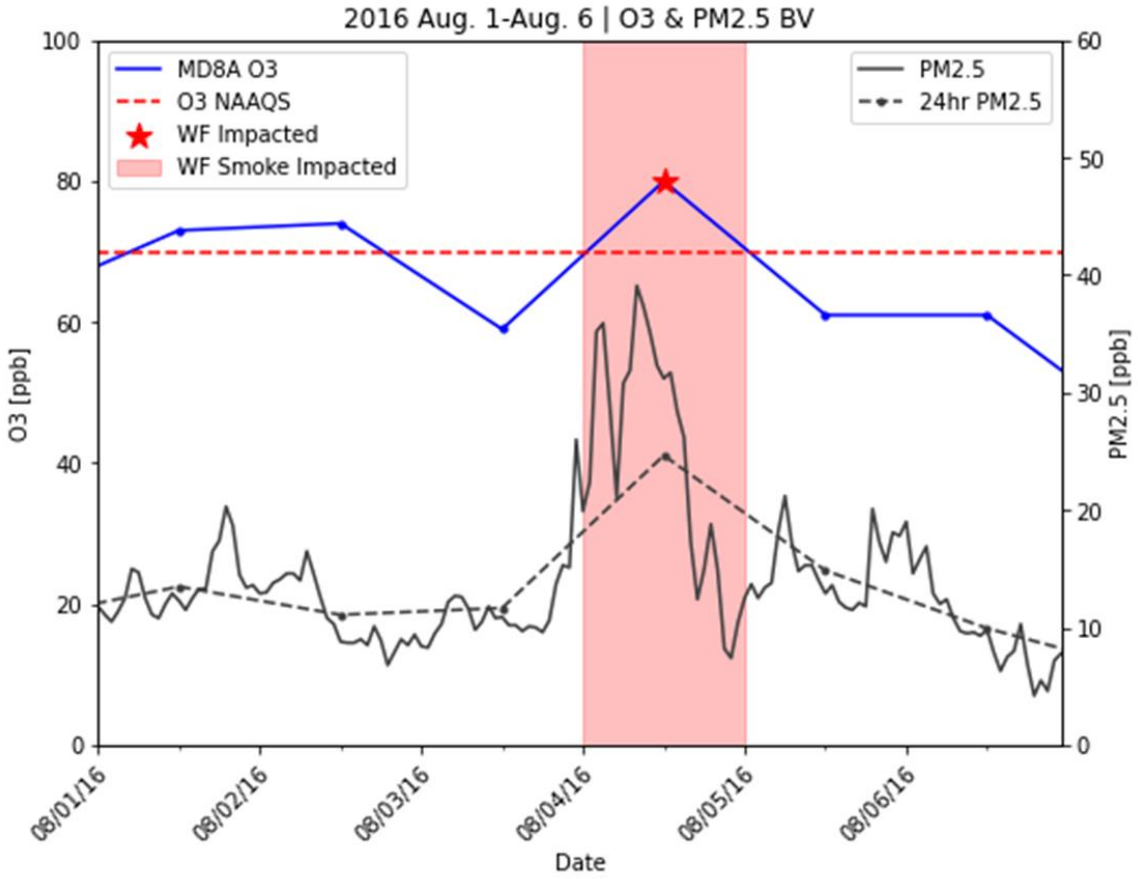

Figure 25. Observed concentrations at the BV monitor of MD8A O3 concentrations **(blue solid line)**, PM2.5 (**black solid line**), 24hr averaged PM2.5 (**dashed black line**). The 2015 MD8A O3 NAAQS is overlaid (**red dashed line**) and the red shaded area represents the event period. Red star marks the MD8A O3 value impacted by wildfire smoke.

Figure 26 - H3: MD8A and PM2.5 Aug. 1-6

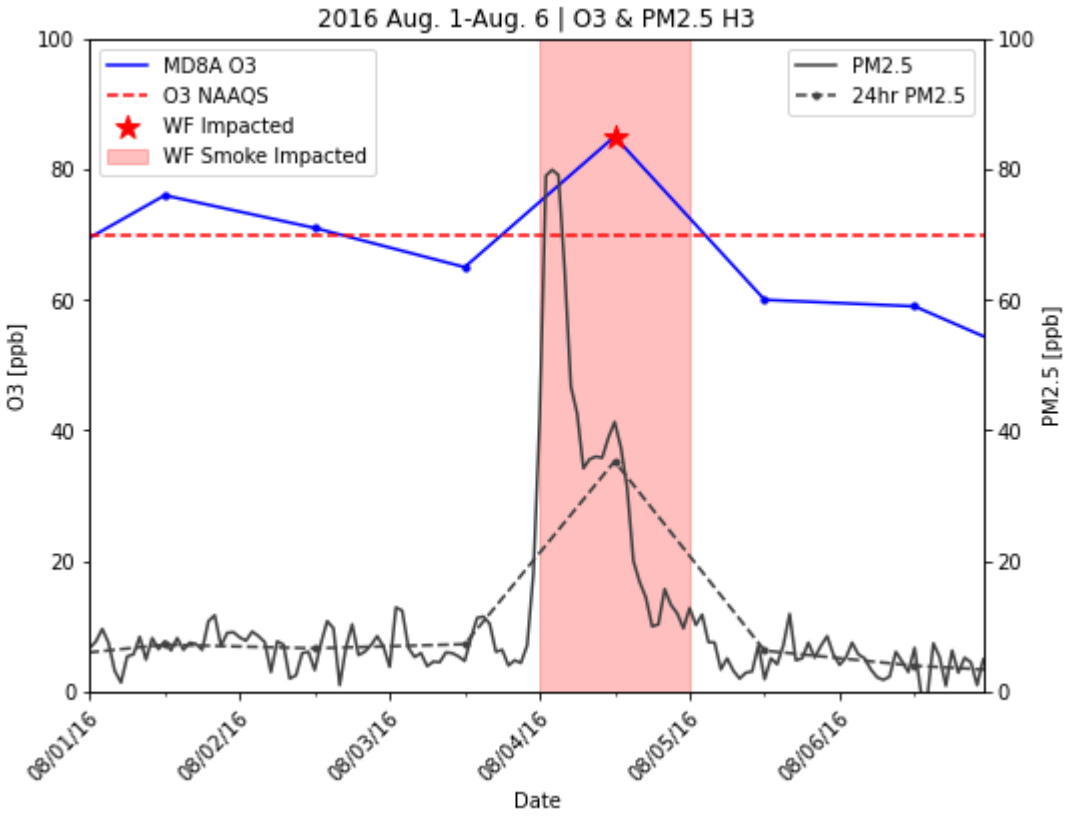

Figure 26. Observed concentrations at the H3 monitor of MD8A O3 concentrations **(blue solid line)**, PM2.5 (**black solid line**), 24hr averaged PM2.5 (**dashed black line**). The 2015 MD8A O3 NAAQS is overlaid (**red dashed line**) and the red shaded area represents the event period. Red star marks the MD8A O3 value impacted by wildfire smoke.

In **Figures 24-26**, it is evident that lower O3 and PM2.5 concentrations frame the period before and after August 4, 2016. In particular, PM2.5 levels reached a local minimum at sites on August 3, 2016, coinciding with the cold frontal passage and subsequent enhanced emission ventilation. The cold front initially helped mix out other emissions that had been residing across the region in the days prior to August 4 due to stagnant upper level conditions. This process was most evident at the HW and BV monitors, where hourly PM2.5 concentrations were slightly higher on August 1 and 2 before decreasing on August 3 with the short-wave trough and attendant dry cold frontal passage late morning and early afternoon (**Figure 24 and 26**). However, at 21-00Z August 3, 2016 as the cold front progressed SE and the upper level ridge built in over the Wasatch PM2.5 levels increased and became elevated (**Figure 27**). During the period 21-00Z smoke plumes from the northern Utah and central Idaho fires were transported into the state as the mean winds shifted N-NW from the surface to 700 mb. This shift in the mean steering flow and subsequent transport of smoke to the Wasatch Front corresponds temporally to the observed surface PM2.5 concentrations (**Figure 27**). **Table 5** shows the observed 24-hour average PM2.5 concentrations August 1-6 at the HW monitor compared to the PM2.5 monthly statistics for the site. The observed PM2.5 concentrations on August 4 were nearly equal to the 95th percentile, indicating the influx of wildfire smoke emissions was of considerable magnitude.

Table 5 - PM2.5 Statistics Aug.2-6

Date	24hr PM2.5	Monthly Avg. PM2.5	μ+1σ	95th percentile PM2.5
08-02-16	8.2	9.3	15.1	21.05
08-03-16	9.4	9.3	15.1	21.05
08-04-16	**20.8**	**9.3**	**15.1**	**21.05**
08-05-16	10	9.3	15.1	21.05
08-06-16	3.3	9.3	15.1	21.05

Table 5. Observed PM2.5 and PM2.5 statistics at the HW monitor site. The statistics are based on PM2.5 observations for the period 2014-2020.

Figure 27 - Winds and PM2.5 Aug. 3-4

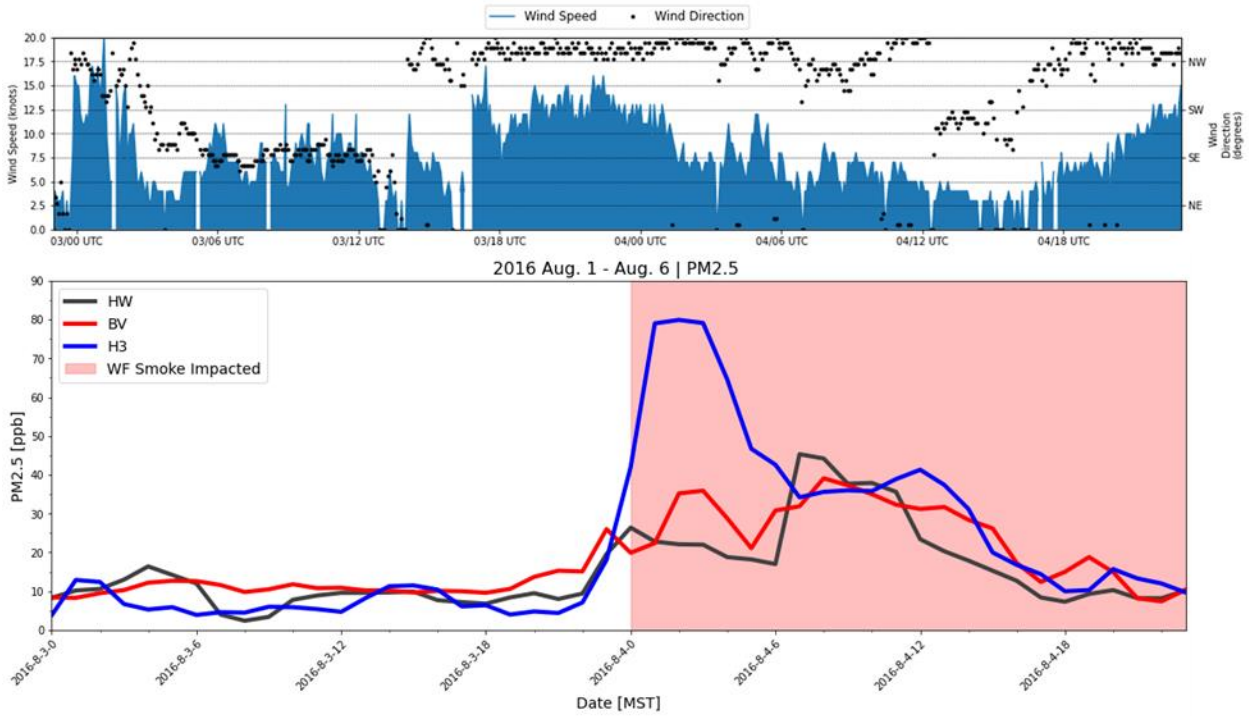

Figure 25. Top: KSLC surface wind observations August 3 00Z - 00Z August 5; **Bottom:** Time series of observed PM2.5 concentrations at HW, BV, and H3 between August 3 00Z - 00Z August 5. The increase in PM2.5 concentrations at the three sites corresponds to the surface to 700mb winds shifting N-NW between August 3 18Z and 00Z August 4.

Other than the strong relationship between PM2.5 and O3, the relationship between temperature and O3 or lack thereof can help distinguish the impact of wildfire smoke. The observed temperatures leading up to August 4 were > 5 degrees F above average (**Figure 28**). However, marginal cold air advection behind the cold front decreased temperatures on August 4 to slightly below to near normal across the

region and 7-10 degrees cooler than before the cold frontal passage (**Table 4** and **Figure 28**). A closer examination of the O3 concentration trends in **Figures 24-26** and observed high temperatures in **Table 4** reveals that the MD8A values at all three monitors were lower on the days prior to August 4 but had higher temperatures. This means O3 concentrations were less likely to be influenced by high temperatures on August 4 and more likely to be influenced by the influx of wildfire smoke as similarly noted in the study Lindaas et al. (2017).

Figure 28 - KSLC Observed 2m Temp

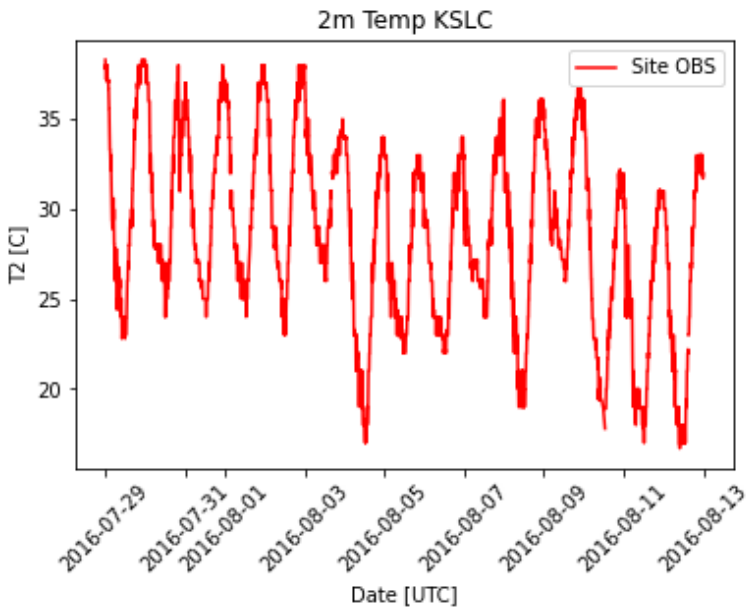

Figure 27. Time series of observed 2m temperature (degrees C) at KSLC between July 29 - August 14, 2016. Dip in temperature noted between August 3-4 with the cold frontal passage.

HYSPLIT 48hr backward trajectories ending at August 4 18Z for 100m, 100m, and 5000m levels over the UDAQ HW monitor were computed utilizing the High Resolution Rapid Refresh version 1 (HRRRv1) 3km model for the time period August 2 18Z-August 4 18Z (**Figure 29 and 30**). The meteorological and wildfire conditions analysis indicates that a large portion of the wildfire smoke emissions that were transported across the Wasatch Front on August 4 was composed of near-surface smoke. This was due to the fact that wildfire smoke was transported behind a surface cold frontal passage, and both synoptic and mesoscale forcing mechanisms contributed to the transport smoke near the surface. Therefore, in our HYSPLIT analysis we chose the 100m and 100m trajectory levels to represent air parcels sourced near the surface within the PBL, while the 5000m trajectory level was chosen to represent air parcels above the PBL and transported within the free atmosphere.

The backward HYSPLIT trajectories make it evident that the source areas for air parcels vary depending on the vertical level within the atmosphere. In **Figure 30**, the air residing at 100m at HW on August 4 18Z is shown to have originated from the Box Elder Co, UT fire complex (8/04/2016 at 0900Z) and south-central Idaho (8/03/2016 at 12Z) where a complex of wildfires is also noted. Investigation of the mid-level wind field (700 mb) and 100m trajectory shows that northerly winds were responsible for the transport of wildfire smoke from Box Elder and Idaho wildfires to HW (**Figure 31**). At the more elevated

level of 5000m, air parcels are shown to be sourced from north-central California. This source region also had ongoing active wildfires with large smoke plumes as exhibited in **Figures 15 and 16**, which points to the potential for elevated layers of smoke to be transported over the northern Wasatch Front from these areas.

Figure 29 - HYSPLIT 48hr Backward Trajectories Aug. 4 18Z - Aug. 2 18Z – West CONUS

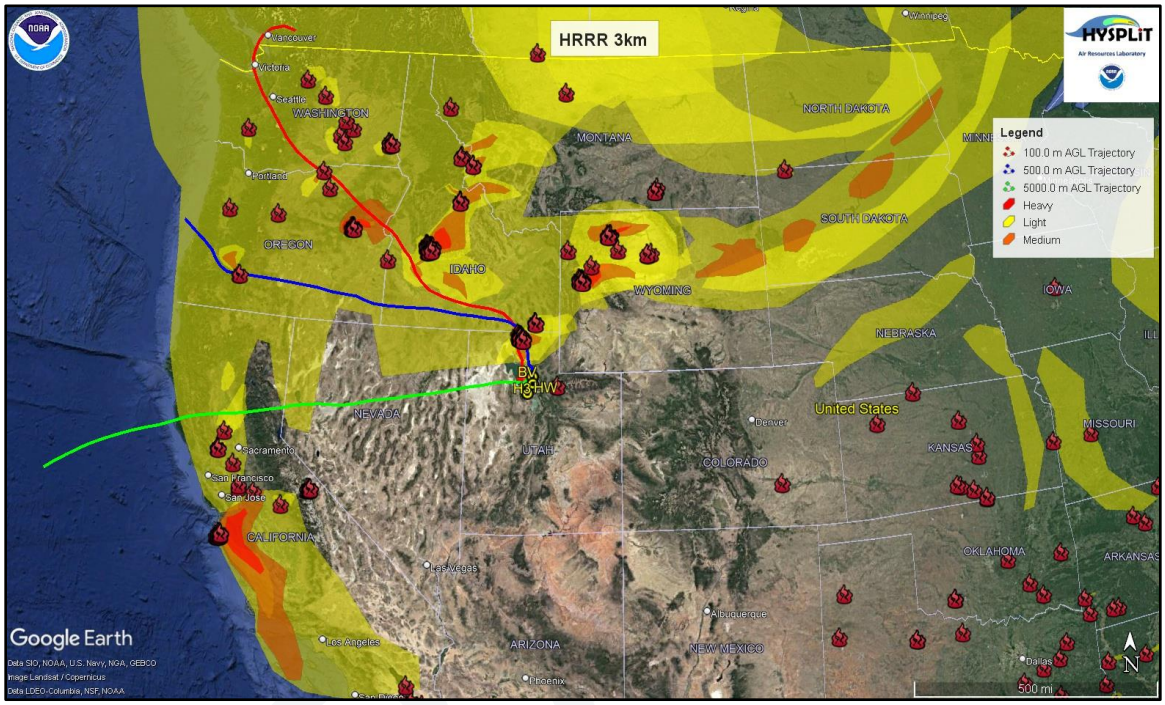

Figure 29. HYSPLIT 48hr backward trajectories starting at August 4 18Z and ending at August 2 18Z with endpoints at 100 m, 500m, and 5000 m AGL over the HW monitor. VIIRS/MODIS active fire detections and thermal anomalies (**red flames**).

Figure 30 - HYSPLIT 48hr Backward Trajectories Aug. 4 18Z - Aug. 2 18Z - Utah

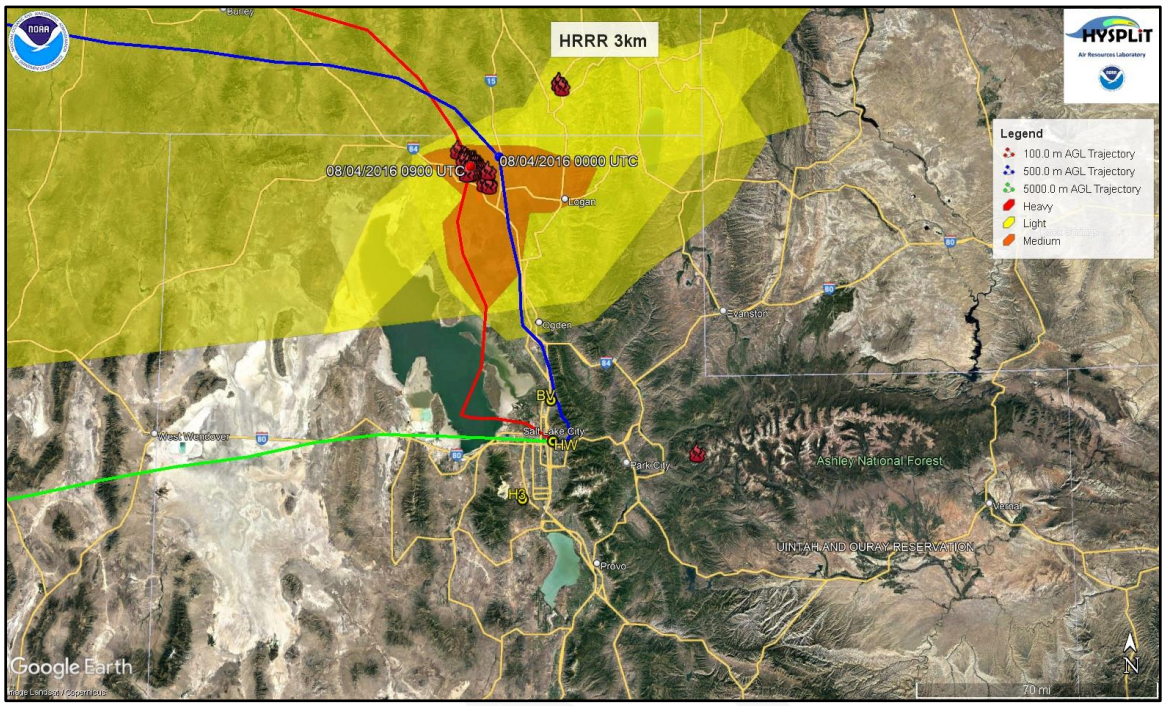

Figure 30. Same as **Figure 29** but zoomed over the Wasatch Front nonattainment area. HYSPLIT 48hr backward trajectories starting at August 4 18Z and ending at August 2 18Z with endpoints at 100 m, 500m, and 5000 m AGL over the HW monitor. VIIRS/MODIS active fire detections and thermal anomalies (**red flames**).

Figure 31 - HRRRv1 Analysis and 100m HYSPLIT Backward Trajectory

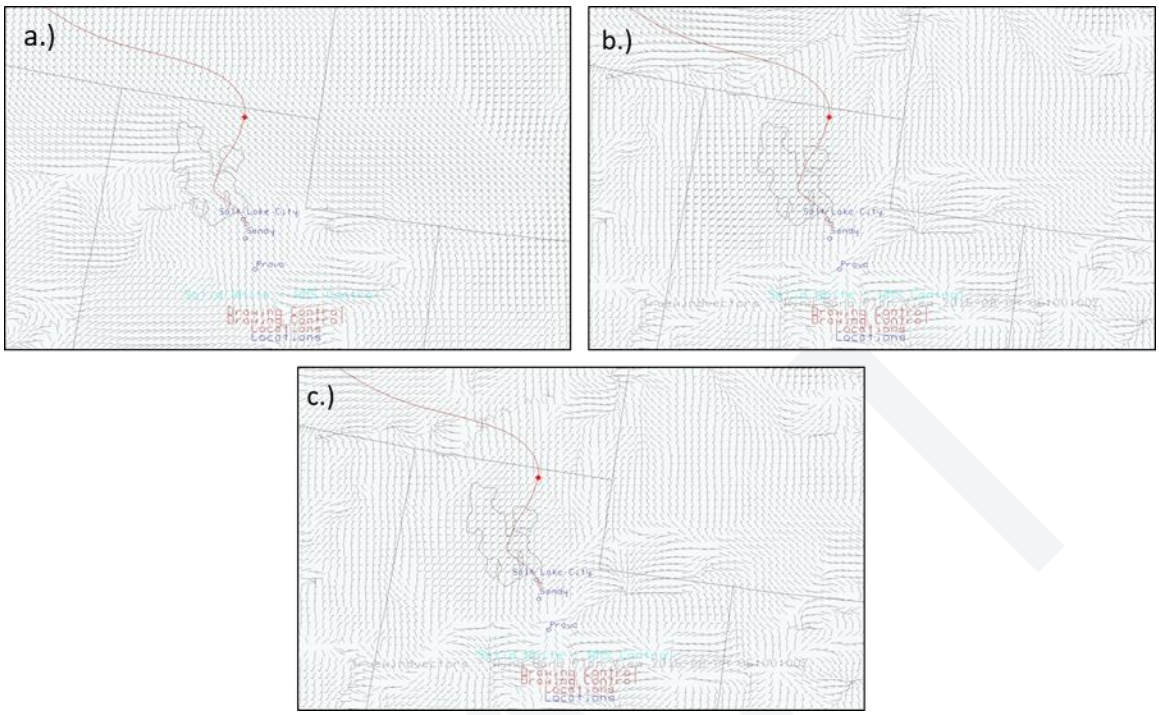

Figure 31. HRRRv1 analysis for 06Z on August 4 **a.)** 700mb, **b.)** 850mb, and **c.)** 1000mb wind vectors, with HYSPLIT 48hr backward trajectory for 100m at the HW monitor overlaid (**red solid line**). Winds from the surface to 700mb are shown as N-NW, transporting wildfire smoke emissions from Box Elder County fire (**red diamond**).

3.2 September 2, 2017 Flagged Event

3.2.1 Meteorological Conditions

To understand the relevant meteorological conditions, we start by investigating the progression of the weather pattern beginning on August 30, 2017 and ending on September 2, 2017. This allows the development of a clear meteorological framework to build our analysis. On August 30, a 500 mb ridge was centered across the Four Corners region as an upper level shortwave trough began to progress into the PNW (**Figure 32a**). Winds at 500 mb were SW across Utah as shown in **Figure 32a**. The trough translated east over the course of August 30 and 31, increasing SW winds from the surface up to the upper levels (**Figure 32b**). By 00Z September 1, the trough had grazed across Utah and moved east across the continental divide, with a weak attendant cold front and marginal moisture passing over the Wasatch Front (**Figure 32c**). Winds from the surface to upper levels veered from SW on August 31 to N-NW between 12Z September 1 and 00Z September 2 in response to the upper level pattern shift. Enough moisture was available as the disturbance moved over the Wasatch Front to produce a few scattered light showers across the region, however, conditions remained largely dry with increased cloud cover being the main impact. After the trough passage early September 1, an upper level ridge began to build in across the western CONUS and firmly established itself by 00Z September 2 (**Figure 32d**). The development of the upper level ridge overhead created a weaker and more stagnated wind field across Utah as synoptically quiescent conditions formed.

Figure 32 - 500 mb Heights and Winds Aug. 30 - Sept. 2

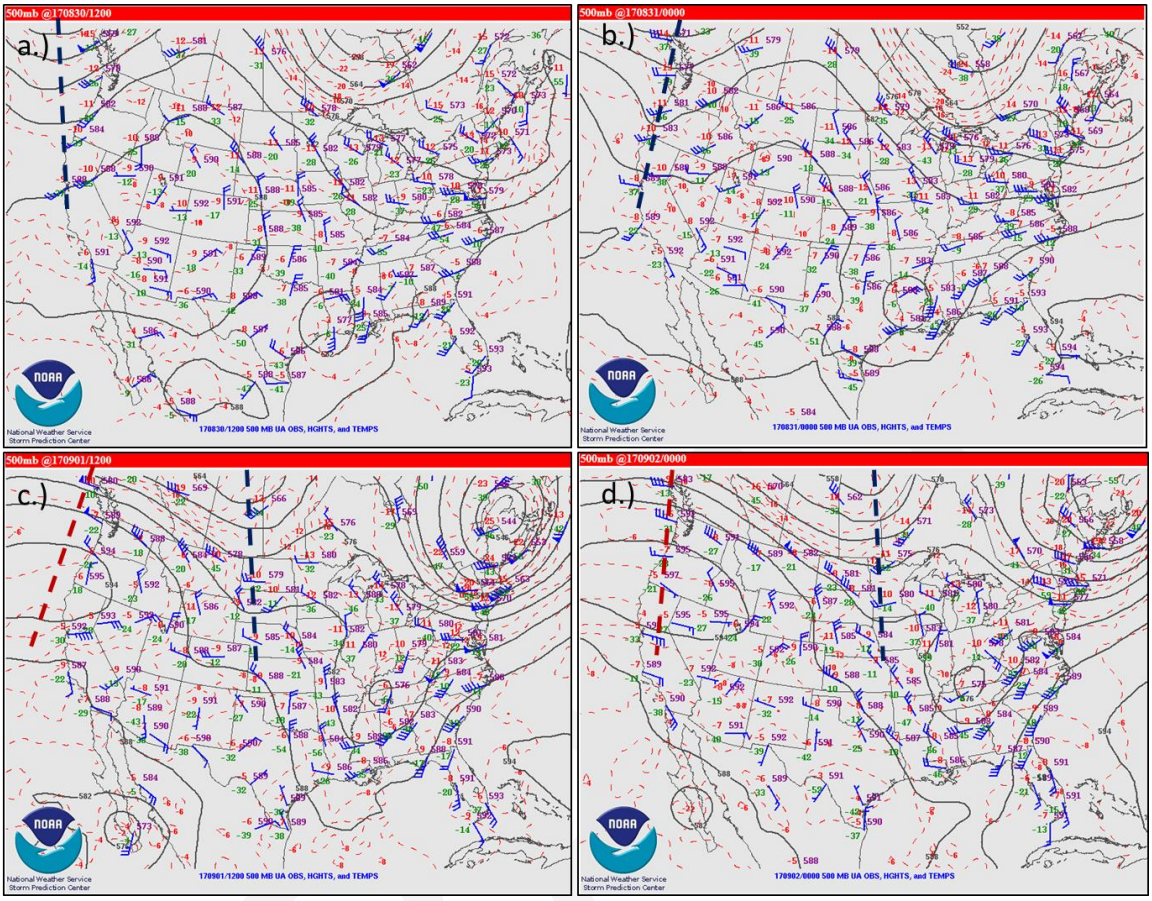

Figure 32. Upper air 500 mb heights and wind observations/analysis for **a.)** 2017-08-30 12Z, **b.)** 2017-08-31 00Z, **c.)** 2017-09-01 12Z, and **d.)** 2017-09-02 00Z. The blue dashed line represents the 500 mb trough axis and red dashed line represents the 500 mb ridge axis.
(Source: https://www.spc.noaa.gov/obswx/maps/)

Although not explicitly described, the conditions on August 29 were even more influenced by the Four Corners upper level ridge than August 30, with surface high temperatures 10-15 degrees above normal on that day as seen in **Table 6**. Temperature trends show a mild temperature swing between August 30 and August 31, with 5-10 degree above normal temperatures on August 30 before a brief cool down on August 31 associated with the cool frontal passage and increased cloud cover (**Table 6**). As the upper level ridge built in on September 1, a warming trend is evident with temperatures moderating 5-10 degrees above average by September 2.

The progression of the meteorological pattern, as described above, becomes increasingly important when discussing the link between wildfire smoke impacts and ozone in the following sections. By providing a short historical context of the weather conditions preceding September 2, we are able to provide a basis for how wildfire smoke was transported and impacted ozone across the Wasatch Front.

Table 6 - Observed and Climate Normals Aug. 29 - Sept. 4

Date	Observed Low (F)	Observed High (F)	Normal Low (F)	Normal High (F)	Observed Precipitation (inches)	Normal Precipitation (inches)
8/29/2017	71	99	60	87	0	0.03
8/30/2017	73	94	60	87	0	0.03
8/31/2017	71	87	59	86	0	0.03
9/1/2017	66	92	59	86	0	0.03
9/2/2017	**64**	**94**	**59**	**85**	**0**	**0.03**
9/3/2017	68	98	58	85	0	0.03
9/4/2017	67	98	58	85	0	0.03

Table 6. Observed and average high/low temperature and precipitation accumulations for KSLC from 8/29/2017 - 9/12/2017. The event date 9/2/2017 is bolded.
(Source: NWS SLC https://www.weather.gov/slc/CliPlot)

On September 2, 2017, 500 mb composite mean and composite anomalies (**Figure 33**) indicate a strong dome of high pressure was situated across the western U.S, with synoptically benign and quiescent conditions across Utah. **Figure 34** shows that the 500 mb ridge axis extended roughly on a SW to NE axis through the Great Basin region, with clockwise flow circulating around the central 594 dm height. The location of the ridge axis and 500mb high circulation contributed to weak and ambiguous flow at the surface and mid to upper levels across much of Utah (**Figure 35 and Figure 36**). However, **Figure 36** reveals that at 500 mb NW winds downstream of the ridge axis managed to infiltrate across the northern tier of state. These NW winds are shown to extend as far south as the Wasatch Front (**Figure 35 and Figure 36**). Below 500 mb, **Figure 37 and 38** reveal how the wind field varied from the mid to lower levels (700 mb-surface) on the morning of September 2 (1500Z) and the afternoon (2100Z), respectively. The wind does exhibit noteworthy variability and stratification through the vertical column 700 mb-surface, which corresponds to the relatively weak synoptic forcing under the strong upper level ridge. In **Figure 37 and 38**, 850 mb-surface winds contain an easterly component across the Wasatch, particularly corresponding to the locations of westerly oriented drainages and canyons. At 700 mb-surface, a nose of S-SE winds extends north from SE Utah to the central Wasatch, while 700 mb winds with an E-NE component dominate most other areas of northern Utah (**Figure 37 and 38**). Above 700 mb, winds back to W-NW up to 500 mb as noted in **Figure 36**.

Figure 33 - NCEP Reanalysis 500 mb Height Composites Sept.1-3

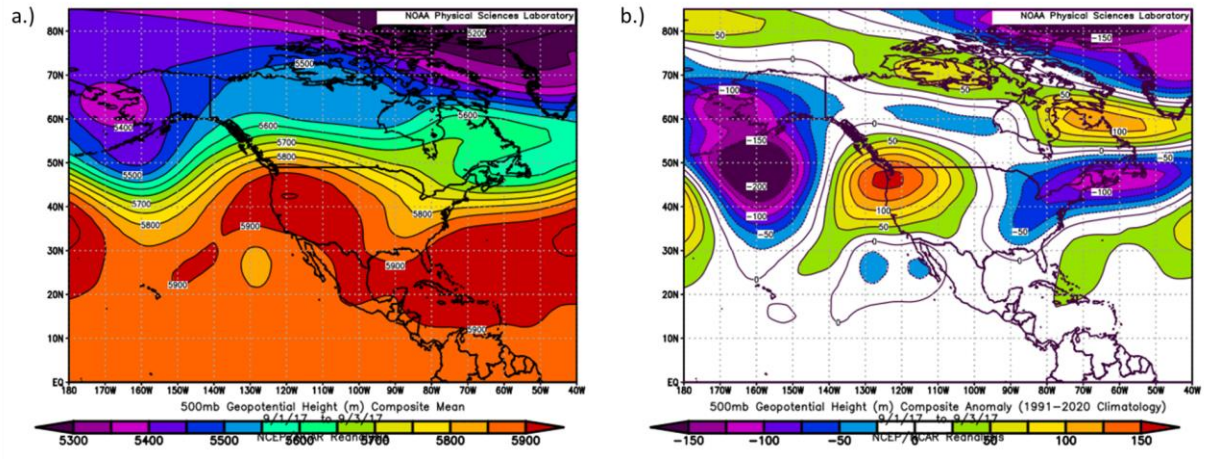

Figure 33. NCEP Reanalysis 500 mb geopotential height **a.)** composite mean and **b.)** composite anomalies for the period September 1-3. (Source: https://psl.noaa.gov/data/composites/day/)

Figure 34 - GFS 0.25 Analyzed 500 mb Winds and Heights Sept. 2 18Z

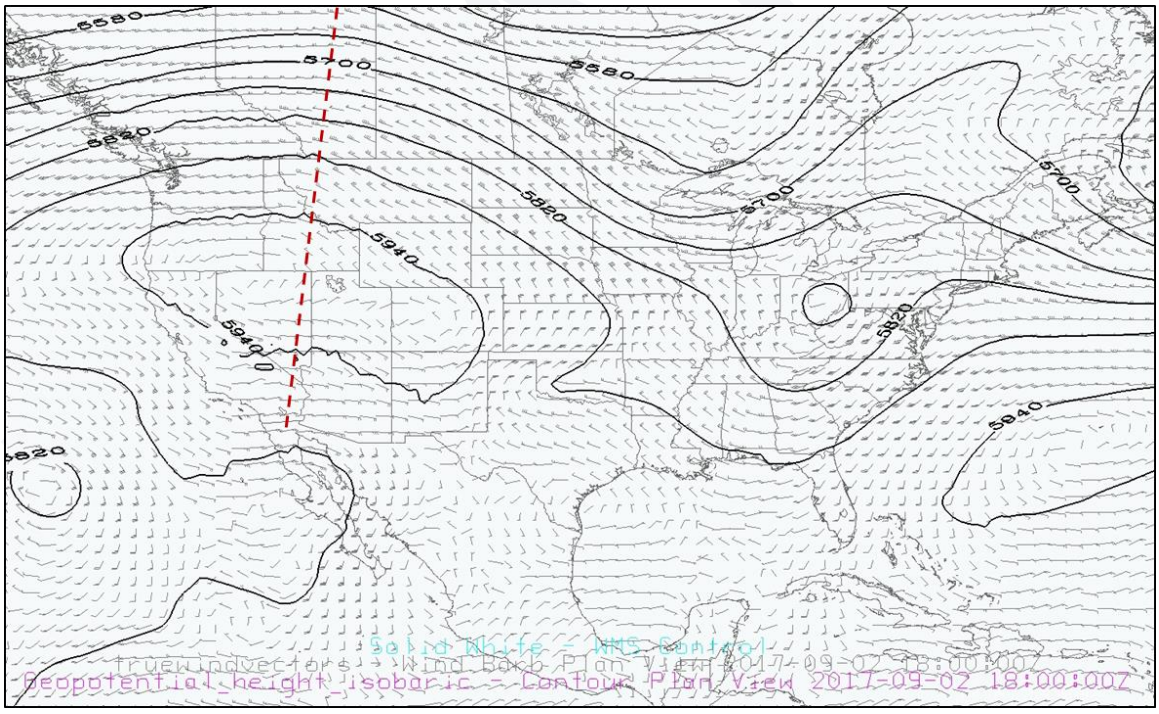

Figure 34. GFS 0.25 degree 500 mb wind and geopotential height analysis valid for 2017-09-02 1800Z with 500 mb ridge axis analyzed (red dashed line).

Figure 35 - GFS 0.25 degree 500 mb Wind Analysis Sept. 3 00Z

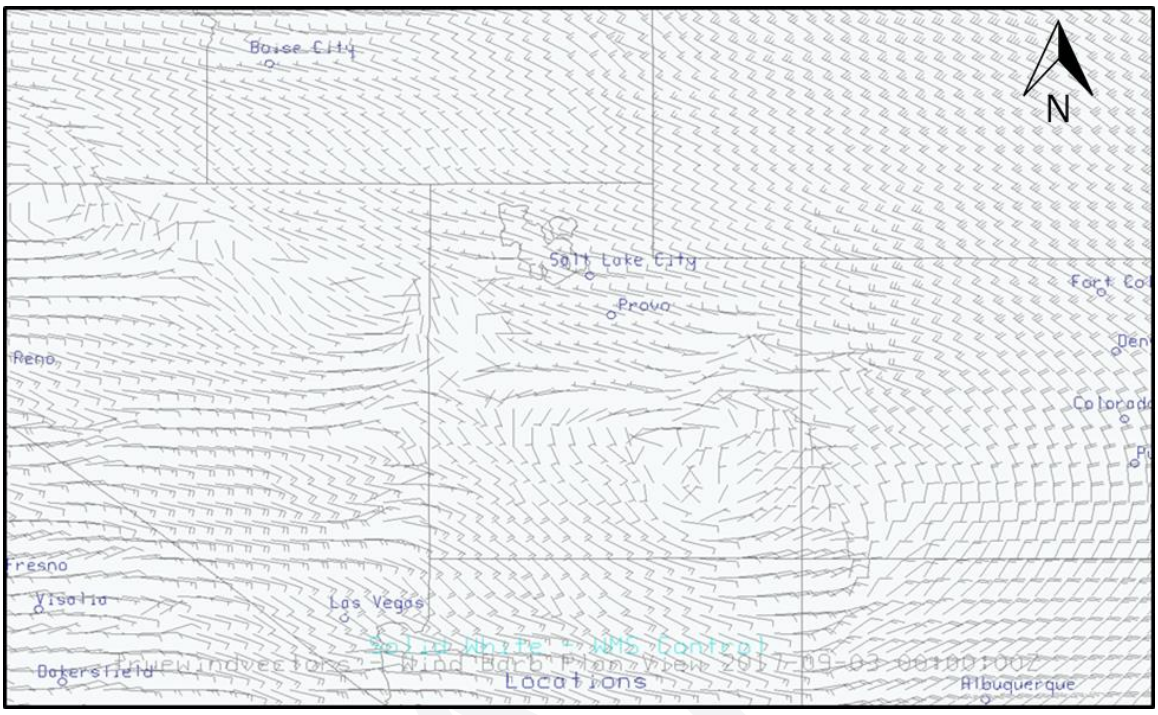

Figure 35. GFS 0.25 degree 500 mb wind analysis 2017-09-03 00Z

Figure 36 - HRRRv1 500 mb Wind Analysis Sept. 2

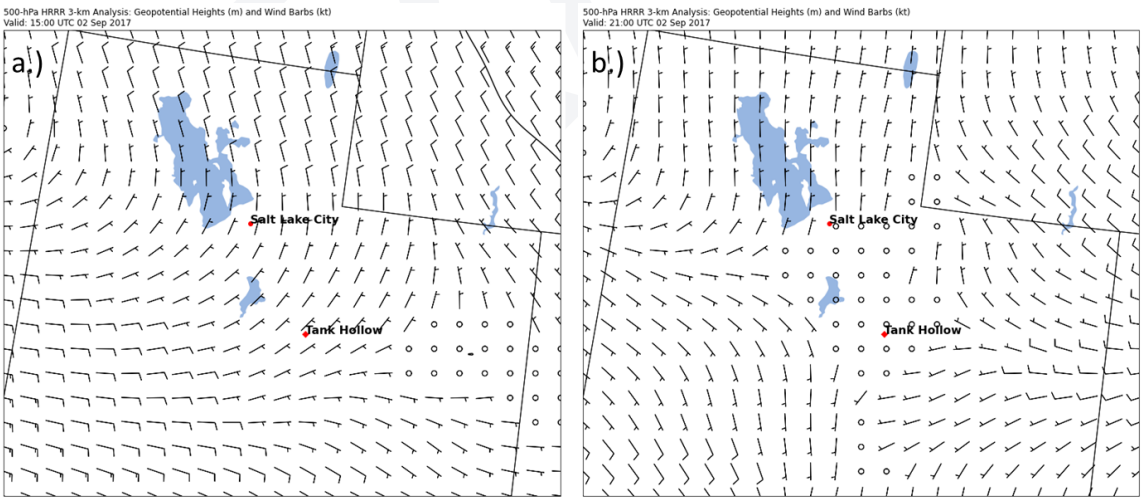

Figure 36. HRRRv1 500 mb wind barb and height analysis for 2017-09-02 **a.)** 1500Z and **b.)** 2100Z.

Figure 37 - HRRRv1 700, 850, 925, and Surface Wind Analysis Sept. 2 15Z

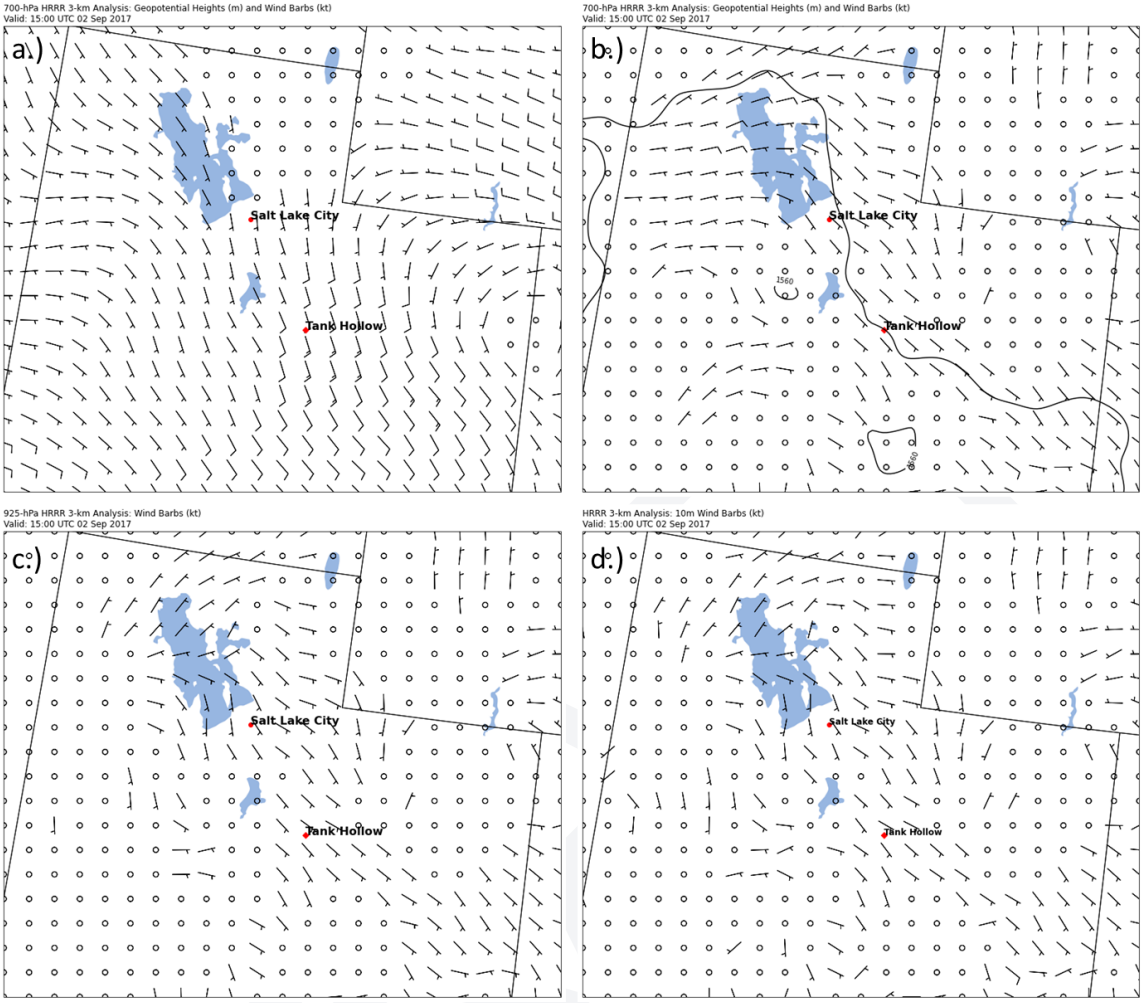

Figure 37. HRRRv1 wind barbs and heights (700 mb and 850mb) valid for 2017-09-02 1500Z at **a.)** 700 mb, **b.)** 850 mb, **c.)** 925 mb, and **d.)** surface (10m).

Figure 38 - HRRRv1 700, 850, 925, and Surface Wind Analysis Sept 2. 21Z

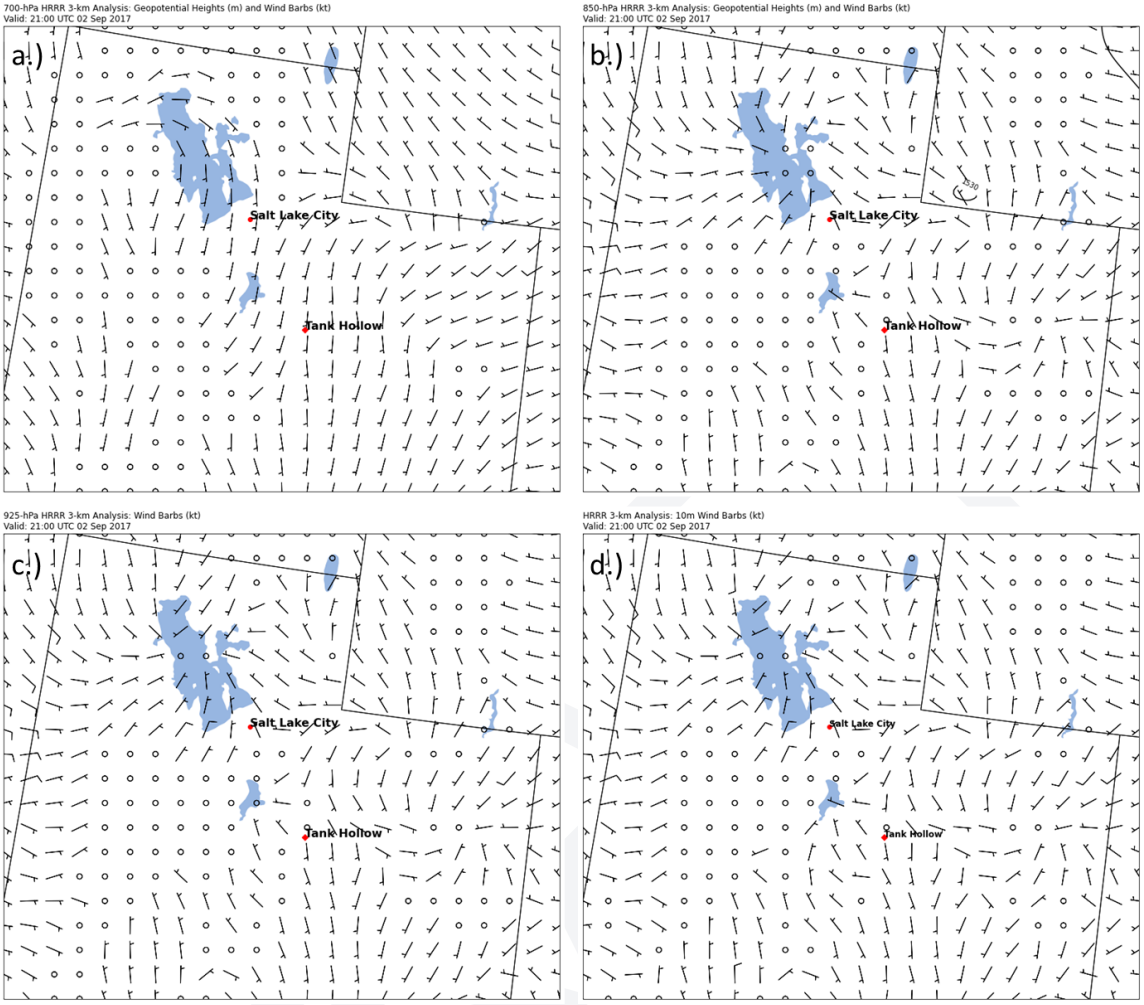

Figure 38. HRRRv1 wind barbs and heights (700 mb and 850mb) valid for 2017-09-02 2100Z at **a.)** 700 mb, **b.)** 850 mb, **c.)** 925 mb, and **d.)** surface (10m).

In addition to the relatively stagnant conditions with weak forcing, the synoptically benign pattern facilitated the formation of diurnal canyon, valley winds, and lake breeze on September 2. An overview of surface conditions across northern Utah on the morning of September 2 (1500Z) are shown in **Figures 39-41**. Upon closer inspection, diurnal canyon flows and down valley winds were present on the morning of September 2 (**Figure 41**). As seen in **Figure 41**, easterly down-canyon winds are evident out of Spanish Fork Canyon, American Fork Canyon, Millcreek Canyon, and Parleys Canyon in addition to down valley southerly winds in Utah County and Salt Lake Country. In order to see the shift in valley and canyon flows through the course of the day, surface conditions are given for the afternoon of September 2 (2100Z) in **Figures 42 and 43**. Surface analysis on the afternoon of September 2 shows that the valley and canyon winds transitioned to their daytime regime, with the N-NW lake-valley breeze in the Salt Lake Valley, Tooele Valley, Davis Co/Bountiful and up-canyon winds evident in Parleys and Provo canyons (**Figures 42 and 43**). The full temporal progression of observed nighttime S-SE valley winds to afternoon N-NW lake breeze within the Salt Lake Valley is exhibited in **Figure 44**.

Figure 39 - Surface Analysis Sept. 9 12Z

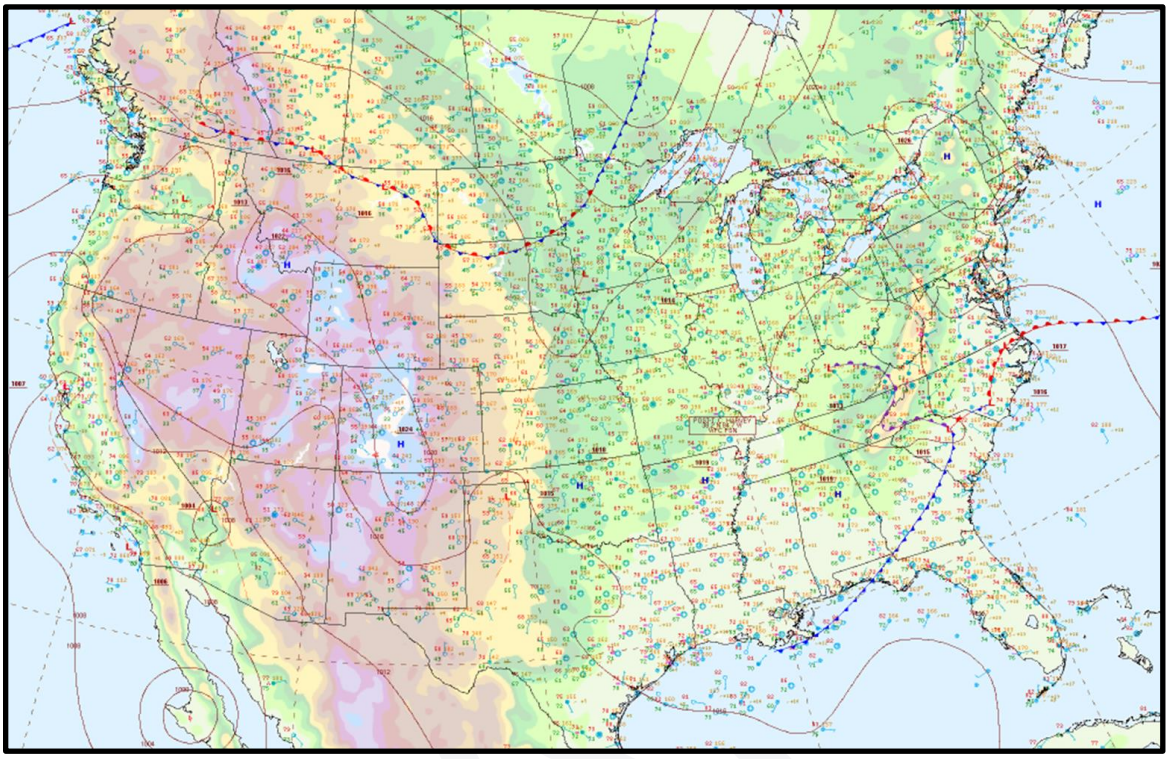

Figure 39. Weather Prediction Center (WPC) surface analysis 2017-09-02 1200Z.
(Source: https://www.wpc.ncep.noaa.gov/html/sfc-zoom.php)

Figure 40 - Surface Met Observations Sept. 2 15Z - Utah Valley

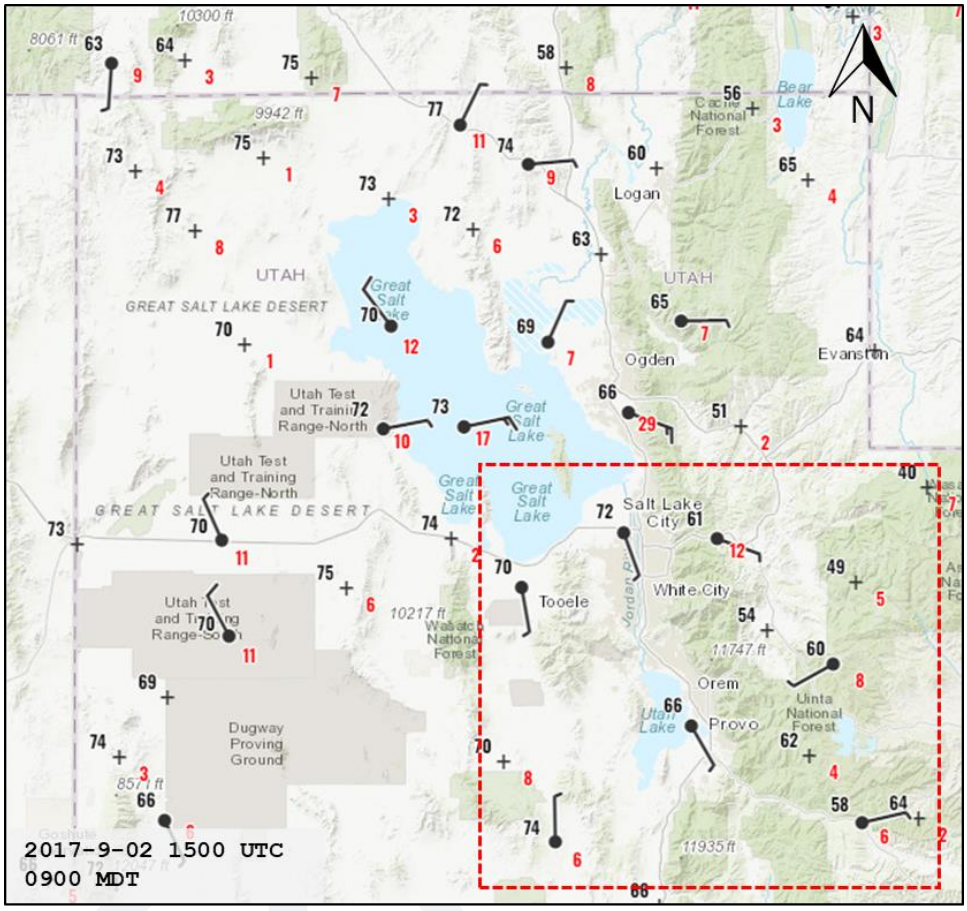

Figure 40. Surface temperature and wind observations across Utah on 2017-09-02 at 15Z. Red box identifies the zoomed in area in **Figure 39**. (Source: https://www.wrh.noaa.gov/map/)

Figure 41 - Surface Met Observations Sept. 2 - Valley Breeze

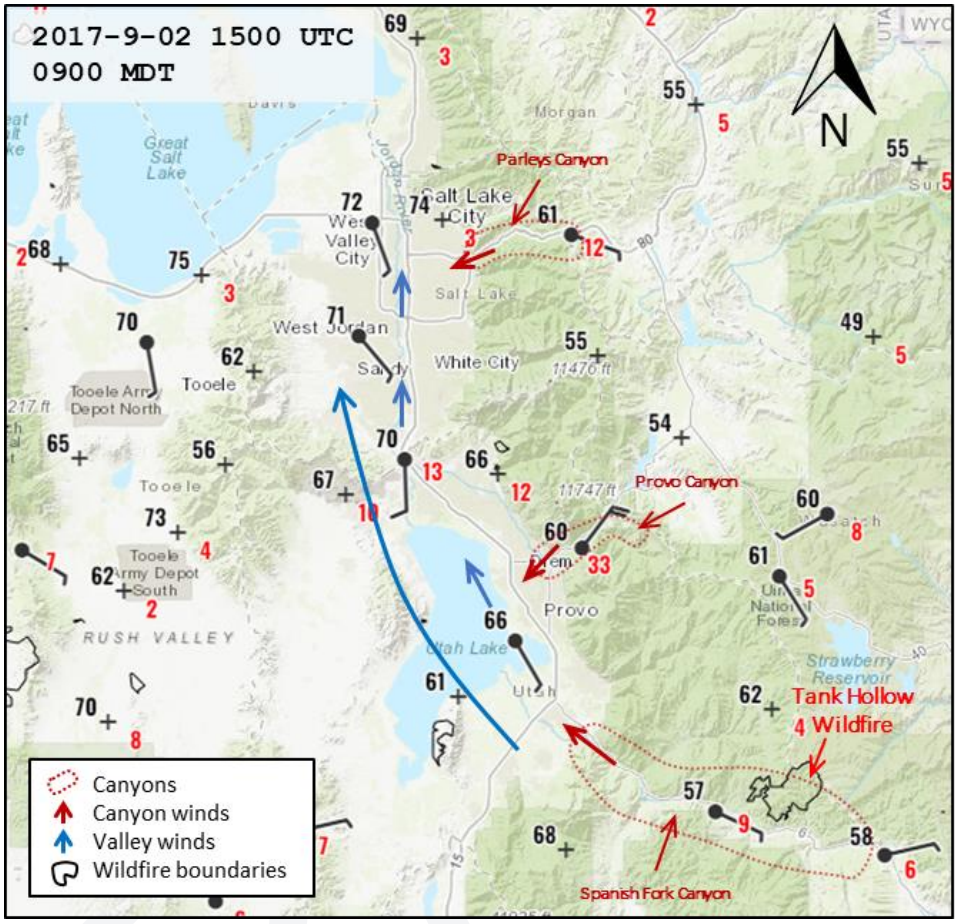

Figure 41. Surface temperature and wind observations along the southern Wasatch Front on 2017-09-02 at 15Z. Major canyons are highlighted (red-dotted lines), with nighttime/morning down-valley S-SE winds (blue arrows) and down-canyon easterly winds (red arrows) identified from observations.
(Source: https://www.wrh.noaa.gov/map/)

Figure 42 - Surface Met Observations Sept. 2 - SL Valley

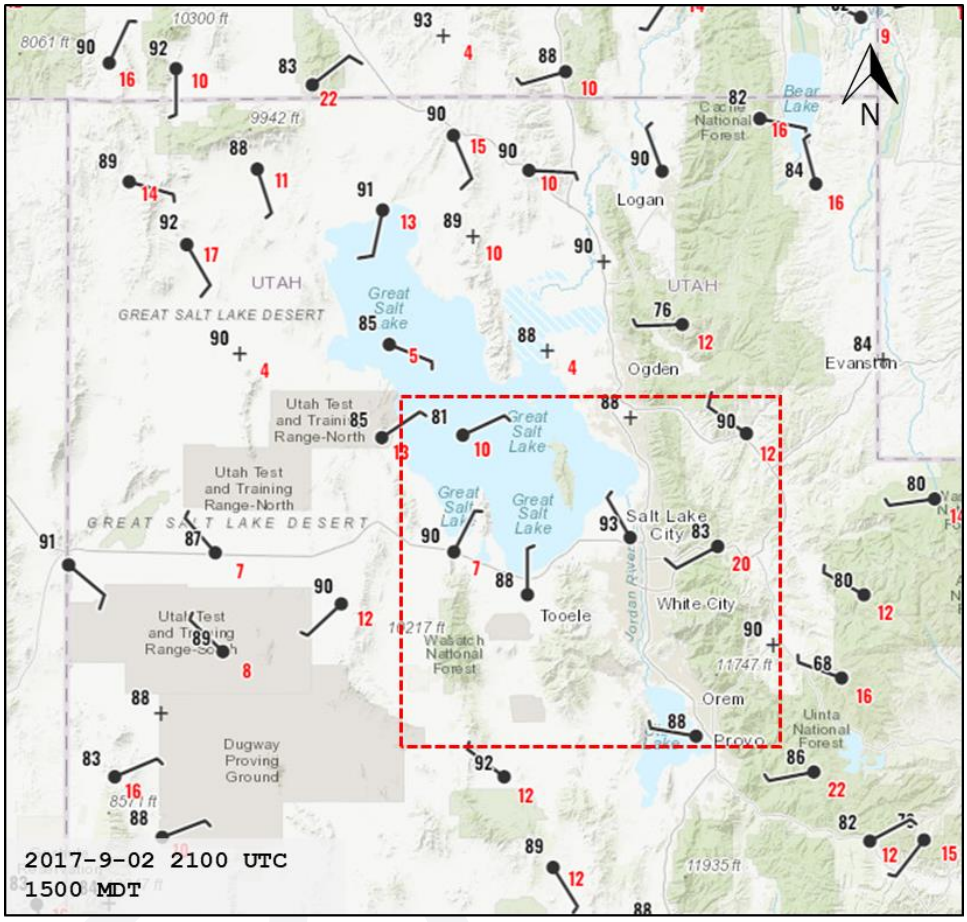

Figure 42. Surface temperature and wind observations across Utah on 2017-09-02 at 15Z. Red box identifies the zoomed in area in **Figure 39**. (Source: https://www.wrh.noaa.gov/map/)

Figure 43 - Surface Met Observations and Lake Breeze Sept. 2

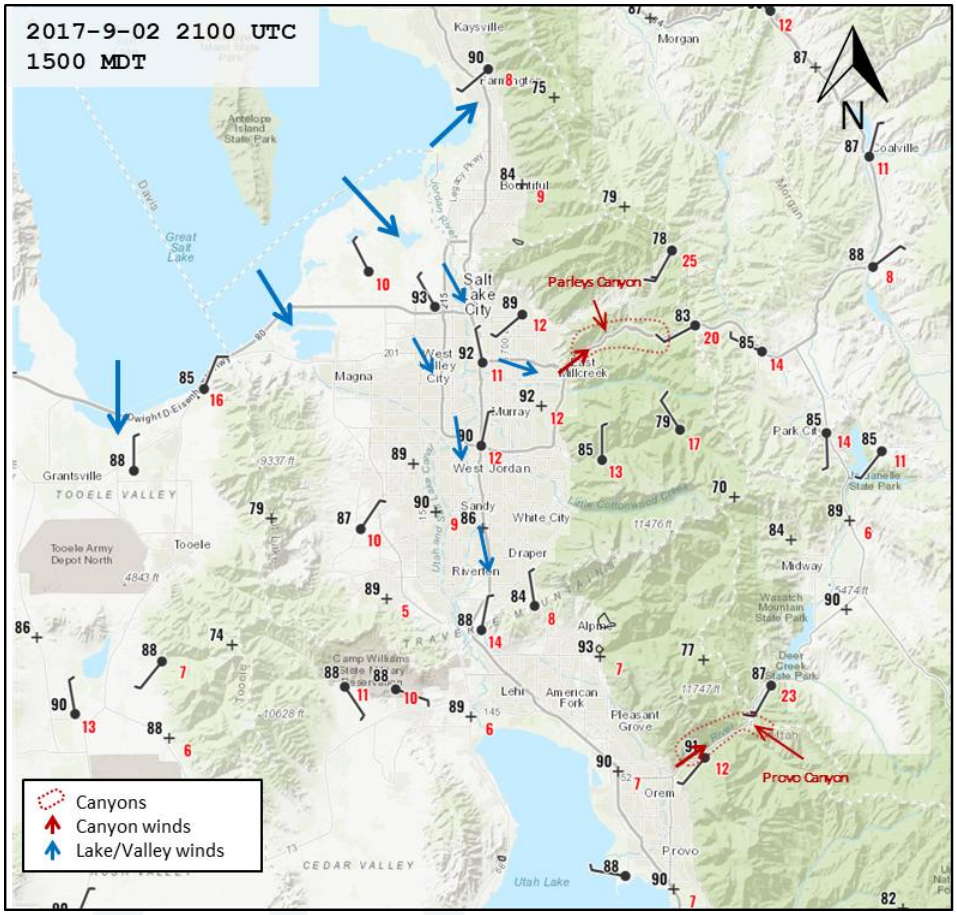

Figure 43. Surface temperature and wind observations along the southern Wasatch Front on 2017-09-02 at 15Z. Major canyons are marked (red-dotted lines), with nighttime/morning up-valley N-NW winds (blue arrows) and up-canyon westerly winds (red arrows) highlighted from observations.
(Source: https://www.wrh.noaa.gov/map/)

Figure 44 - KSLC Surface Met Observations Aug. 30 - Sept. 3

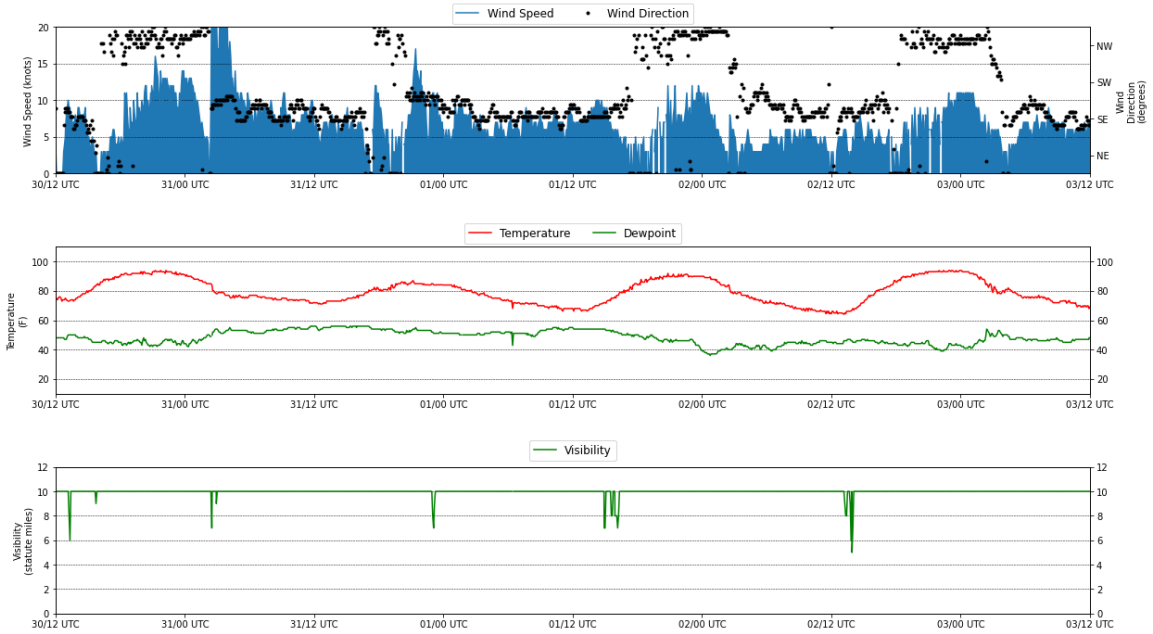

Figure 44. Surface wind observations at KSLC for the period September 2 00Z - September 3 00Z. Winds are S-SE between September 2 03Z - 17Z and N-NW 18Z - 00Z, marking the nighttime valley winds and daytime lake breeze, respectively.

Temperatures were above normal on September 2 and conditions were dry (**Table 5 and Figure 52**). Afternoon (00Z) KSLC radiosonde observations reveal subsidence associated with the upper level ridge as well as a deep dry adiabatic layer from the surface to 600 mb, corresponding to the PBL mixed layer (**Figure 43**). The descending air associated with subsidence is evident by the dry adiabatic temperature profile between 400-600 mb. Within this layer, air is sinking and warming down to the capping inversion which marks the top of the PBL and entertainment zone 580-600 mb. The vertical wind profile at 00Z September shows the depth of the N-NW lake breeze from the surface to about 790 mb, with E-SE flow above this level to 600 mb and N-NW flow at 500 mb.

Figure 45 - KSLC Radiosonde Skew-T's Sept. 2-3

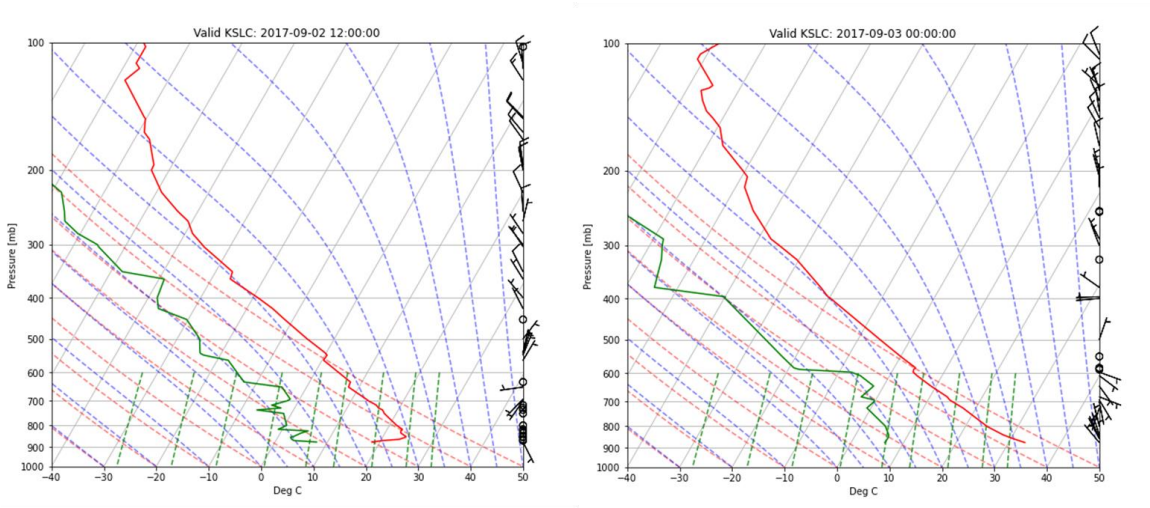

Figure 45. Radiosonde observations from KSLC on 2017-09-02 at 12Z (**left**) and 2017-09-03 at 00Z (**right**), with dew point (**green solid line**), temperature (**red solid line**), and wind barbs (**right vertical axis**) plotted to 100 mb. (Source: Integrated Global Radiosonde Archive (IGRA) - https://www.ncei.noaa.gov/access/metadata/landing-page/bin/iso?id=gov.noaa.ncdc:C00975)

3.2.2 Wildfire Conditions

In order to gain better context on the spatial and temporal variability of wildfire smoke coverage on September 2, we investigate the progression of wildfire smoke transport across the Wasatch Front beginning on August 30 and ending on the day of the event September 2. Multiple wildfires were ongoing in California, Oregon, Washington, Idaho, Montana, and Utah on August 30 through September 1, spreading smoke plumes vast distances (**Figure 46**). HRRR Smoke analyzed/forecasted smoke fields and visible satellite imagery with GFS 0.25 degree analyzed 500 mb heights and wind barbs at 18Z on August 30 and 31 and September 1 and 2 are used to reveal two important elements related to the transport of wildfire smoke into the Wasatch Front during this period. These elements include 1.) the trend in the synoptic weather pattern across the western U.S, and 2.) the subsequent trend in wildfire smoke transport.

Figure 46 - MODIS Terra/Aqua True Color Image Sept. 2

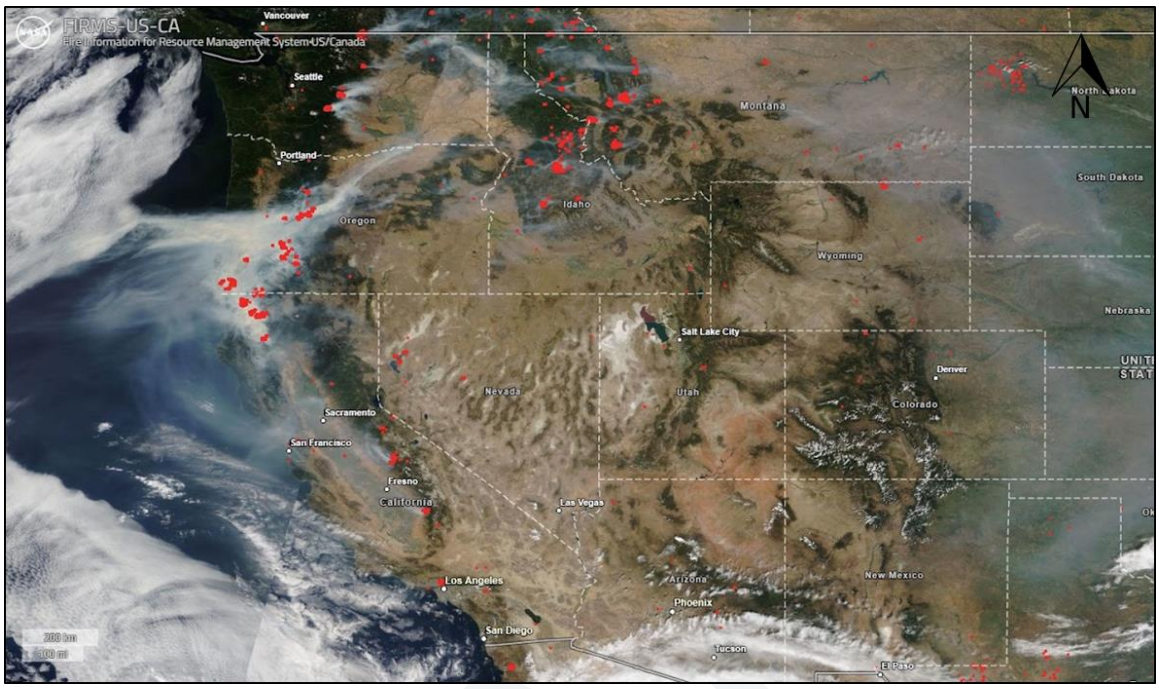

Figure 46. MODIS Terra/Aqua True Color image on September 2, 2017. Red markers indicate VIIRS/MODIS active fire detections and thermal anomalies (hot spot detection).
(Source: https://firms.modaps.eosdis.nasa.gov/usfs/map/).

As shown in **Figure 47 and 48** and described in the previous section, a weak disturbance moved over the Wasatch Front August 30-31, producing some clouds and shifting winds from the SW to NW. On August 30, GOES visible satellite imagery and HRRR Smoke shows moderate to heavy areas of smoke over eastern Washington, western Idaho, and northwestern NV, which correspond to the anticyclonic side of the main shortwave trough axis. No areas of smoke were analyzed over northern Utah, on the cyclonic side of the trough axis, by HRRR Smoke or are noted by GOES visible satellite imagery on August 30 (**Figure 47 and 48**). The disturbance translated eastward and dug south on August 31, with satellite imagery revealing a swath of diffuse wildfire smoke across southern Idaho and northern Nevada trailing the trough axis of the main disturbance. This smoke is evidenced by the subtle milky/opaque color in the visible satellite imagery in **Figure 47 and 48** and as the light to moderate analyzed smoke in the vertically integrated and near-surface smoke HRRR Smoke fields in **Figure 49 and 50**. As the disturbance progressed east out of the Wasatch Front and the upper level ridge built in, winds shifted N-NW allowing wildfire smoke from fires across Idaho, Washington, northern California, and Oregon to be transported east and south into Utah by September 1 (**Figure 48-50**). A broad region of diffuse wildfire smoke is present in the visible satellite imagery across the Wasatch Front beginning on September 1 and continuing into September 2 (**Figure 48**), indicating the transport of wildfire smoke over the region and smoke inundation under the upper level ridge. The presence of surface and elevated smoke across the Wasatch Front on September 1-2 is further verified by HRRR Smoke analyzed light to moderately dense vertically integrated and near-surface smoke over the area (**Figure 49 and 50**).

Figure 47 - GOES East True Color Image Aug. 30 - Sept. 2 - West CONUS

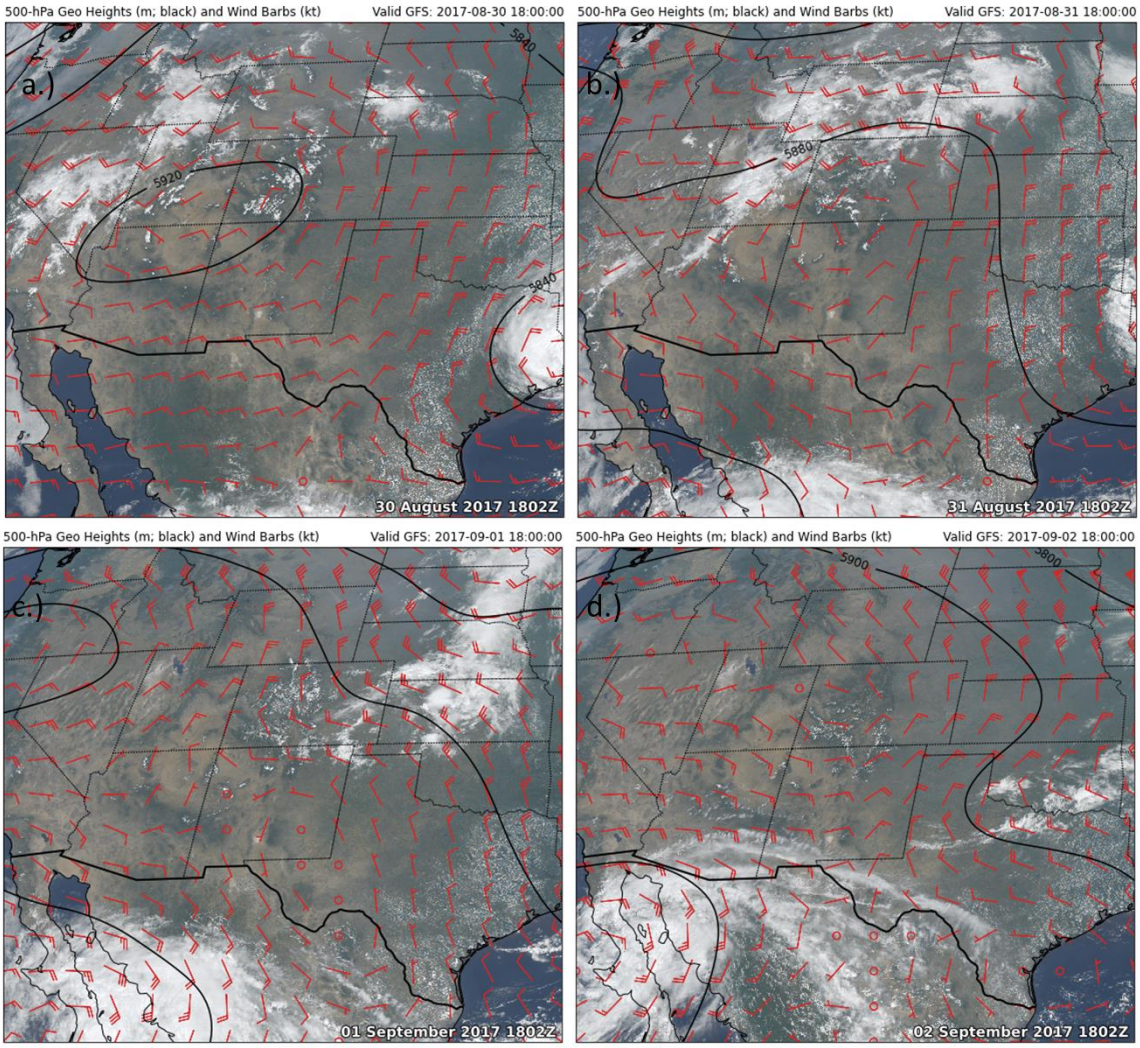

Figure 47. GOES East True Color imagery focused over the Intermountain West with GFS0p5 degree analyzed 500 mb geopotential heights and winds for **a.)** 2017-08-30 18Z, **b.)** 2017-08-31 18Z, **c.)** 2017-09-01 18Z, and **d.)** 2017-09-02 18Z.

Figure 48 - GOES East True Color Image Aug. 30 - Sept. 2 - Utah

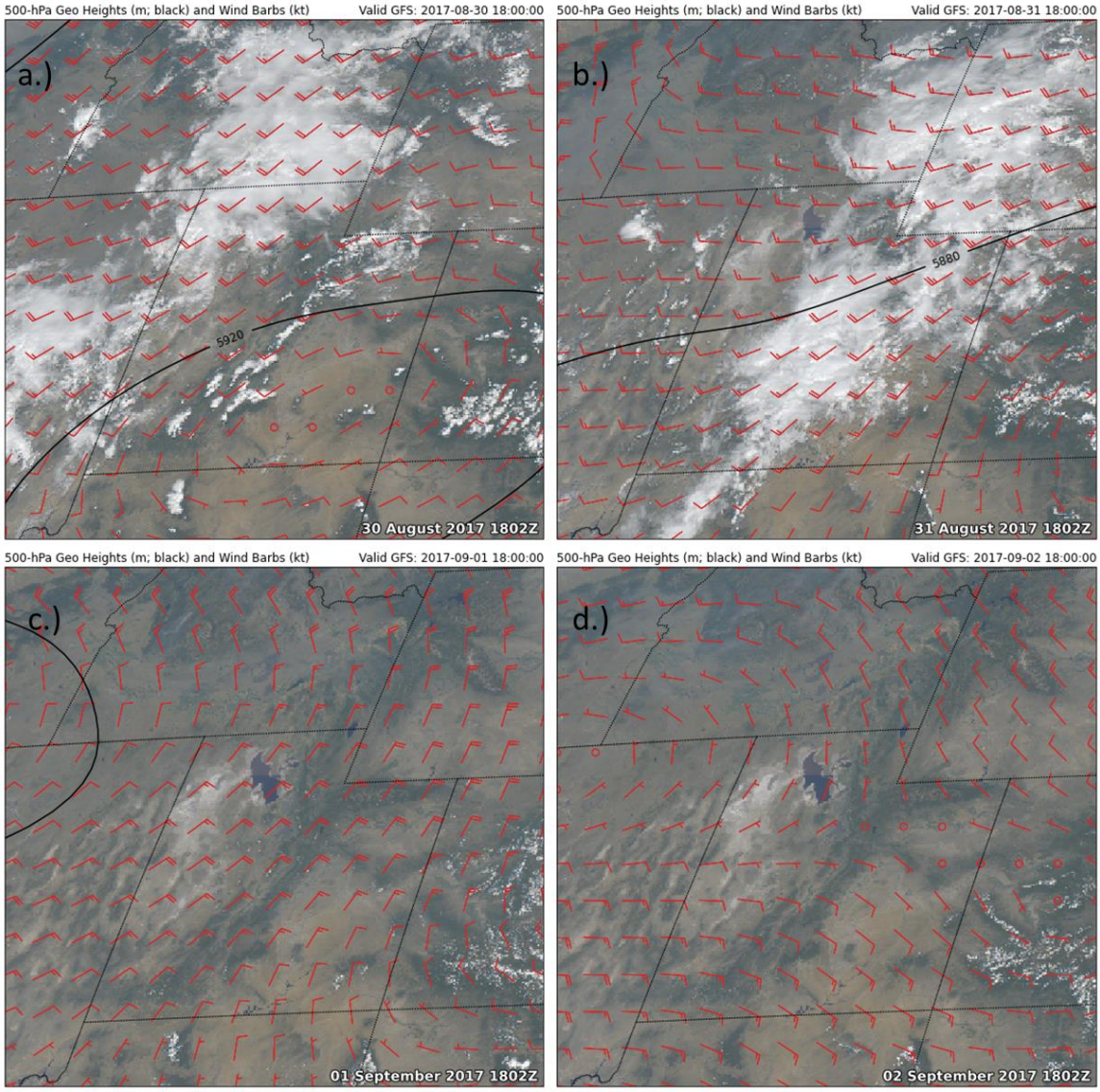

Figure 48 GOES East True Color imagery focused over Utah with GFS0p5 degree analyzed 500 mb geopotential heights and winds for **a.)** 2017-08-30 18Z, **b.)** 2017-08-31 18Z, **c.)** 2017-09-01 18Z, and **d.)** 2017-09-02 18Z.

Figure 49 - HRRR Smoke Vertically Integrated Smoke Aug. 30 - Sept. 2

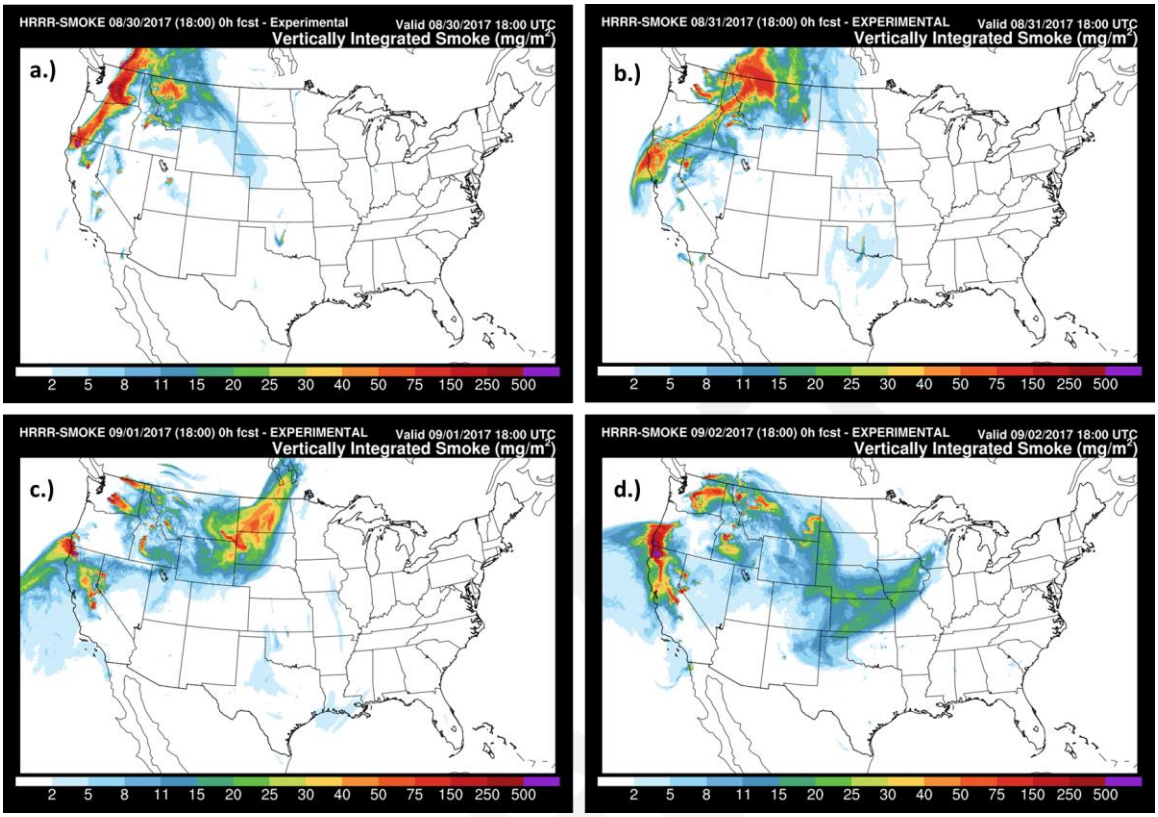

Figure 49. HRRR SMOKE analyzed vertically integrated smoke (mg/m²) on **a.)** 2017-08-30 18Z, **b.)** 2017-08-31 18Z, **c.)** 2017-09-01 18Z, and **d.)** 2017-09-02 18Z.

Figure 50 - HRRR Smoke Near-Surface Smoke Aug. 30 - Sept. 2

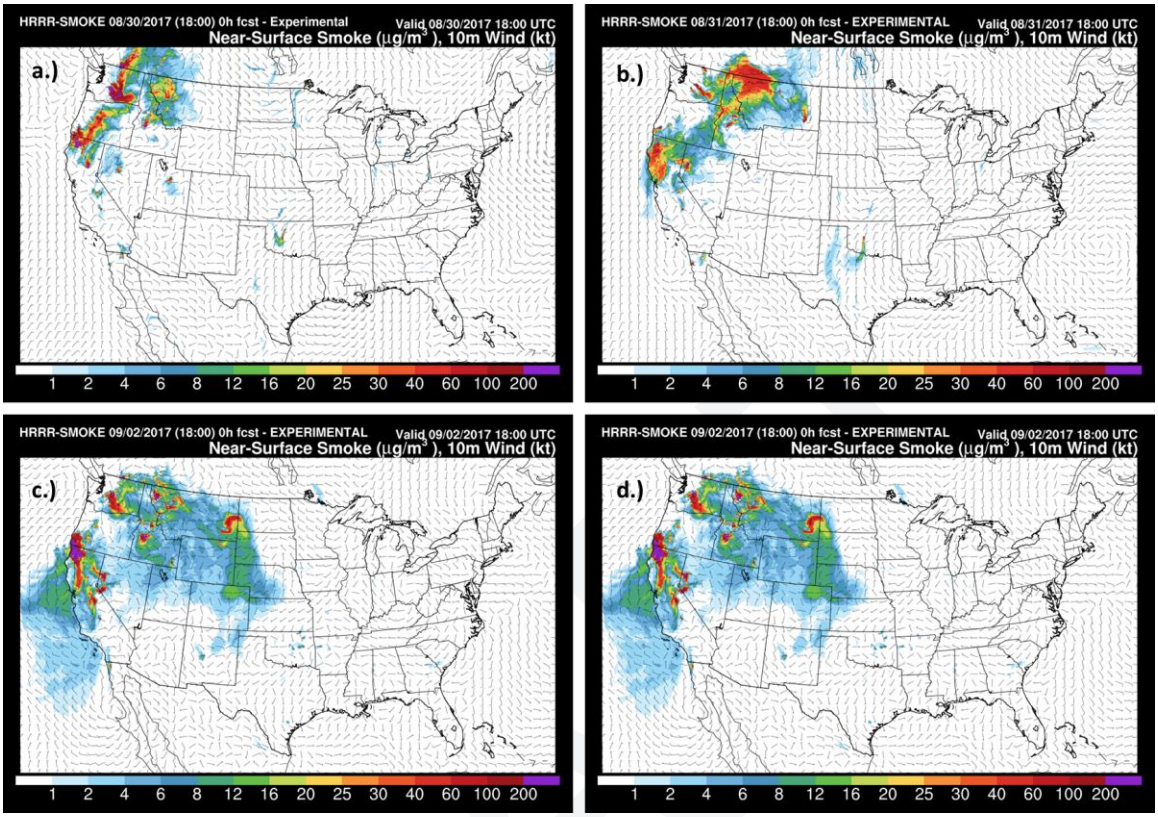

Figure 50. HRRR SMOKE analyzed near-surface smoke ($\mu g/m^3$) and surface winds on **a.)** 2017-08-30 18Z, **b.)** 2017-08-31 18Z, **c.)** 2017-09-01 18Z, and **d.)** 2017-09-02 18Z.

On September 2, 2017. GOES-16 visible satellite imagery and VIIRS/MODIS thermal hot spot detection shows the location of active wildfires and wildfire smoke coverage (**Figure 46**). As seen in **Figure 46**, a large number of these wildfires were located in Idaho, Oregon, Washington, Wyoming, Montana, and California. Inspection of the 500 mb wind field and the spatial variability of wildfire smoke coverage indicates that the wildfire smoke was generally transported by the clockwise swirling 500 mb wind field associated with the dome of high pressure across the western U.S (**Figure 34 and Figure 46**). Satellite visible imagery also displays the accumulation of wildfire smoke under the upper level ridge as air parcels under and around the ridge had a difficult time escaping. The light milky color in the GOES visible satellite imagery across Utah and much of the intermountain west signifies the presence of diffuse wildfire smoke. The progression of wildfire smoke transport across the Wasatch Front is further illustrated by snapshots of the Salt Lake Valley from August 28 - September 2 (**Figure 51**). On August 28, visibility was at its best, indicating the air was the cleanest with the least amount of wildfire smoke emissions present (**Figure 51**). Inspection of the images from August 29-31 reveals varying degrees of visibility, with features and key landmarks being only very slightly obscured at times. By September 1, visibility decreased significantly with landmarks and features totally or largely obscured due to the wildfire smoke. Visibility was at its relative lowest (< 5 statute miles at KSLC) miles the afternoon of September 2 when the greatest amount of wildfire smoke was observed.

Figure 51 - Camera Images Salt Lake Valley Aug. 28 - Sept. 2

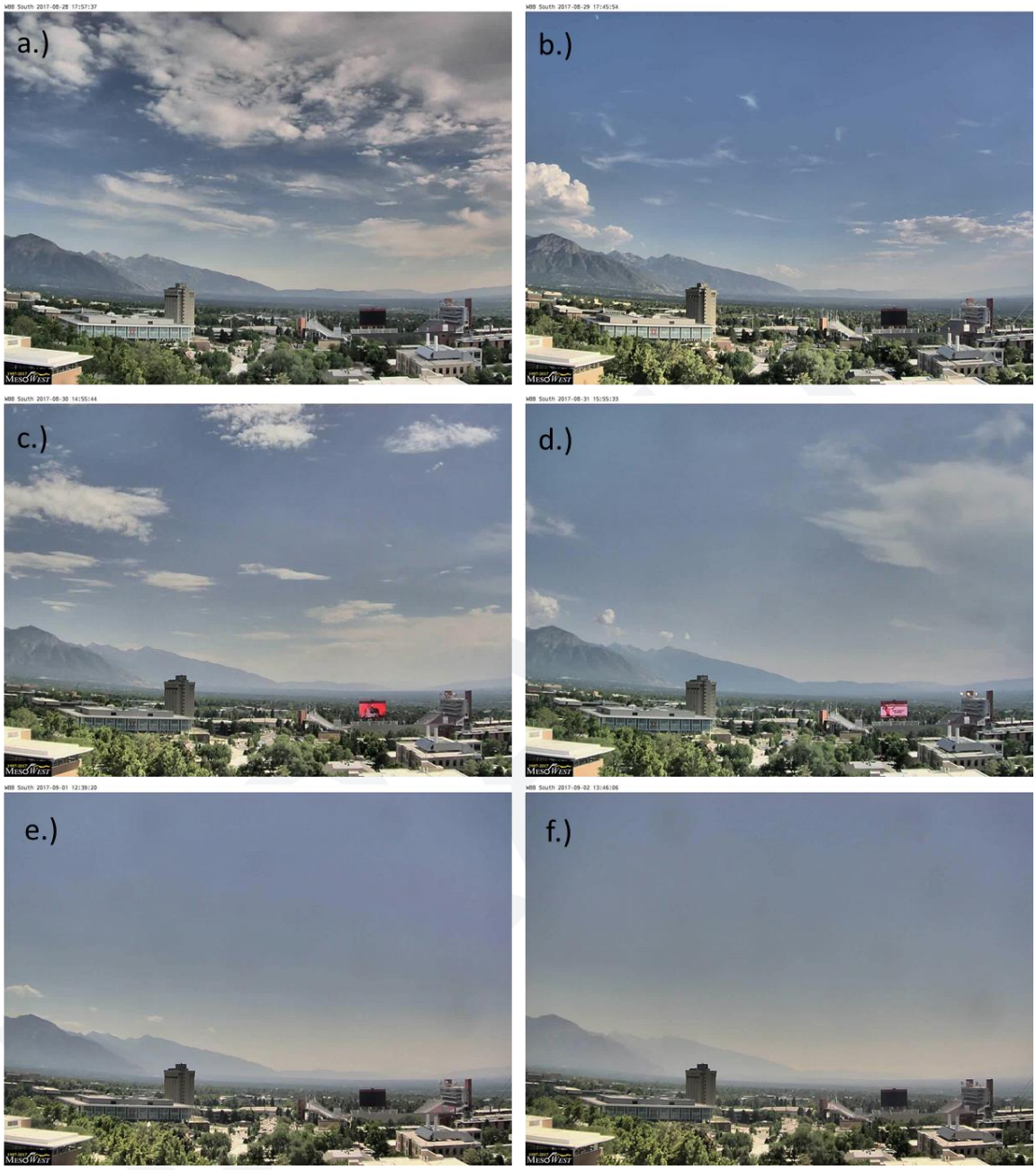

Figure 51. Snapshots from the University of Utah-MesoWest WBBS camera on **a.)** 2017-08-28, **b.)** 2017-08-29, **c.)** 2017-08-30, **d.)** 2017-08-31, **e.)** 2017-09-01, and **f.)** 2017-09-02. (Perspective: downtown facing south in the Salt Lake Valley)

Analysis by the HMS smoke tool distinguishes a large swath of wildfire smoke across the western U.S and Canada, with heavy and dense smoke associated with large wildfire complexes highlighted across California, Oregon, Washington, Idaho, and Montana the presence of smoke across Utah and the Wasatch Front (**Figure 52**). The transport of smoke from these fires extended light to heavy smoke across the entire intermountain west and even as far east as the Mississippi. Light to moderately dense smoke is analyzed

across Utah and the Wasatch Front, with VIIRS/MODIS thermal hot spot detection noting the location of the Tank Hollow fire approximately 60 miles to the SE of the HW site and a few other smaller fires located to the west and north of the Salt Lake Valley. In addition to the large plume of light smoke detected over Utah, HMS smoke also reveals a light to moderate smoke plume extending NW from the Tank Hollow wildfire into the Salt Lake Valley. Observations of AOD from ground-based aerosol remote sensing instrumentation near the Wasatch Front corroborate the presence of diffuse wildfire smoke with increased observed AOD values of 0.15-0.30 (**Figure 53**). On a typical clear day without wildfire smoke, AOD for visible light (wavelengths 400-700 nm) are < 0.10. Satellite observed AOD from MODIS Terra/Aqua MAIAC and ECMWF/CAMS indicate AOD values from 0.25-0.30 (**Figure 53)** over the Wasatch Front, with a satellite derived OMPS Aerosol Index layer of 1-2, indicating particulate matter within the atmosphere (**Figure 55**).

Figure 52 - HMS Smoke Detection Sept. 2

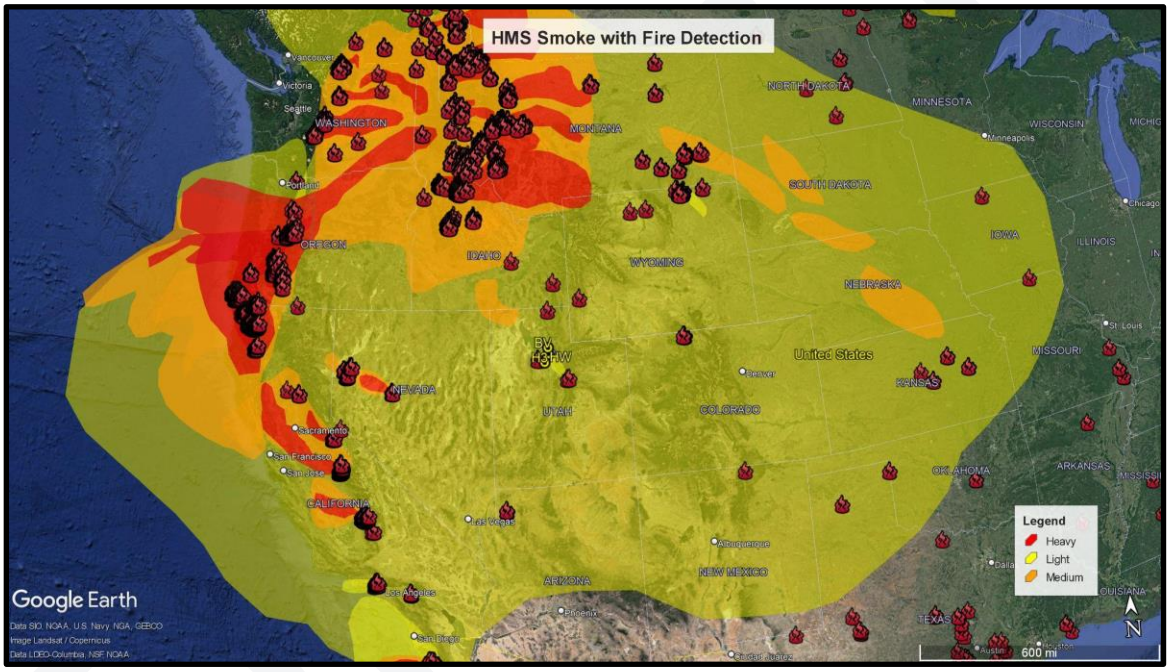

Figure 52. HMS smoke detection (yellow: light smoke, orange: moderate smoke, and red: heavy smoke) and VIIRS/MODIS active fire detections and thermal anomalies (**red flames**) on September 2, 2017. UDAQ monitors (HW, BV, and H3) are marked (**yellow filled circles**).
(Source: https://globalfires.earthengine.app/view/hms-smoke).

Figure 53 - AERONET AOD Sept. 2

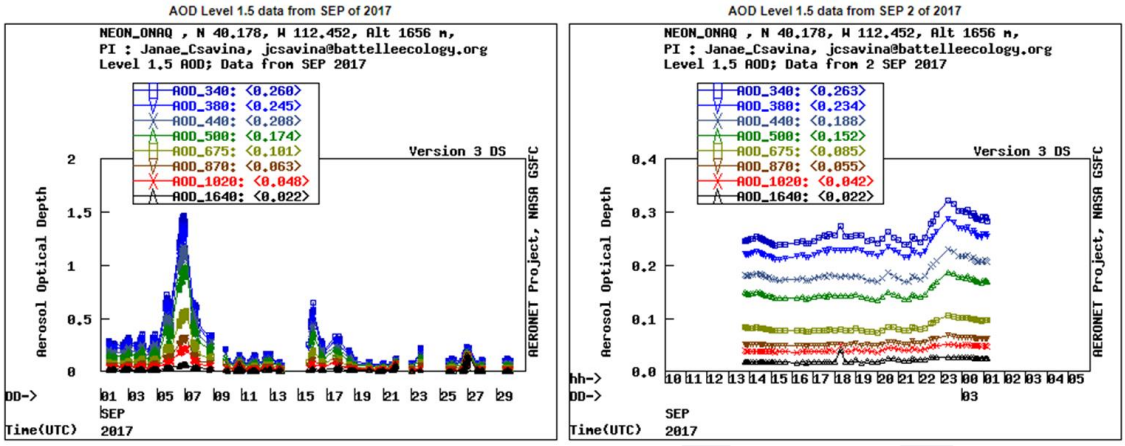

Figure 53. Time series of Aerosol Optical Depth (AOD) measured by the AERONET observation network at NEON_ONAQ site (40.17759 N, 112.45244 W) for **left:** September 1-30, 2017 and **right:** September 2 10Z - September 3 05Z. (Source: https://aeronet.gsfc.nasa.gov)

Figure 54 - MODIS Terr/Aqua MAIAC AOD Sept. 2

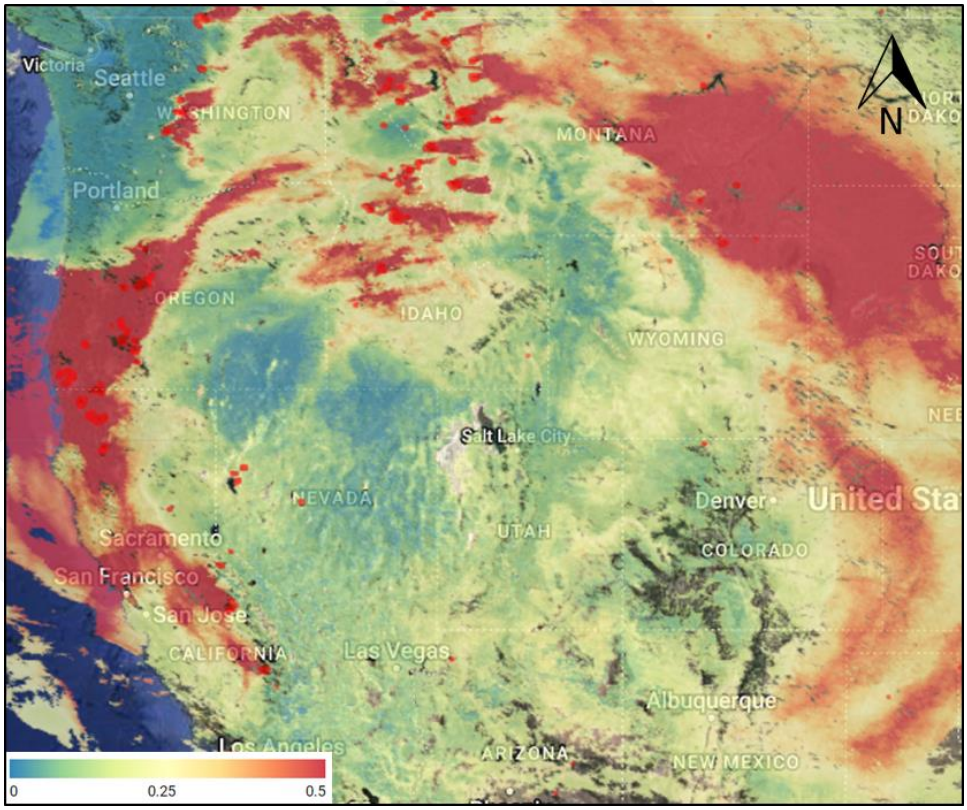

Figure 54. MODIS Terra/Aqua MAIAC Optical Depth (AOD) at 550 nm on September 2, 2017. Red markers indicate VIIRS/MODIS active fire detections and thermal anomalies (hot spot detection). (Source: https://firms.modaps.eosdis.nasa.gov/usfs/map/)

Figure 55 - OMPS Aerosol Index Sept. 2

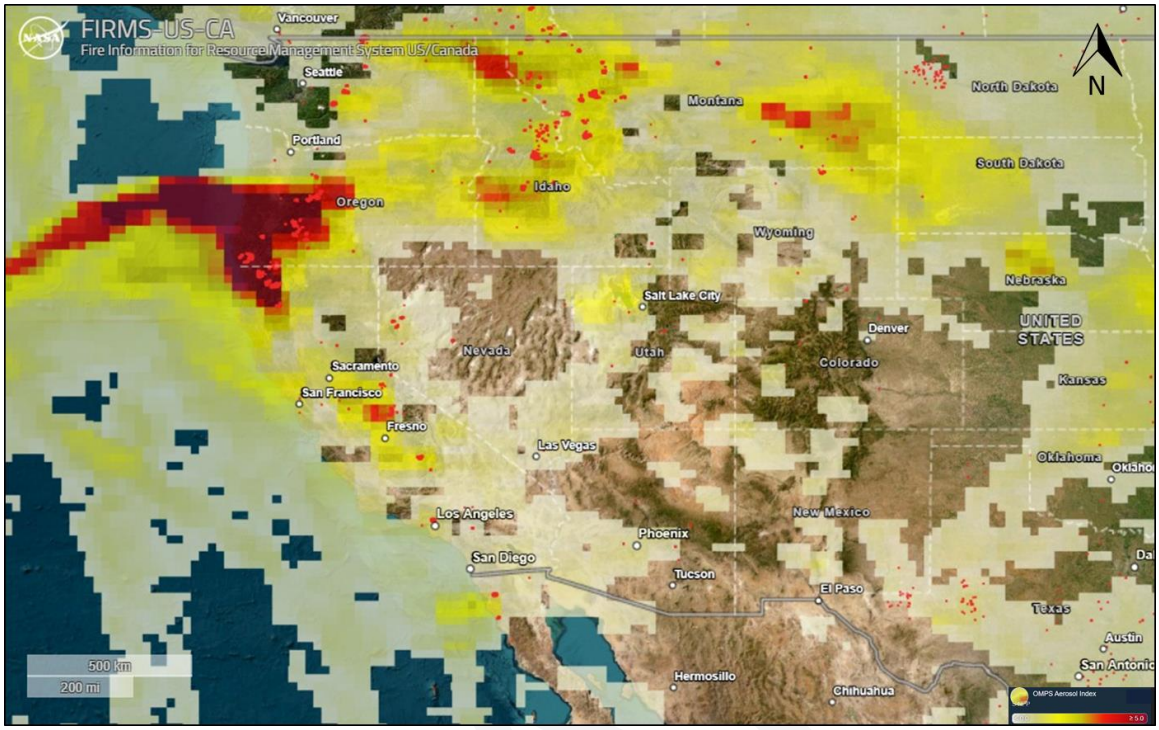

Figure 55. The OMPS Aerosol Index layer on Sep. 2, 2017. OMPS Aerosol Index layer indicates the presence of ultraviolet (UV)-absorbing particles in the air (aerosols) such as soot particles in the atmosphere; it is related to both the thickness of the aerosol layer located in the atmosphere and to the height of the layer. The Aerosol Index is a unitless range from < 0 to >= 5, where 5 indicates heavy concentrations of aerosols from biomass burning smoke located in the lower troposphere (1-3 km).
(Source: https://firms.modaps.eosdis.nasa.gov/usfs/map/)

Other satellite products, including GMAO's (Global Modeling and Assimilation Office) MERRA-2 (Modern-Era Retrospective analysis for Research and Applications, Version 2), show the total column and surface mass of Black Carbon and Organic Carbon on September 2 (**Figure 56 and 57**). Similar to PM2.5 and CO, black and organic carbon can be used as a tracer for wildfire smoke. In **Figure 56 and 57**, assimilated satellite observations and meteorological data exhibit the transport of black and organic carbon concentrations by the mean circulation across the western U.S. The highest black and organic carbon concentrations in **Figure 56 and 57** are associated with the large fires and fire complexes across California, Oregon, Washington, Idaho, and Montana. Transport vectors show that black and organic carbon was being transported from the wildfire regions across northern Utah. Specifically, moderately elevated total column (~2-3 mg/m^2) and surface (~1-2 µg/m^3) black carbon concentrations and elevated organic carbon total column (~30-40 mg/m^2) and surface (~16-24 µg/m^3) concentrations are analyzed over the Wasatch Front in **Figure 56** and **Figure 57**, respectively, indicating the presence of wildfire smoke.

Figure 56 - MERRA-2 Vertically Integrated and Surface Mass BC

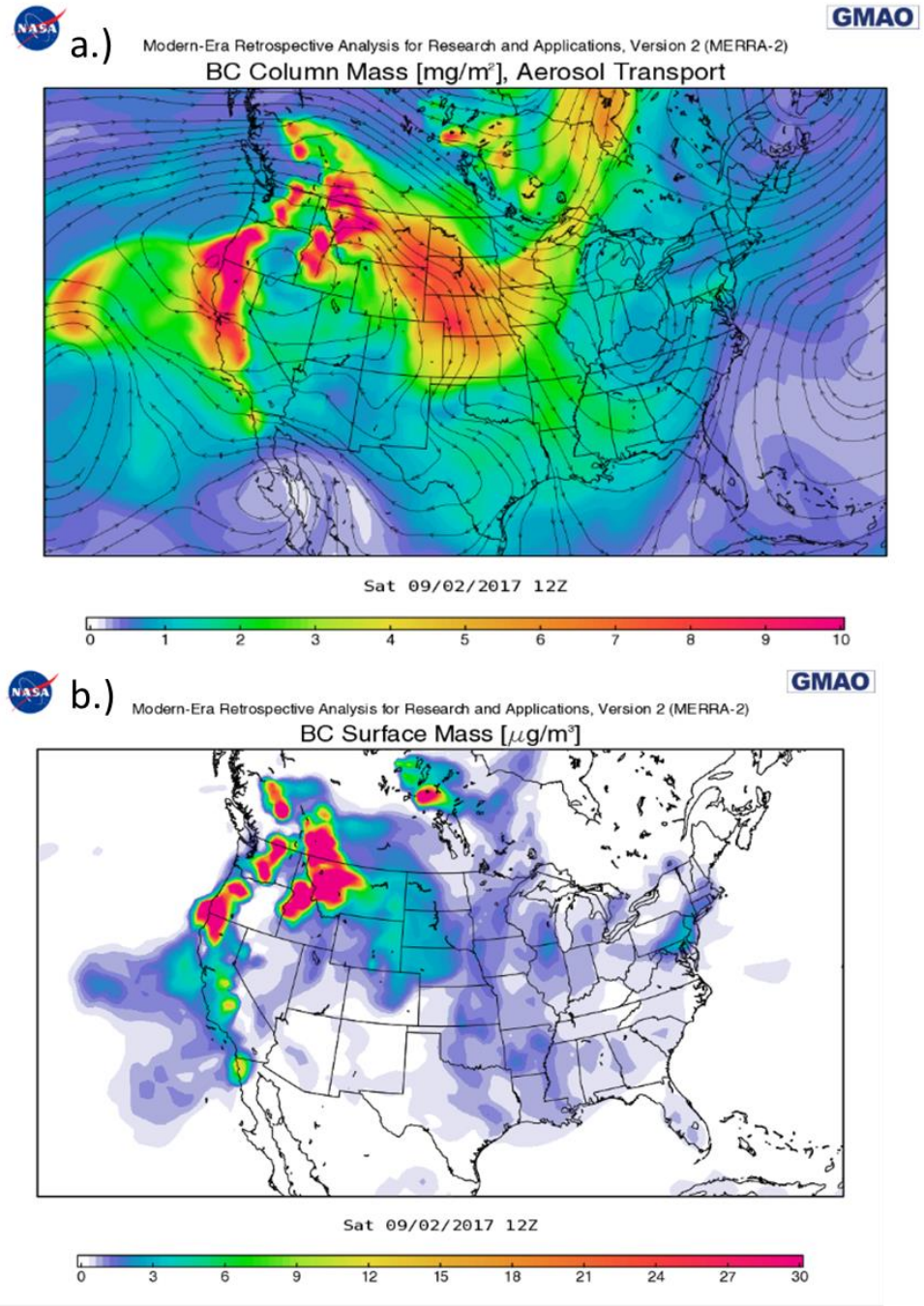

Figure 56. MERRA-2 satellite and model analyzed: **a.)** vertically integrated (column mass) black carbon (BC) with aerosol transport vectors on 2017-09-02 12Z and **b.)** surface mass black carbon (BC) on 2017-09-02 12Z

Figure 57 - MERRA-2 Vertically Integrated and Surface Mass OC

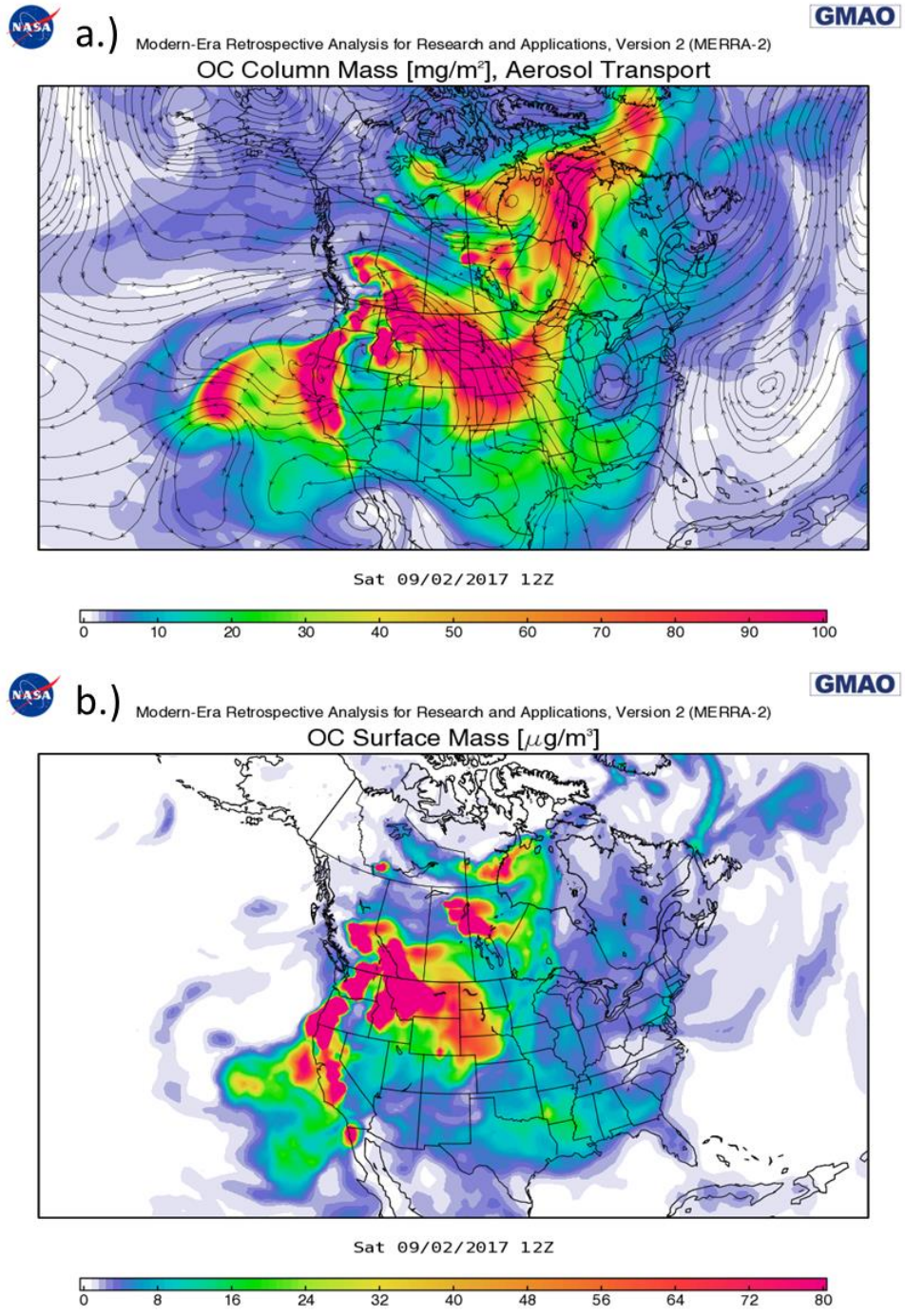

Figure 57. MERRA-2 satellite and model analyzed: **a.)** vertically integrated (column mass) organic carbon (OC) with aerosol transport vectors on 2017-09-02 12Z and **b.)** surface mass organic carbon (OC) on 2017-09-02 12Z.

3.2.3 Event Analysis September 2, 2017

In this section, we incorporate parts of the previous meteorological and wildfire analysis with the analysis of observed air quality variables related to wildfire smoke and O3. The purpose here is to reveal a strong link between the timing and arrival of wildfire smoke emissions and the timing of the MD8A O3 exceedance on September 2, 2017. We provide a time series of wildfire smoke tracers PM2.5, CO, brown carbon along with MD8A O3 to analyze and determine the impact wildfire smoke had on enhanced O3 concentrations during the flagged event period (**Figures 58-62**). Additionally, HYSPLIT backward and frequency trajectories as well as some meteorological analysis are given to substantiate the ground-based observations of wildfire smoke tracers and the wildfire smoke transport analysis. By investigating the trends in these tracers and O3 in conjunction with analysis from the meteorology and spatiotemporal variability of wildfire smoke, we show the concurrence of wildfire smoke transport across the Wasatch Front and high O3 concentrations. Ultimately, this analysis provides evidence that there is a strong relationship between the presence of wildfire smoke and subsequent impact on the MD8A O3 exceedance on September 2.

Wildfire smoke from regional and local sources was transported at multiple levels within the atmosphere across the Wasatch Front on September 2, 2017. This combination of the varied smoke source locations and stratified smoke layers makes the analysis of wildfire smoke impact on O3 complex. Based on the meteorological and smoke analysis in the previous section, we distinguished two possible primary source locations of wildfire smoke that were transported over the Wasatch Front. The first smoke source was a conglomerated mass of wildfire smoke from the northern California, Oregon, Washington, and Idaho fires. This wildfire smoke was shown to be transported at lower to upper levels behind the shortwave trough that moved across the Wasatch from August 30 - September 2. The second smoke grouped source area, which is more subtle, was from the Tank Hollow Fire that was 60 miles to the SE of the HW monitor and from fires in southern Idaho and Wyoming. This smoke was transported over the Wasatch Front by a combination of canyon and valley wind systems that were shown to be present on September 2 as well as mesoscale wind features in the mid-levels.

To stay in line with the previous section's analysis, we take a step back and begin our analysis in the preceding days from the flagged event period then move into September 2. On August 29, PM2.5 concentrations at HW, BV, and H3 were slightly above to near the monthly average and CO and brown carbon were marginally elevated (**Figure 58-62**). The slightly higher than average concentrations can be explained by the presence of an upper level ridge, that up August 29, facilitated the buildup of emissions to a mild degree across the Wasatch Front. However, by August 30-31 a disturbance began to track into the area and PM2.5, CO, and brown carbon concentrations began to decrease. At all three UDAQ sites, a local minimum is evident in observed PM2.5 concentrations during the period August 30-31, with CO and brown carbon also showing a minimum (**Figure 58-62**). The minimum observed concentrations in PM2.5, CO, and brown carbon corresponds to a period of emission ventilation, which was due to a decrease in atmospheric stability and increase in surface to upper level winds as the disturbance/short-wave trough pushed across the area. Emissions and wildfire smoke that had been residing before August 31 were swept out of the area as synoptic forcing associated with the disturbance temporarily mixed things out. Interestingly, a local minimum in MD8A O3 also occurred on August 31 at HW and H3 and on August 30 at BV as PM2.5, CO, and brown carbon concentrations were at their respective lowest levels. The

progression of this disturbance and associated trough axis is described in the meteorological and wildfire analysis sections.

Figure 58 - HW: MD8A and PM2.5 Aug. 29 - Sept. 4

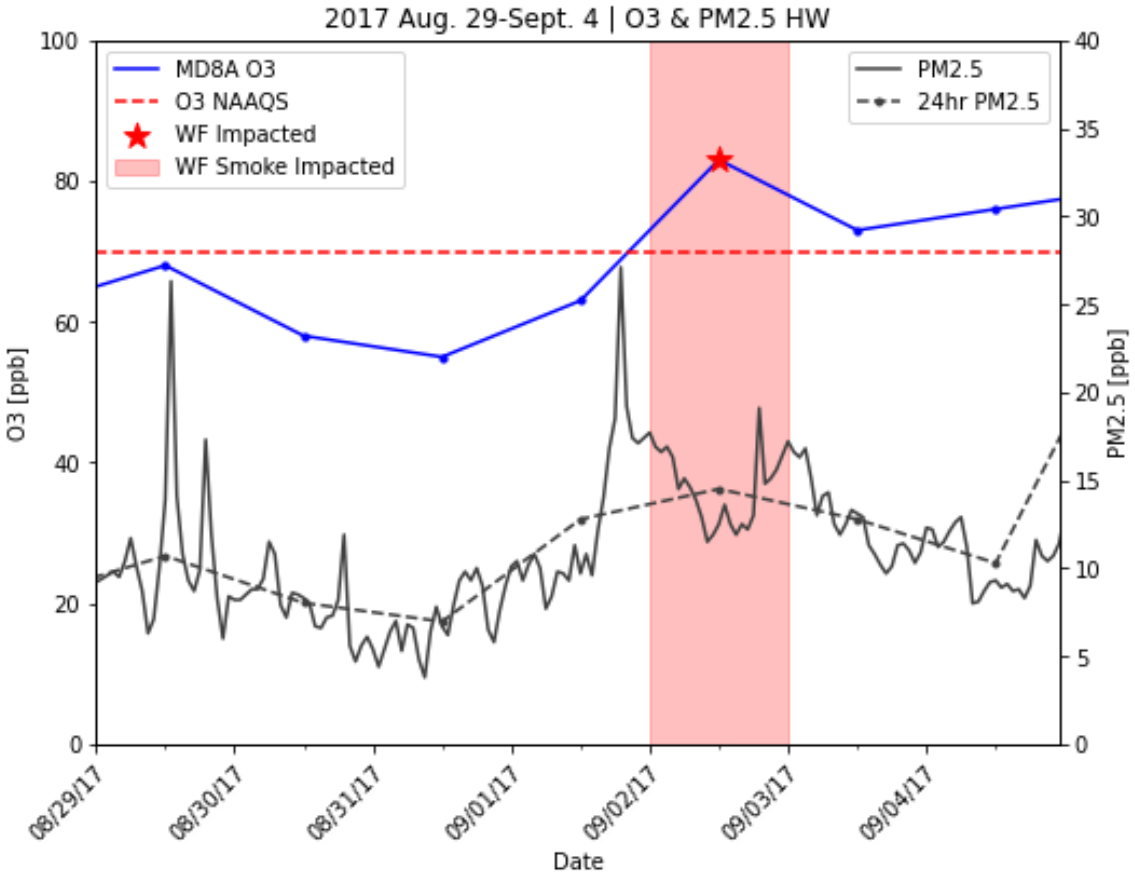

Figure 58. Observed concentrations at the HW monitor of MD8A O3 concentrations **(blue solid line)**, PM2.5 (**black solid line**), 24hr averaged PM2.5 (**dashed black line**). The 2015 MD8A O3 NAAQS is overlaid (**red dashed line**) and the red shaded area represents the event period. Red star marks the MD8A O3 value impacted by wildfire smoke.

Figure 59 - BV: MD8A and PM2.5 Aug. 29 - Sept. 4

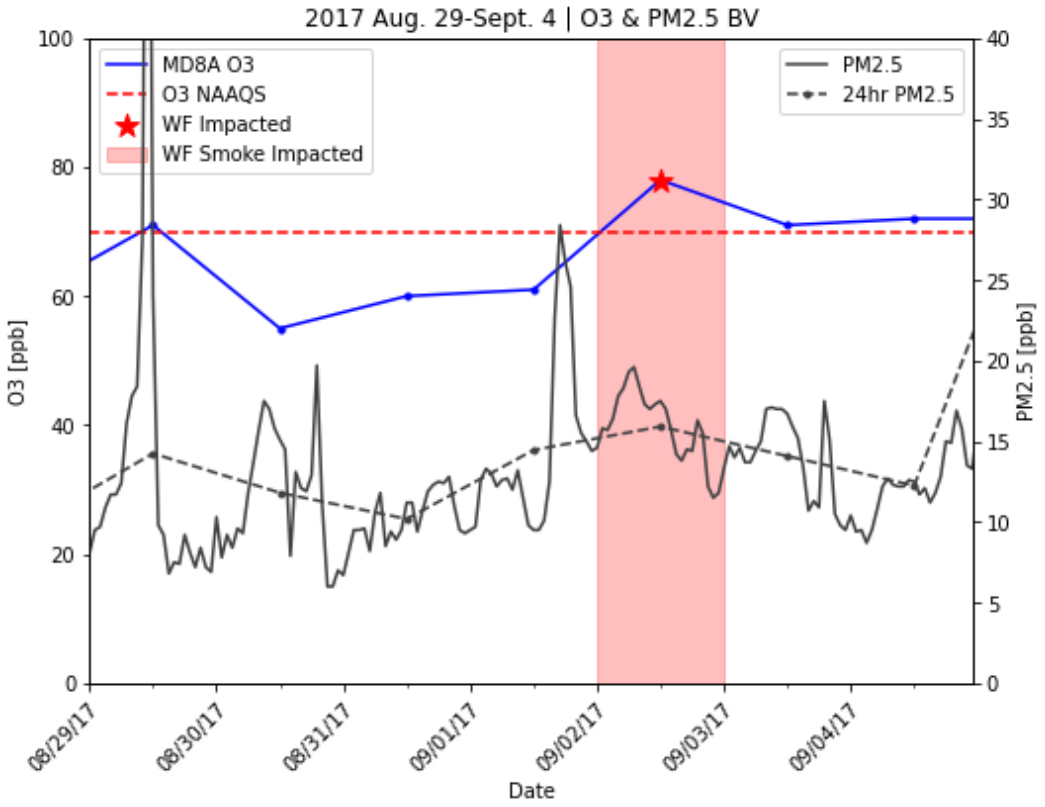

Figure 59. Observed concentrations at the BV monitor of MD8A O3 concentrations **(blue solid line)**, PM2.5 (**black solid line**), 24hr averaged PM2.5 (**dashed black line**). The 2015 MD8A O3 NAAQS is overlaid (**red dashed line**) and the red shaded area represents the event period. Red star marks the MD8A O3 value impacted by wildfire smoke.

Figure 60 - H3: MD8A and PM2.5 Aug. 29 - Sept. 4

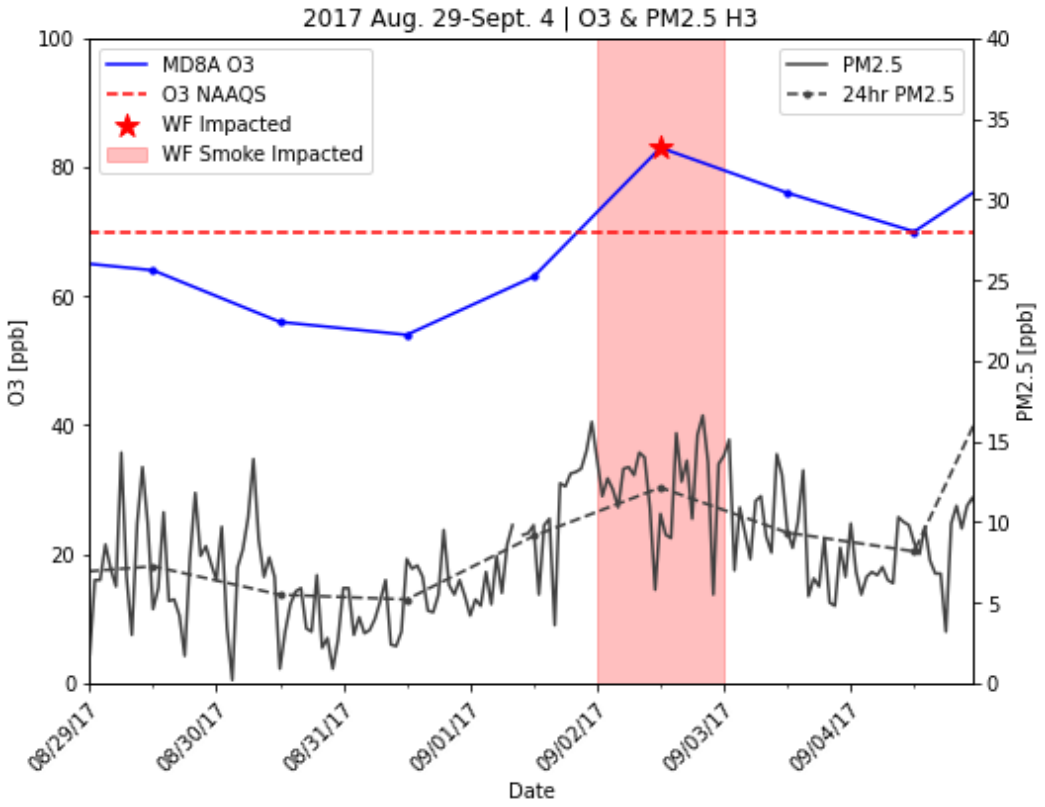

Figure 60. Observed concentrations at the H3 monitor of MD8A O3 concentrations **(blue solid line)**, PM2.5 (**black solid line**), 24hr averaged PM2.5 (**dashed black line**). The 2015 MD8A O3 NAAQS is overlaid (**red dashed line**) and the red shaded area represents the event period. Red star marks the MD8A O3 value impacted by wildfire smoke.

Figure 61 - HW: CO Aug. 28 - Sept. 12

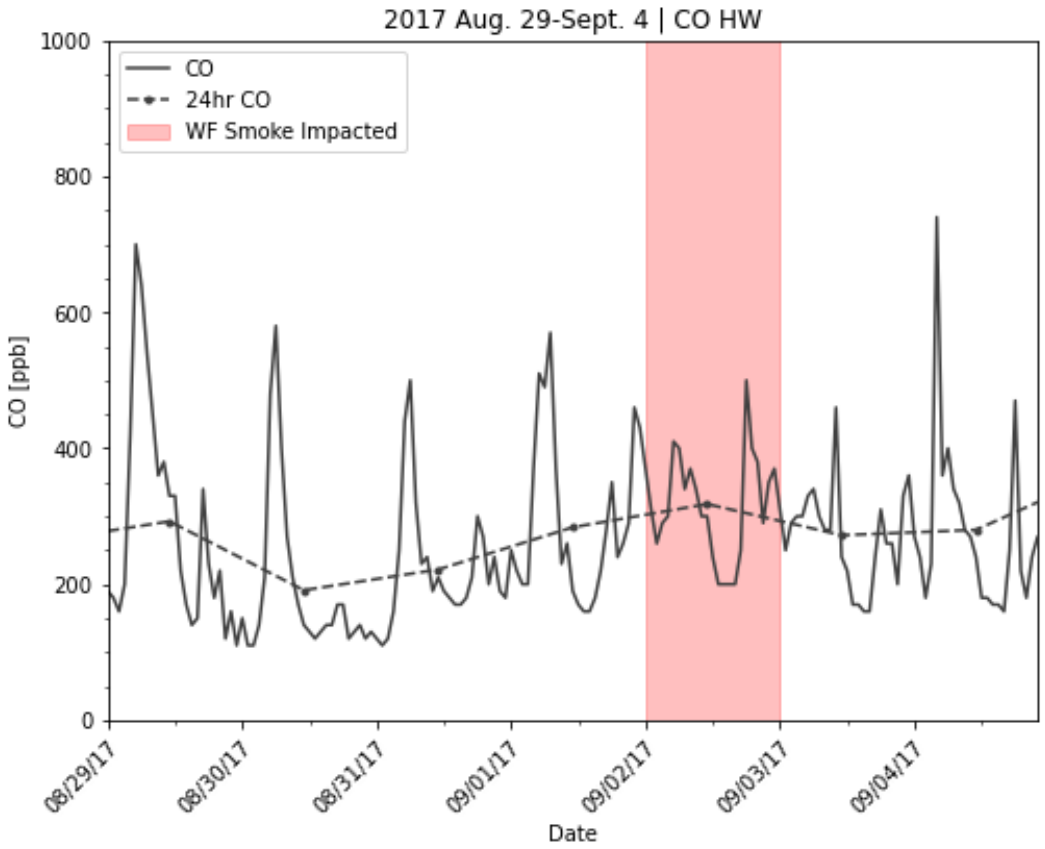

Figure 61. Carbon monoxide (CO) hourly observations (ppb) from HW August 28 - September 12, 2017. The red shaded area represents the flagged event period September 2.

Figure 62 - BV: Brown Carbon Aug. 28 - Sept. 12

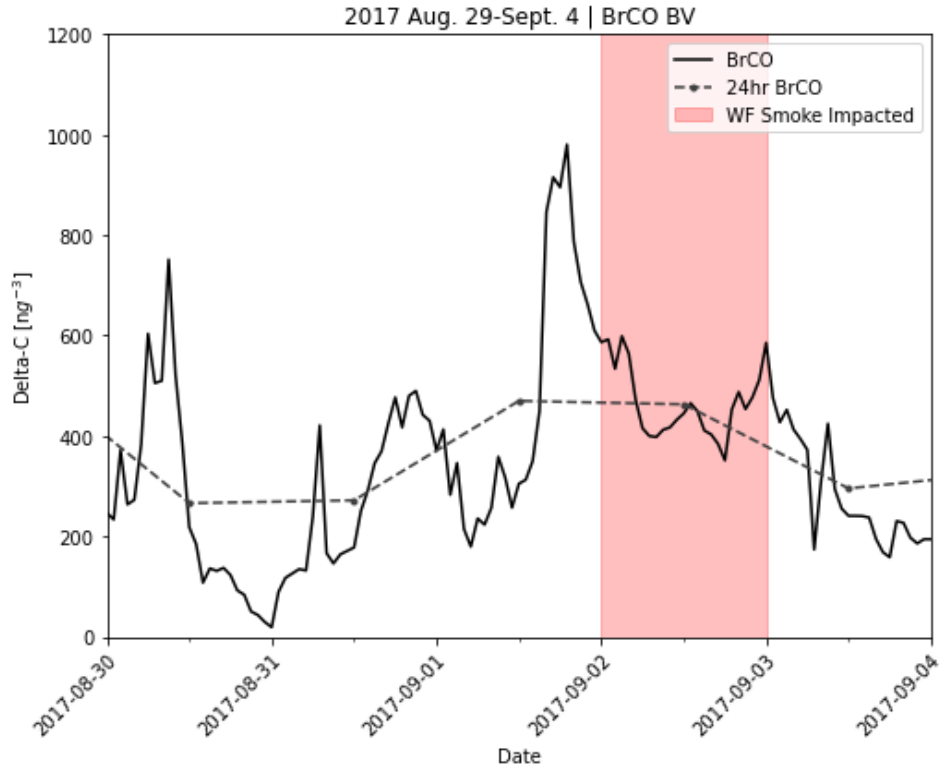

Figure 62. Brown carbon (Delta) observations (black solid line), 24-hour average brown carbon (dashed black line) at the BV UDAQ site August 28 - September 10, 2017. Red shaded areas represent the two flagged event periods in September (9/2 and 9/5-6).

Figure 63 - Observed PM2.5 at HW, BV, H3 Aug. 31 - Sept. 3

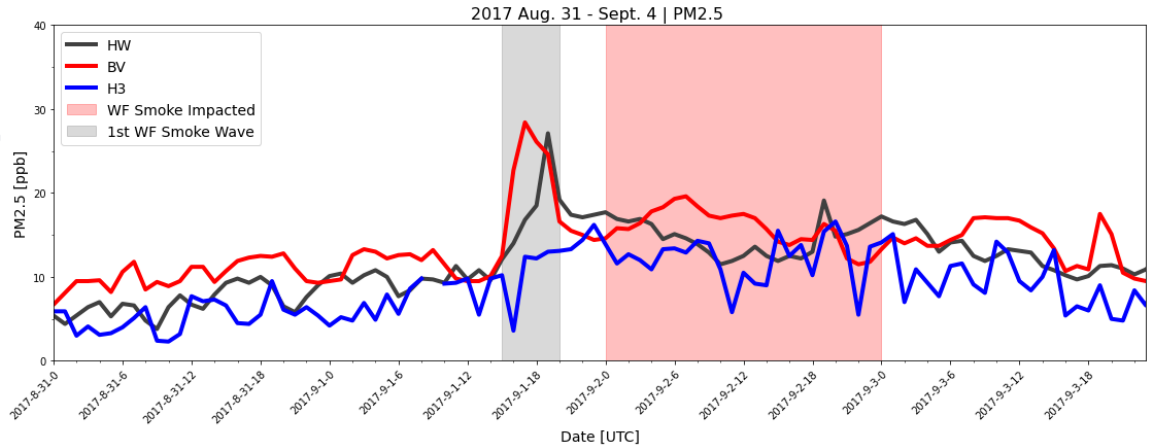

Figure 63. Observed PM2.5 at UDAQ monitors HW (black), BV (red), and H3 (blue) monitors August 31 00Z - September 4 00Z. Red highlight areas represent the flagged event period (September 2) and the gray shaded region marks a primary peak in PM2.5 associated with a swath of wildfire smoke moving across the Wasatch Front.

After the disturbance passed to the east late August 31, PM2.5, CO, and brown carbon concentrations began to increase. Specifically, there are two peaks or spikes in PM2.5, CO, and brown carbon that mark the passage of the short-wave trough axis to the east of the Wasatch Front and associated transport of wildfire emissions. We delineate these two peaks as wildfire smoke wave one and wave two. In **Figure 63**, a primary peak in PM2.5 is evident at all three UDAQ monitors between the hours 15-00Z September 1. This first peak corresponds to a relatively denser swath of wildfire smoke that was transported across the Wasatch Front by the N-NW clockwise flow around the upper level ridge. **Figure 63** reveals that the highest levels of PM2.5 occurred with this wave of smoke. Peaks in the observed CO and brown carbon trends also are evident between the hours 15-21Z September 1 (**Figure 61 and 62**), which temporally matches the peak in PM2.5 (**Figure 63**). After 21Z September 1, the densest smoke diffused across the region and PM2.5, CO, and brown carbon slightly decreased before leveling out by 00Z September 2.

At varying times during the period after 00Z September 2 through 16Z, a mild rebound in wildfire smoke tracer concentrations is noted, indicating the contribution of additional wildfire smoke emissions over the UDAQ sites. The addition of wildfire smoke emissions was potentially connected to a subtler and overlapping influence of the transport of wildfire smoke emissions from a few different sources to the UDAQ sites the early morning of September 2 (after 06Z September 2) (**Figures 58-60**). These sources included the Tank Hollow (UT), Little Valley (ID), Maple Creek 2 (ID), and Pole Creek (WY) fires, as well as reservoir wildfire smoke emissions from the Wasatch Back. **Figures 58-60** show a few periods of slight increase in PM2.5 at H3 and BV and increased CO at HW between 06-16Z September 2, which corresponds to the formation of the nighttime southerly valleys' winds and easterly canyon winds. As described in the meteorological analysis section, these wind systems were observed overnight September 1 through the morning of September 2 and had the potential to aid in the transport of wildfire smoke from the aforementioned wildfires to the Salt Lake Valley and to the UDAQ sites (**Figure 41 and 43**). Other than the near-surface transport of wildfire smoke, wildfire smoke emissions were potentially transported at more elevated levels by the southeasterly 700 mb winds extending from the Tank Hollow fire to the Wasatch Front (**Figure 37a and 38a**). However, due to the stratified nature of the atmosphere during the nighttime boundary layer, this layer of wildfire smoke likely remained above the nocturnal inversion layer and was not mixed down to the surface until the afternoon.

The developmental timing of the topographical flows corresponds well to the periods of slight increase in PM2.5 at BV and H3 and CO at HW between 06-16Z September 2. However, a clear relationship is difficult to draw, solely based off of ground-based measurements, between the wildfire tracer trends we see between 00-16Z September 2 and the transport of wildfire smoke emissions from these fires. This is mainly due to observational limitations, including the lack of VOC observations and the need for greater spatial coverage of aethalometer brown carbon observations. The addition of these two types of observational datasets would give a more refined picture of the transport of wildfire smoke and associated O3 precursors to the UDAQ sites by the diurnal canyon/valley winds. Therefore, to help trace the trajectory of wildfire smoke emissions into the Wasatch Front, we incorporate HYSPLIT backward trajectory analysis to investigate the potential source location of air parcels overnight September 1 through the morning of September 2 (00-18Z September 2) at HW, BV, and H3.

HYSPLIT 18hr 27-member ensemble backward trajectories, utilizing the Global Data Assimilation System (GDAS) 0.5 degree and High Resolution Rapid Refresh version 1 (HRRRv1) 3km model, reveal a few

different potential source locations of air parcels at the UDAQ monitoring sites (**Figure 64 and 65**). In **Figure 64**, GDAS backward trajectories show that air at 500m above H3 largely originated over the Tank Hollow wildfire, air parcels at HW originated near the Tank Hollow Fire and from easterly sources across the Wasatch crest (Wasatch Back), and air parcels at BV originated from easterly sources across the Wasatch crest (Wasatch Back). The backward trajectories using the HRRRv1 model provide similar results as GDAS but allow for the potential incorporation of higher resolved transport features in the trajectory analysis (**Figure 65**). The 18hr backward trajectories at H3 suggest that air parcels overnight September 1 to the morning of September 2 largely originated from the Tank Hollow fire area, providing supporting evidence between the wildfire smoke tracer trends and transport by the observed valley/canyon flows. Trajectories at both HW and BV suggest air parcels were largely sourced from the Wasatch Back and were transported via easterly canyon winds over the Wasatch crest into the Wasatch Front. While HYSPLIT has limitations, particularly in complex topography, the backward trajectories using GDAS and HRRRv1 provide supporting documentation that additional wildfire smoke emissions were likely transported via canyon and valley winds from the Tank Hollow fire and from residing smoke across the Wasatch Back from Idaho fires (Maple Creek 2 and Little Valley) and Wyoming fires (Pole Creek) over the UDAQ monitoring sites 00Z-18Z September 2.

Figure 64 - HYSPLIT GDAS 0.5 Ensemble 18hr Backward Trajectories

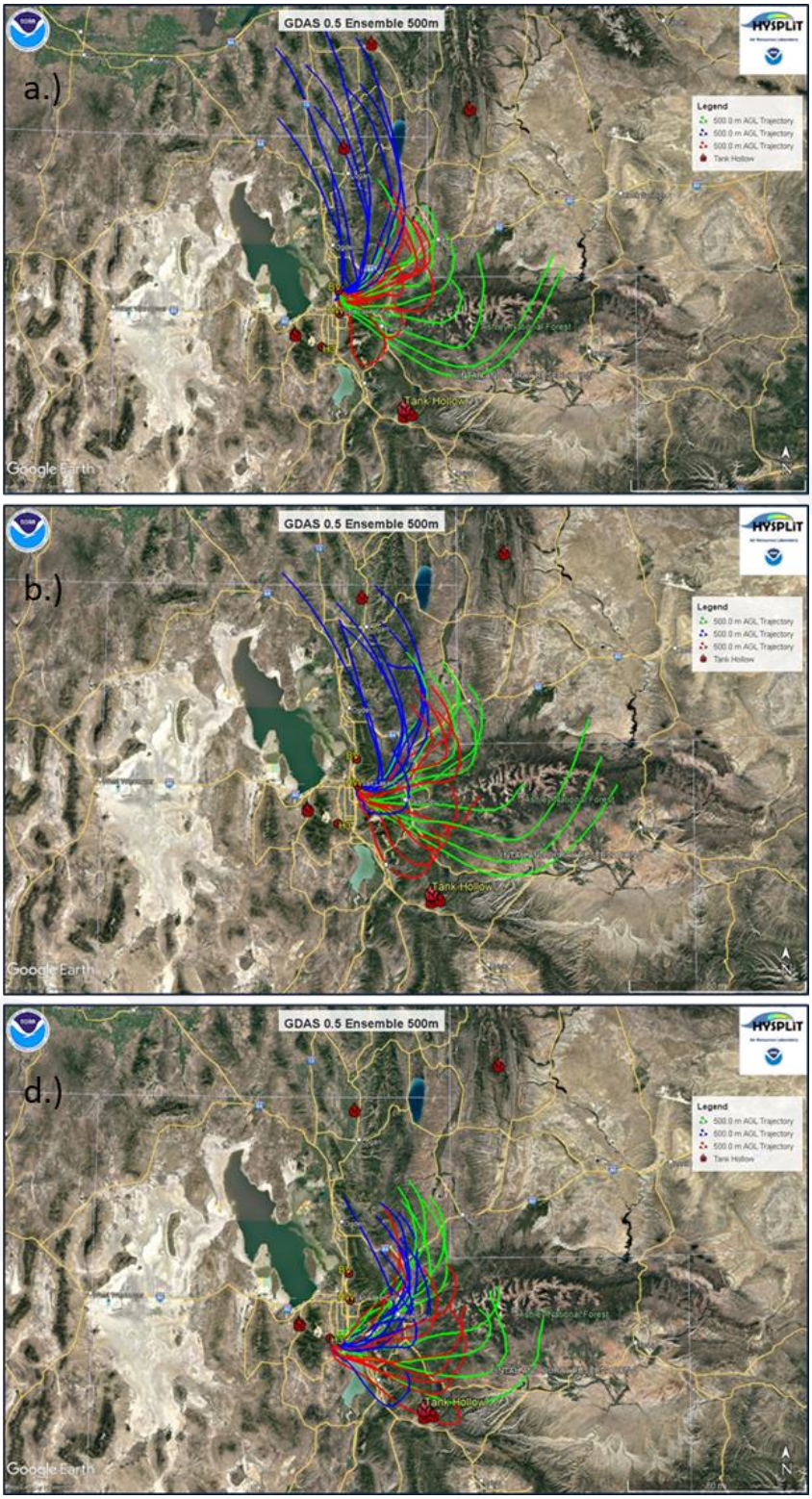

Figure 64. HYSPLIT GDAS0p5 degree 27-member ensemble 18hr September 2 18-00Z backward trajectory ending at 500m at the UDAQ monitors **a.)** HW, **b.)** BV, and **c.)** H3. VIIRS/MODIS active fire detections and thermal anomalies (**red flames**).

Figure 65 - HYSPLIT HRRRv1 Ensemble 18hr Backward Trajectories Sept. 2

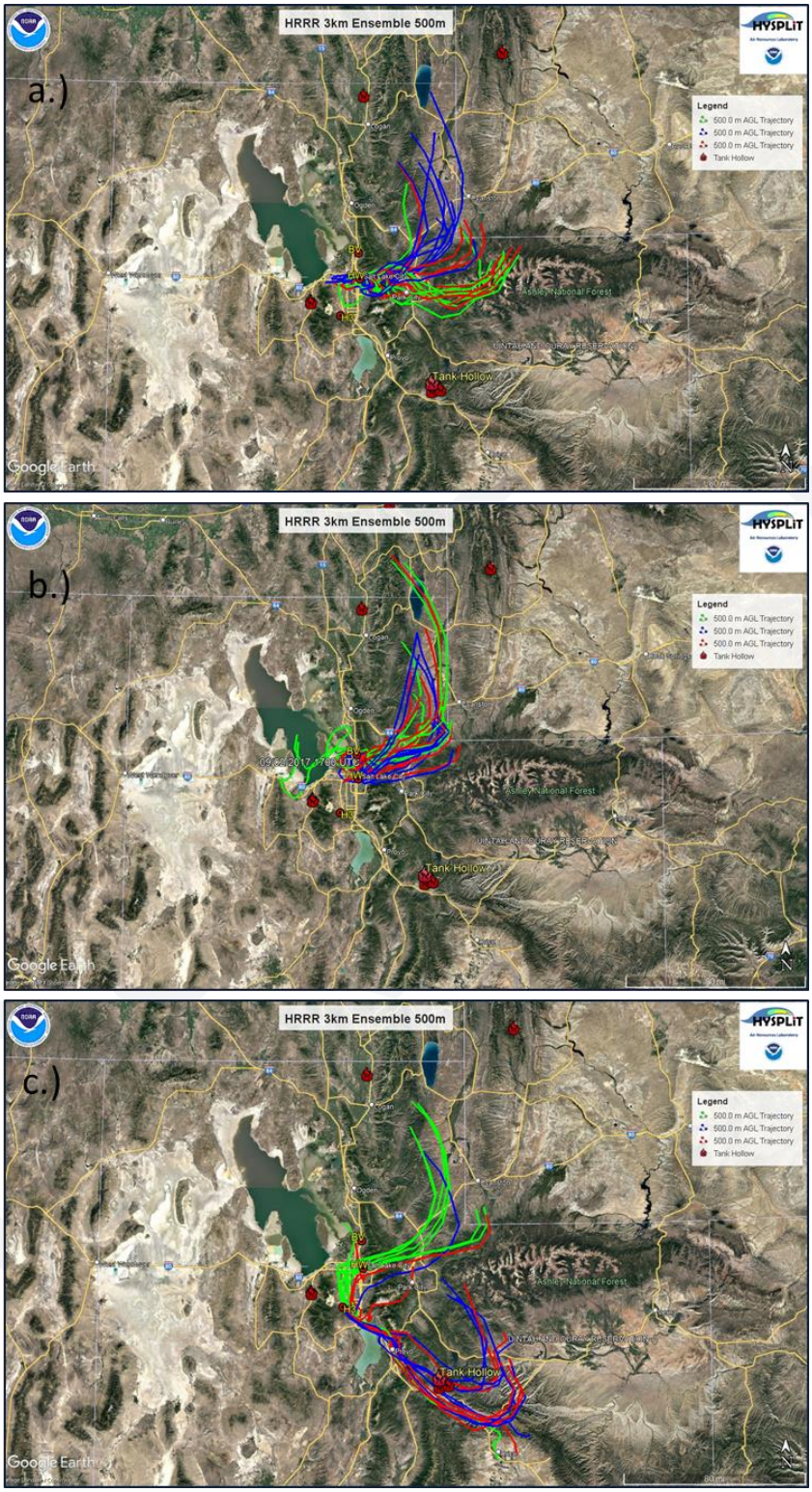

Figure 65. HYSPLIT HRRRv1 3km 27-member ensemble 18hr September 2 18-00Z backward trajectory ending at 500m at the UDAQ monitors **a.)** HW, **b.)** BV, and **c.)** H3. VIIRS/MODIS active fire detections and thermal anomalies (**red flames**).

During the period 00-18Z September 2, we deduct that O3 precursors and reservoir species were transported by the nocturnal drainage flows (canyon/valley) from mountain basins/valleys and brought into the Wasatch Front area. The emissions transported by the drainage flows were likely made up of a reservoir of wildfire emissions, transported into the mountain basins/valleys by the preceding day's diurnal canyon/valley winds as well as wildfire smoke emissions from the fires in southern Idaho and Wyoming. The recapture and recirculation of these emissions allowed the local accumulation of O3 precursors within the Wasatch Front airshed, and additionally allowed precursors with lower reactivities more time to contribute to high local O3 formation. This type of local O3 enhancement by emission recapture from thermally driven and diurnal wind systems has been documented by previous research (e.g. Reddy and Pfister, 2016). In the case of the flagged period of September 2, the recapture of O3 precursors and increased residence time of these precursors was of particular importance for the development of high O3 concentrations at HW, BV, and H3.

The afternoon of September 2 is the last period where PM2.5 and brown carbon concentrations are noted to increase in connection with wildfire smoke transport and observed meteorological mechanisms. **Figures 58-60** reveals a few different spikes in wildfire tracers 18-21Z September 2, which correspond to the evolution of the planetary boundary layer (PBL) mixed layer across the Wasatch Front. Sounding analysis from KSLC exhibits a deep and well mixed boundary layer up to about 600 mb or ~3.2 km AGL that formed the afternoon of September 2 (**Figure 45**). The stratification of the atmosphere is also shown by the sounding profile, with two main layers in the PBL analyzed, including a lower layer (< 790 mb) characterized by the NW lake breeze winds and an upper layer characterized by SE winds (790-600 mb). Above the PBL (> ~600 mb), there is a layer characterized by weak N-NW flow and a subsidence inversion followed by an adiabatic temperature profile. The subsidence inversion indicates sinking and warming air below the upper level ridge down to the entertainment zone or top of the PBL at ~600 mb. These layers within and above the PBL all contained wildfire smoke emissions from varied sources and contributed to near-surface wildfire smoke concentrations on the afternoon of September 2 by the following mechanisms: 1) Convective mixing within the PBL mixed layer transported elevated wildfire emissions from ~700 mb (source, Tank Hollow fire) down to the surface, 2) elevated smoke emissions within the free atmosphere (FA) (western U.S. fire sources) > 600 mb descended down to the subsidence inversion ~600 mb and PBL entrainment zone, 3) wildfire smoke emissions at the PBL top and FA interface (entrainment zone) were entrained into the PBL mixed layer where turbulence further transported the emissions down to the surface. The processes described above outline the mechanisms that contributed to the modest increase in PM2.5, CO, and brown carbon during the afternoon of September 2. These specific processes have been described by previous research as potential mechanisms of wildfire smoke transport to the surface under synoptic subsidence (e.g. Alonso-Blanco et al., 2018; Colarco et al., 2004; Duck et al., 2007; Hung et al., 2020a; Miller et al., 2011; Pahlow et al., 2005; Wu et al., 2018, 2021).

During the September 2 flagged period, without the interaction of subsidence and PBL mixing providing a mechanism for the transport of wildfire smoke emissions from the FA to the surface, smoke emissions would have remained trapped aloft having a negligible impact near the surface (Colarco et al., 2004). Wildfire tracer emission concentrations would have likely decreased through the afternoon as concentrations were diffused through a deeper PBL mixed layer, but the contribution of turbulent mixing and entrainment of elevated wildfire smoke emissions helped transport additional emissions to the

surface. Therefore, the noted increases in wildfire tracers from 18Z-00Z September 2 provide evidence that additional wildfire smoke emissions were being mixed down to the surface from elevated levels. This process has been described by previous research (e.g. Reddy and Pfister, 2016; Horel et al., 2016) as a mechanism for recapturing wildfire smoke under upper level ridges from elevated levels and was potentially responsible for the capture of elevated O3 precursor species and elevated O3 within the aged smoke plume over the Wasatch Front. The capture of elevated O3 and O3 precursor species helped contribute to the high concentrations of O3 observed on September 2, 2017 at HW, BV, and H3.

The analysis discussed thus far illuminates three main mechanisms that aided wildfire smoke transport across the Wasatch Front during the September 2 flagged event period. These three mechanisms include the transport of wildfire smoke by 1) the synoptic weather pattern (short-wave trough/cool frontal passage), 2) diurnal topographical wind systems (canyon/valley winds), and 3) interaction between the subsidence inversion and PBL turbulence processes. Subsequently, we determined that wildfire smoke emissions were transported by these mechanisms from both local and distant sources. The distant smoke sources include California/Nevada, the PNW, Idaho, Wyoming and Montana, and the more local sources include the Tank Hollow fire and Wasatch Back. To add to this analysis and gain a comprehensive picture of where air parcels along the Wasatch Front were sourced from over an extended period leading up to September 2, HYSPLIT frequency and ensemble 48hr and 72hr backward trajectory analysis was performed using GDAS 0.5 and HRRRv1 3km model input (**Figures 66-68**).

The GDAS 0.5 model was chosen due to its coarser resolution and ability to provide a smoother representation of trajectory paths, while the HRRRv1 was chosen for its higher resolution and ability to provide a potentially more nuanced depiction of transport. Frequency trajectories were calculated by taking the number of trajectories that passed over a grid cell and normalizing it by the total number of trajectory endpoints. Ensemble backward trajectories were calculated by offsetting the meteorological data by a fixed grid factor (one grid meteorological grid point in the horizontal and 0.01 sigma units in the vertical). This results in 27 members for all-possible offsets in X, Y, and Z (NOAA Air Resources Laboratory). We released the 48hr and 72hr backward trajectories at 1500m, which is in line with previous research conducting long duration backward trajectories for wildfire smoke (e.g. Hung et al., 2020 and 2021) and reduces errors due to trajectory and topography intersections. The purpose of the frequency and ensemble backward trajectories is to reveal the possible origins of air parcels and associated trajectory paths that were present along the Wasatch Front on September 2. Trajectory paths crossing or starting from regions of active wildfires indicate the potential transport of wildfire smoke from these locations to the Wasatch Front. The areas of highest trajectory frequencies and ensemble trajectory paths in **Figure 66** and **Figure 67 and 68**, respectively, correspond to locations of active wildfires during the period August 29 - September 2, with the trajectory paths indicating transport by the mean synoptic winds, under the upper level ridge, and localized transport by the diurnal topographic winds (canyon, valley, and lake breezes). In general, frequency and ensemble trajectories show air parcels mainly originating from three sources: 1.) the Pacific Northwest (PNW), 2.) Idaho and Montana, and North-central California and Nevada, and 3.) the Tank Hollow fire and Wasatch Back.

Figure 66 - HYSPLIT HRRRv1 and GDAS 0.5 Frequency 48hr and 72hr Backward Trajectories Sept. 2

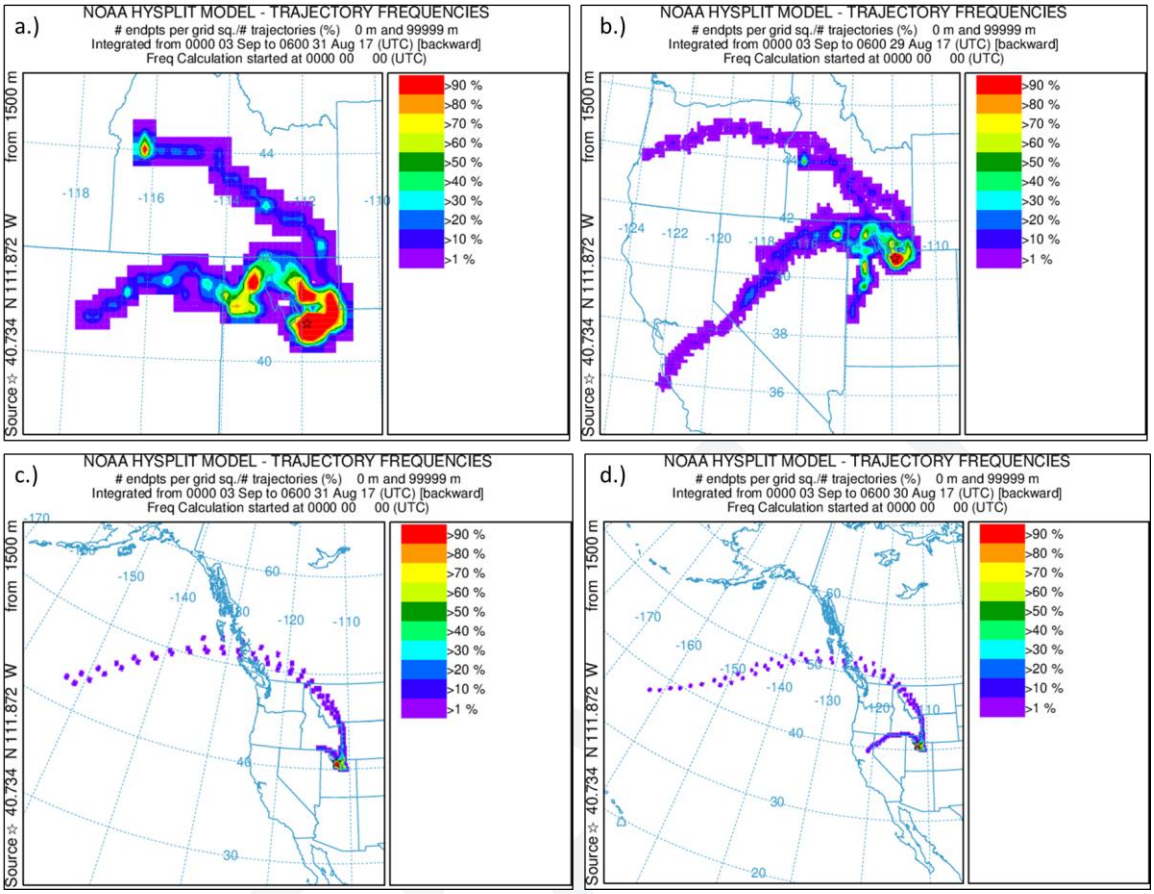

Figure 66. HYSPLIT HRRRv1 **a.)** 48hr September 3 00Z - August 31 06Z and **b.)** 72hr September 3 00Z - August 30 06Z backward frequency trajectory from HW. HYSPLIT GDAS 0.5 degree **c.)** 48hr September 3 00Z - August 31 06Z and **d.)** 72hr September 3 00Z - August 30 06Z backward frequency trajectory from HW.

Figure 67 - HYSPLIT GDAS 0.5 Ensemble 48hr Backward Trajectories Sept. 2

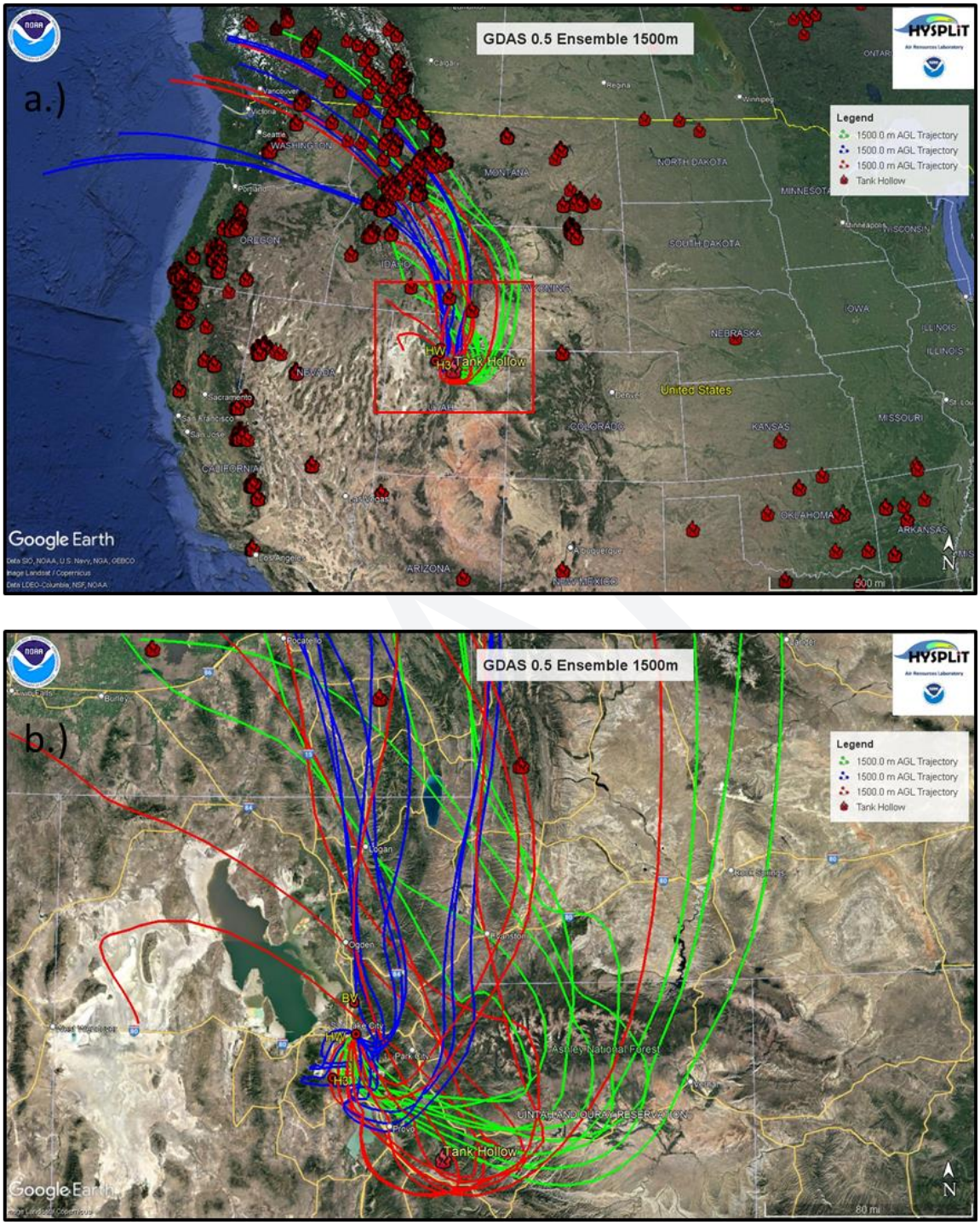

Figure 67. HYSPLIT GDAS 0.5 degree 27-member ensemble 48hr backward trajectory from HW September 3 00Z - September 1 00Z focused **a.)** view over western U.S. and **b.)** focused view over northern Utah. VIIRS fire hotspot thermal detection active wildfires are overlaid (**red flames**).

Figure 68 - HYSPLIT HRRRv1 Ensemble 48hr Backward Trajectories Sept. 2

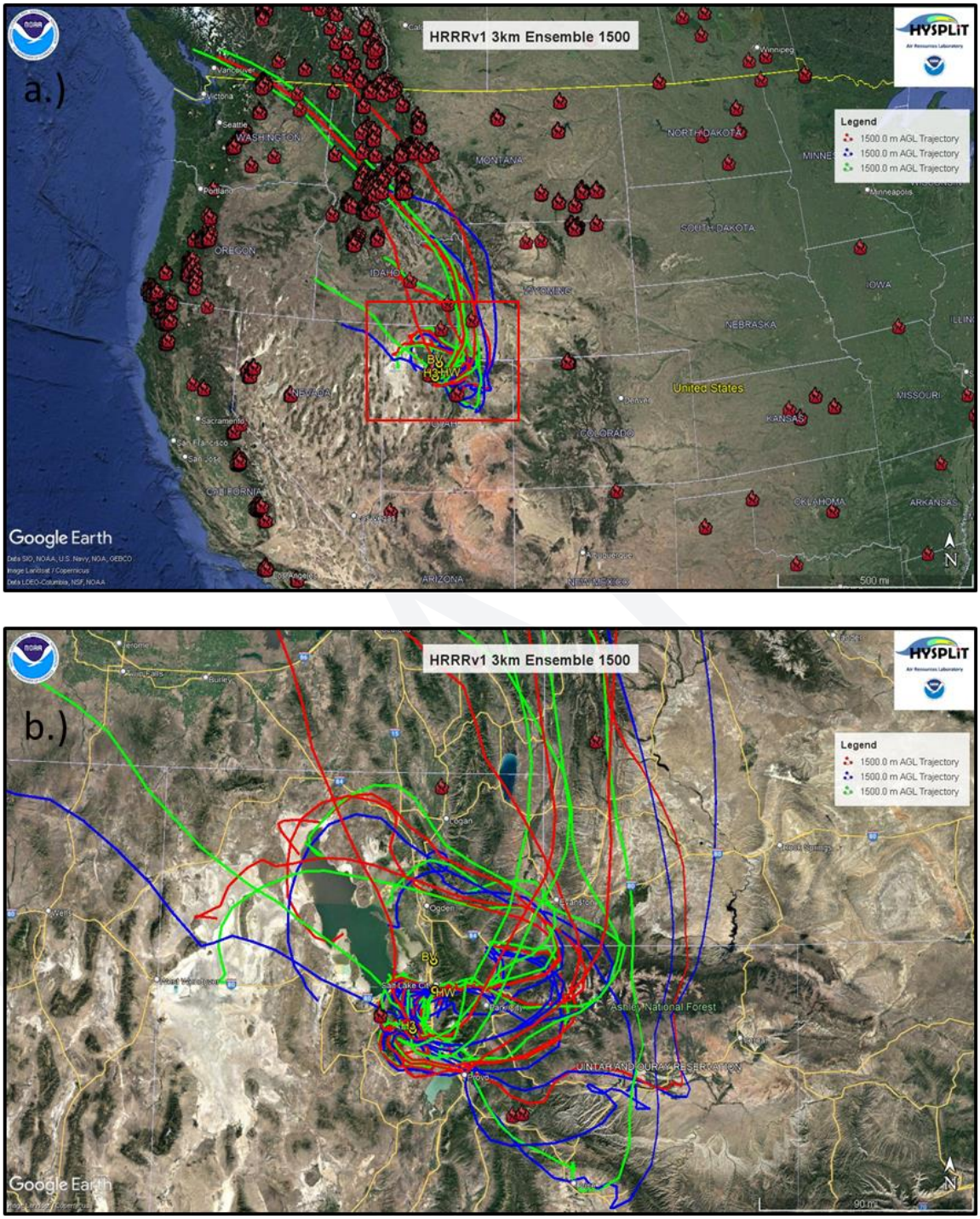

Figure 68. HYSPLIT HRRRv1 3km 27-member ensemble 48hr backward trajectory from HW September 3 00Z - September 1 00Z focused **a.)** view over western U.S. and **b.)** focused view over northern Utah. VIIRS fire hotspot thermal detection active wildfires are overlaid (**red flames**).

Ultimately, all three UDAQ sites reached a local 24hr PM2.5 maximum on September 2, with a local 24hr maximum observed in CO at HW and shared brown carbon maximum between September 1

and 2 at BV (**Figures 58-63**). The positive trend in PM2.5, CO, and brown carbon levels from late August 31 through September 2 corresponds to the transport of wildfire smoke plumes behind the shortwave trough axis as the mean winds shifted to the N-NW, the transport by topographical wind systems, and mixing of elevated smoke layers to the surface due to PBL mechanisms. The trend of MD8A O3 and wildfire tracers shows a fairly strong relationship on the flagged event and in the days preceding and proceeding the event period. Similar to PM2.5, CO, and brown carbon, the MD8A O3 concentration trend exhibits a local minimum on August 31 and a peak on September 2, indicating a close relationship with the trend of wildfire smoke tracers and potential link to wildfire smoke O3 enhancement. Wildfire smoke decreased across the area the days following September 2 as indicated by the gradual decline in tracer trends of PM2.5, CO, and brown carbon concentrations. Interestingly, a decrease in observed MD8A O3 concentrations occurred simultaneously with the decrease in wildfire smoke, further supporting the case that wildfire smoke emissions enhanced O3 at the UDAQ sites on September 2. While temperatures were hotter on September 3 compared to September 2, higher MD8A O3 was observed on September 2 at all sites. Without the additional emissions from wildfire smoke, O3 concentrations would have been lower on September 2 based on the given meteorology. Wildfire smoke emissions composed of O3 precursor species contributed to O3 exceedances at UDAQ monitors.

HYSPLIT frequency and ensemble 48hr and 72hr backward trajectory analysis reveals three main dominant source areas of air parcels through the period September 1 00Z - 00Z September 3 (**Figures 66-68**). The first source region is from the PNW, Idaho, Montana. The second source region is California and Nevada and the third and last main source region is from the Tank Hollow Fire and Wasatch Back. The connection between the peak in PM2.5 and MD8A O3 concentrations and the arrival of wildfire smoke over the Wasatch Front is further substantiated by the corresponding satellite imagery, HMS Smoke, and HRRR Smoke analysis from the previous section, which all reveal the arrival of wildfire smoke between late August 31 and September 2.

3.3 September 5 and 6, 2017 Flagged Event

3.3.1 Meteorological Conditions

In the days leading up to the flagged event, the synoptic weather pattern was characterized as benign, with the main noteworthy feature being the strengthening and amplification of an upper level ridge across the western U.S (**Figure 69**). The amplification of the upper level ridge is noted by the increased meridional component in the upper level heights and winds over the U.S Pacific coast up to BC, Canada and over the Continental Divide. As seen in **Figure 69**, the upper level ridge axis incrementally rotated clockwise from September 4-6. This modest shift in the ridge axis allowed the downstream anti-cyclonic branch of the ridge and associated mid to upper level N-NW winds to move over Utah on September 5-6. With the ridge axis nearly overhead Utah, the pattern on September 5 and 6 was dominated by strong upper level ridging indicated by anomalously high 500 mb heights (**Figure 70**). By September 7 and 8, the upper level ridge translated eastward across the continental divide, shifting the ridge axis so that the cyclonic branch of the ridge and S-SW winds progressed over Utah (**Figure 69**). The progression of the mid-level pattern (700 mb) also reveals N-NW winds across the Wasatch Front during the flagged event period, transitioning to S-SW by September 7-8 (**Figure 71**).

Figure 69 - Observed 500 mb Heights and Winds Sept. 3-6

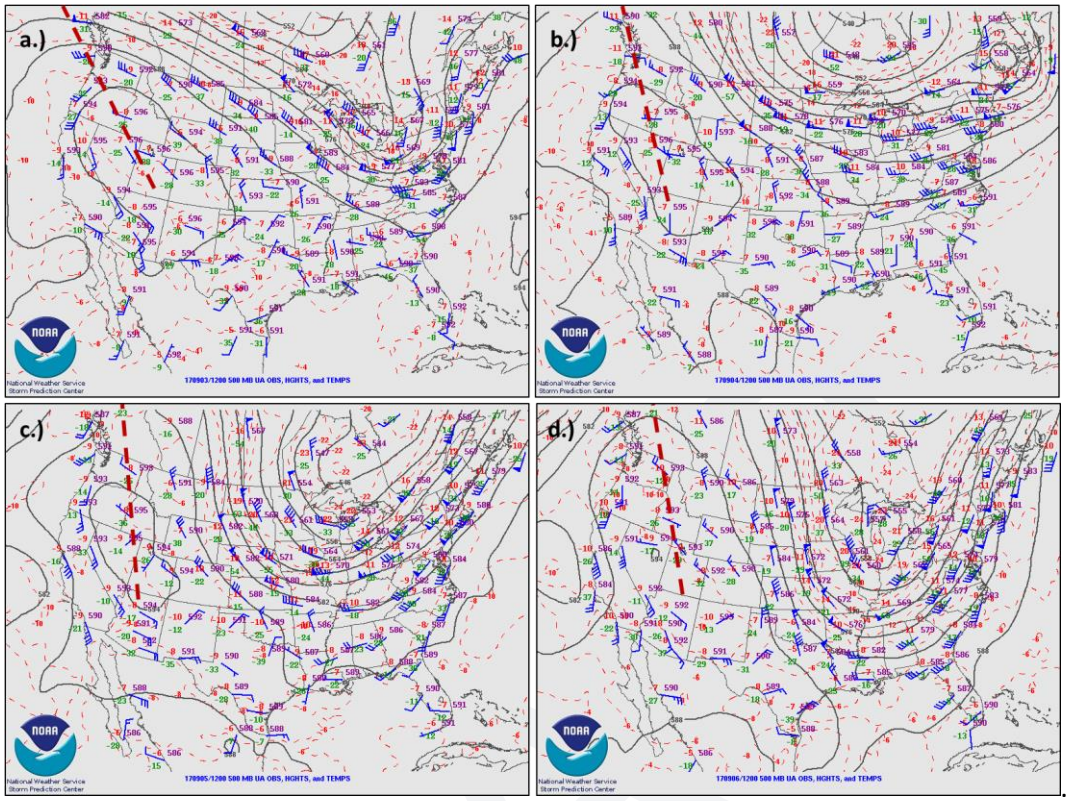

Figure 69. Upper air 500 mb heights and wind observations/analysis for **a.)** 2017-09-03 12Z, **b.)** 2017-09-04 12Z, **c.)** 2017-09-05 12Z, and **d.)** 2017-09-06 12Z. The red dashed line represents the 500 mb ridge axis.

Figure 70 - NCEP Reanalysis 500 mb Height Composites Sept. 5-6

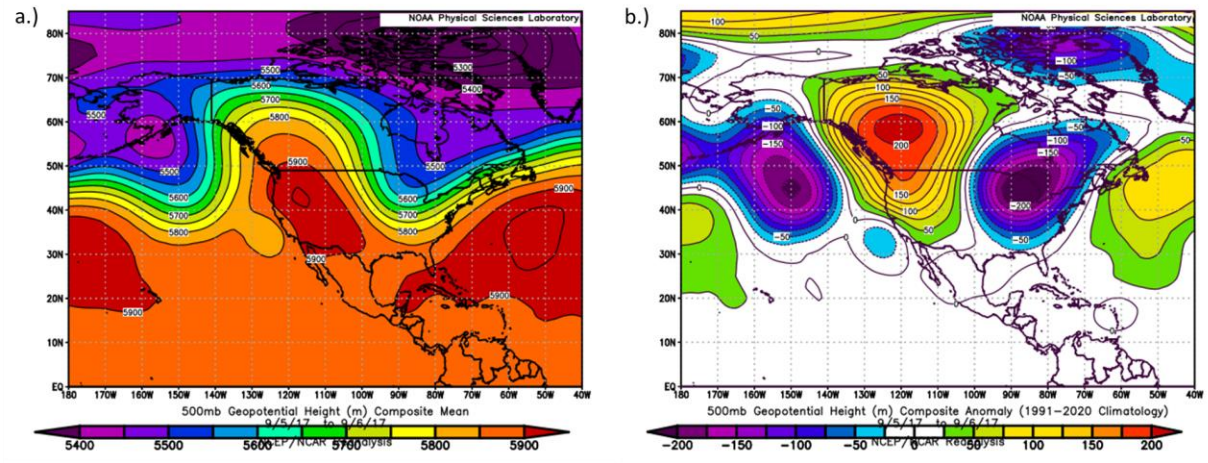

Figure 70. NCEP Reanalysis 500 mb height **a.)** composite mean and **b.)** composite anomalies for September 5-6, 2017.

Figure 71 - HRRR 3km Analyzed 700 mb Heights and Winds Sept. 4-7

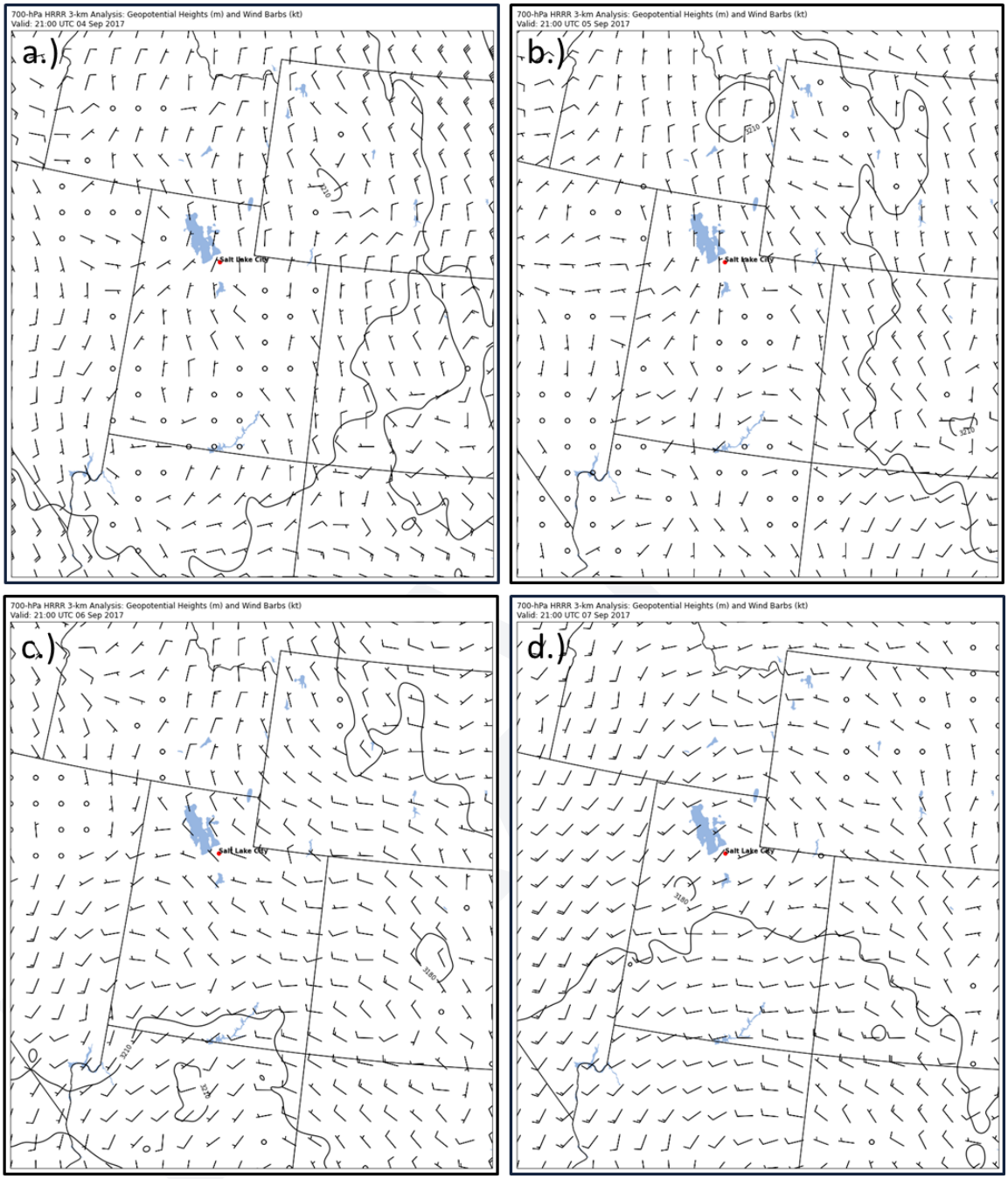

Figure 71. HRRR 3km analyzed 700 mb geopotential heights and winds valid for **a.)** 2017-09-04 21Z and **b.)** 2017-09-05 21Z, **c.)** 2017-09-06 21Z, and **d.)** 2017-09-07 21Z.

Radiosonde soundings from 00Z September 6 and 00Z September 7 reveal a slight stratification from the lower to upper levels (**Figure 72**). The PBL mixed layer is noted to contain the lake breeze in both soundings between the surface and 750 mb on September 5 and 730 mb on September 6. Above the lake breeze, the mixed layer extended up to ~600 mb (3111 m AGL) on September 5 and ~550 mb (3811 m AGL) on September 6. HRRR model analyzed PBL mixed layer heights over the Wasatch Front also exhibit

mixed layer depths of about 2000-3000 m AGL (**Figure 73**). Above the PBL, there are indications of a layer of drying (large dew point depression) and warming air (slight temperature inversion ~500-450 mb), which identifies the sinking air due to subsidence under the upper level ridge on September 5 and 6. Lower to upper level (sfc-400 mb) winds are generally observed as N-NW in both soundings.

Figure 72 - KSLC Radiosonde Skew-T's Sept. 5-6

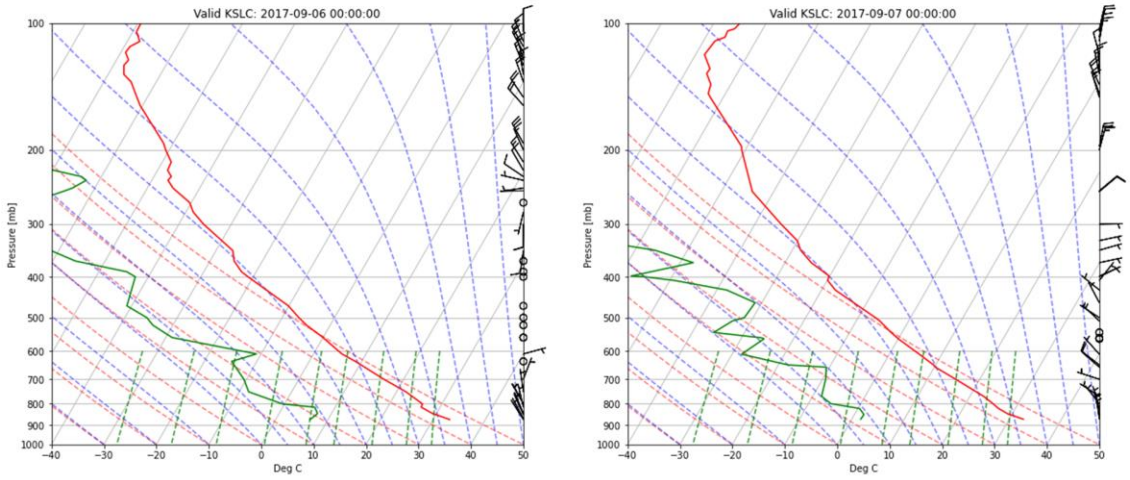

Figure 72. Radiosonde observations from KSLC on 2017-09-06 at 00Z (**left**) and 2017-09-07 at 00Z (**right**), with dew point (green solid line), temperature (red solid line), and wind barbs (right vertical axis) plotted to 100 mb. (Source: Integrated Global Radiosonde Archive (IGRA) https://www.ncei.noaa.gov/access/metadata/landing-page/bin/iso?id=gov.noaa.ncdc:C00975)

Figure 73 - HRRR 3km Analyzed PBL Height Sept. 5-6

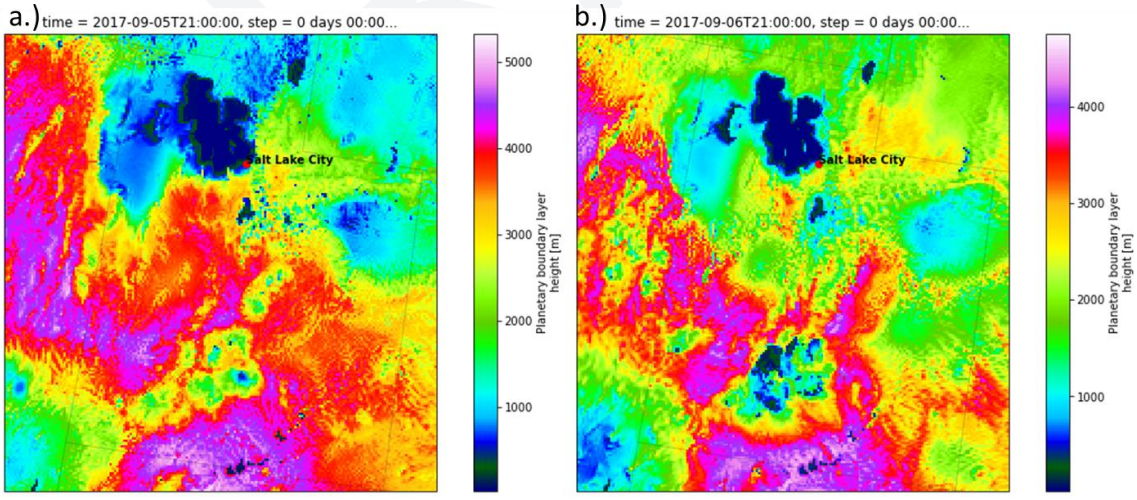

Figure 73. HRRR 3km analyzed PBL height (m AGL) valid for **a.)** September 5 21Z and **b.)** September 6 21Z.

Figure 74 summarizes the observed surface conditions from KSLC September 3-7. Temperatures were above normal through the period, with observed surface highs ~15 degrees F above normal on September 3 and 4 (**Figure 74**). A slight cool down is noted on September 5 and 6, where temperatures

were about 5 degrees F cooler than the preceding two days and topped out approximately 10 degrees F above normal (**Table 7**). The lower temperatures correspond to decreased visibility (< 10 statute miles) measured at KSLC from 12Z on September 5 through September 6 (**Figure 74**). Winds were generally light (<15 knots), indicating relatively calm conditions at the surface, and the observed surface wind direction reveals the presence of the typical summertime diurnal daytime (N-NW lake-breeze) and nighttime (S-SE valley winds) wind cycle each day September 3-7 (**Figure 72**).

Table 7 - Observed and Climate Normals Sept. 3-8

Date	Observed Low (F)	Observed High (F)	Normal Low (F)	Normal High (F)	Observed Precipitation (inches)	Normal Precipitation (inches)
9/3/2017	68	98	58	85	0	0.03
9/4/2017	67	98	58	85	0	0.03
9/5/2017	**65**	**95**	**57**	**84**	**0**	**0.03**
9/6/2017	**66**	**94**	**57**	**84**	**0**	**0.04**
9/7/2017	67	93	57	83	0	0.03
9/8/2017	70	91	56	83	0	0.03

Table 7. Observed and average high/low temperature and precipitation accumulations for KSLC from 9/3/2017 - 9/8/2017. The event dates 9/5/2017 and 9/6/2017 are bolded.
(Source: NWS SLC https://www.weather.gov/slc/CliPlot)

Figure 74 - KSLC Surface Observations Sept. 3-7

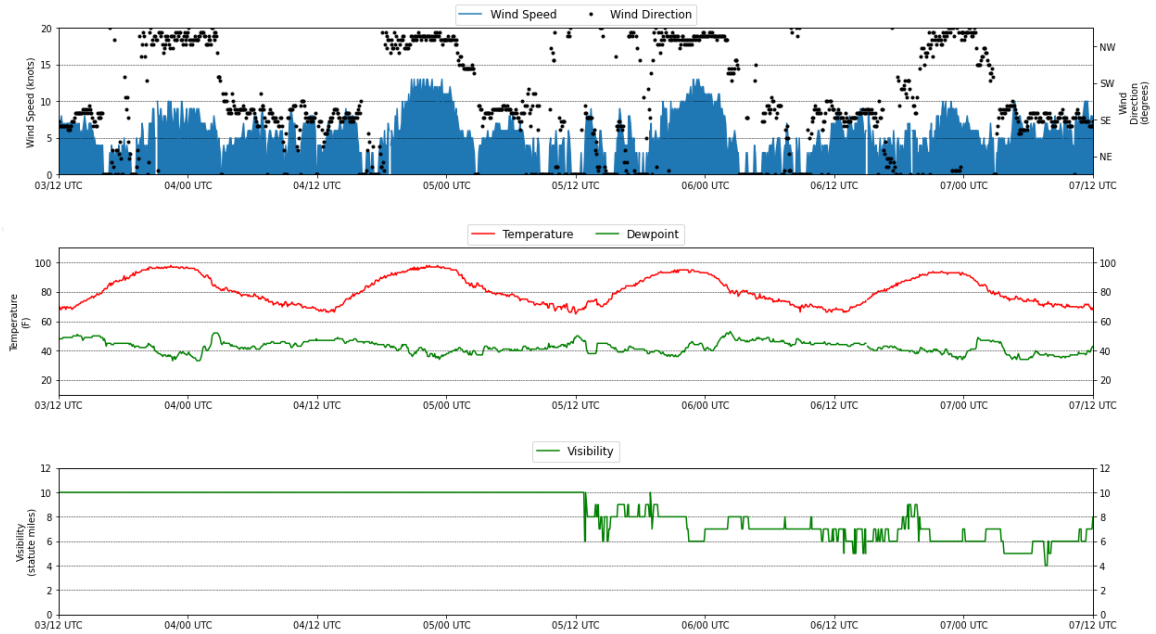

Figure 74. Surface observations from KSLC September 3 12Z - September 7 12Z of wind speed and direction (**top**), temperature and dewpoint (**middle**), and visibility (**bottom**).

3.3.2 Wildfire Conditions

Numerous wildfires across the western U.S were active September 5-6, leading to large plumes of accumulated wildfire smoke extending vast distances over the CONUS (**Figure 75 and 76**). As seen in **Figures 75 and 76**, visible satellite imagery indicates portions of these plumes drifted over northern Utah during the flagged event period. However, while satellite imagery clearly shows large swaths of heavy wildfire smoke in northern Utah on September 5-6, we further examine the characteristics of the wildfire conditions in order to better understand the spatiotemporal characteristics of wildfire smoke transport over the Wasatch Front September 5-6. A better knowledge of the spatial and temporal trends in wildfire smoke emissions is intended to draw a more complete picture between the arrival and departure of wildfire emissions and observed air quality trends in the Wasatch Front. To complete the wildfire smoke analysis, we analyze the progression of wildfire smoke transport before, during, and after the flagged episode. Similar to the previous wildfire analysis for the flagged events on August 4, 2016 and September 2, 2015, we utilize a variety of products and analysis tools to track the transport and presence of wildfire smoke across the Wasatch Front on September 5-6. These tools include HRRR Smoke analyzed smoke fields (vertically integrated and near-surface smoke), visible satellite imagery with GFS 0.25 degree analyzed 500 mb heights and wind barbs from September 4 18Z - September 7 00Z, HMS smoke and fire products, ground and satellite observed aerosol and wildfire smoke emission tracer observations.

Figure 75 - MODIS Terra/Aqua True Color Image Sept. 5

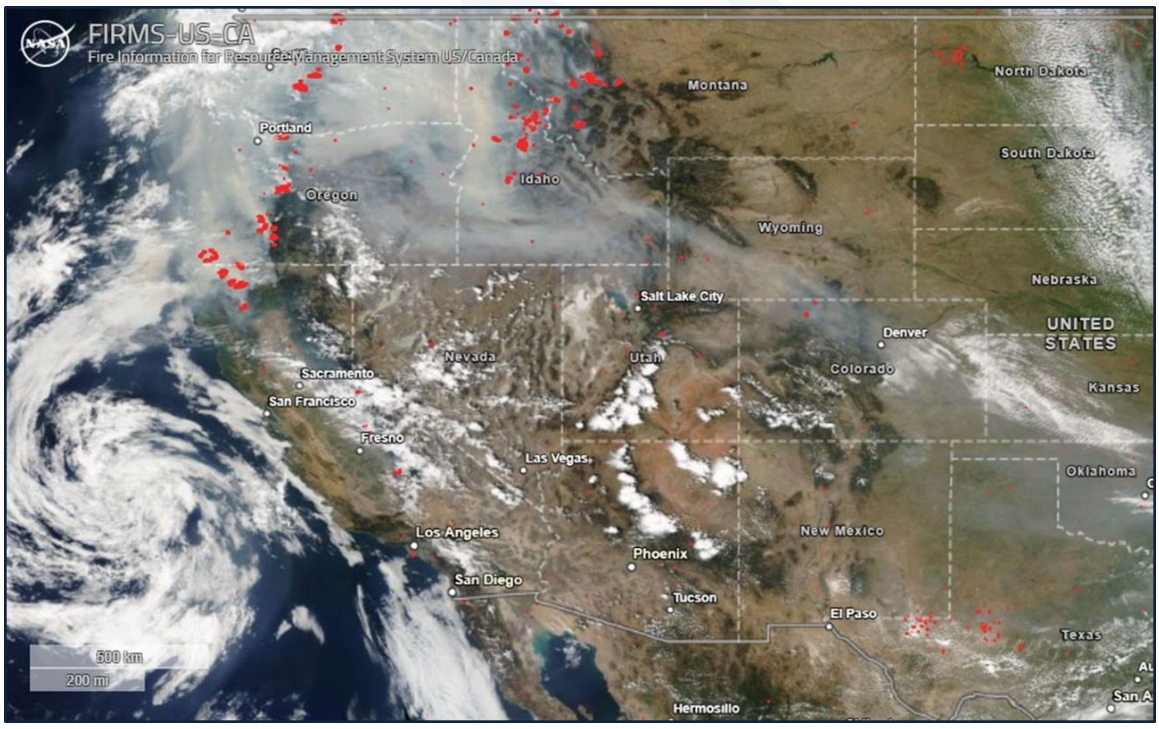

Figure 75. MODIS Terra/Aqua True Color image on September 5, 2017. Red markers indicate VIIRS/MODIS active fire detections and thermal anomalies (hot spot detection).
(Source: https://firms.modaps.eosdis.nasa.gov/usfs/map/).

Figure 76 - MODIS Terra/Aqua True Color Image Sept. 6

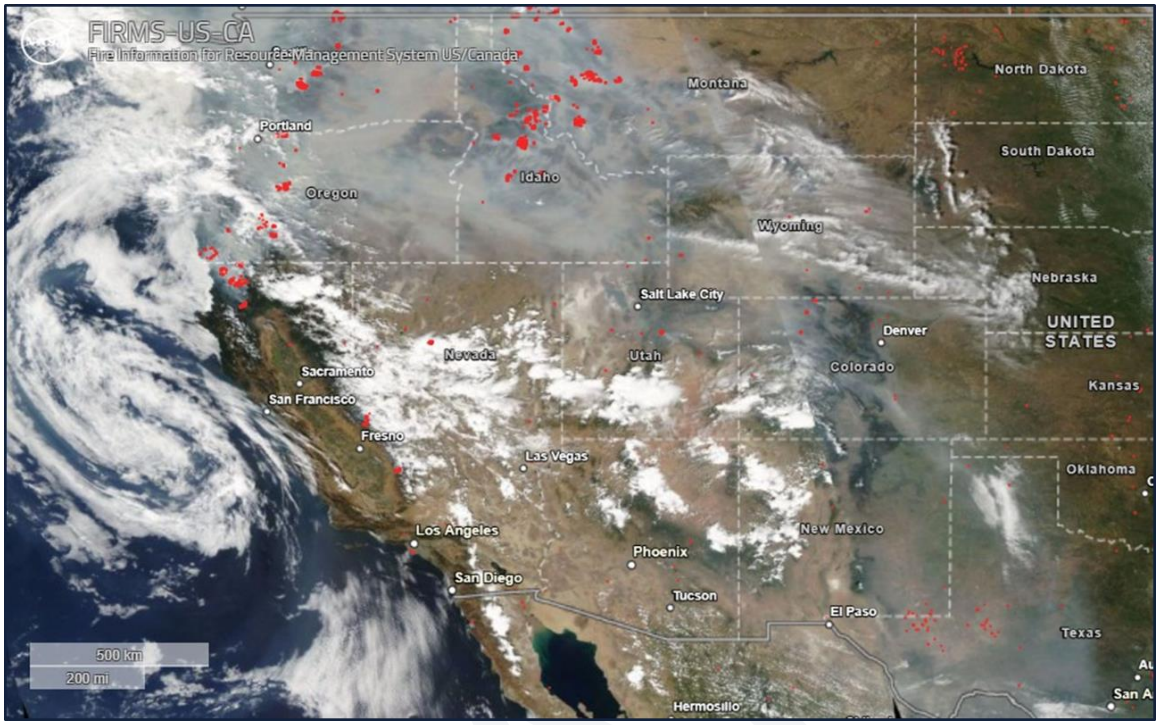

Figure 76. MODIS Terra/Aqua True Color image on September 6, 2017. Red markers indicate VIIRS/MODIS active fire detections and thermal anomalies (hot spot detection).
(Source: https://firms.modaps.eosdis.nasa.gov/usfs/map/).

Satellite imagery and HRRR Smoke products illustrate the progression of wildfire smoke across the Wasatch Front from September 4-7 (**Figures 77-79**). We include the periods of September 4 and September 7 in the satellite and HRRR Smoke analysis to identify the arrival and departure timing of wildfire emissions relative to the flagged event period. In **Figures 77-79**, the smoke field evident in the visible satellite imagery and HRRR Smoke fields reveal how the wildfire smoke plume was transported under the upper-level ridge by the mean winds September 4-7. This transport was roughly directed NW to SE from the PNW down to the southern Great Plains, with wildfire smoke shown to incrementally increase across the Wasatch Front and become heavy on September 5-6. HRRR Smoke fields show the smoke was moderate to dense with the maximum mass of vertically integrated and near-surface smoke occurring on the afternoon of September 6. Additionally, the differential between the HRRR vertically integrated and near-surface smoke fields indicates that the wildfire smoke over the Wasatch Front was composed of both elevated and near-surface smoke (**Figure 79**).

The HMS smoke tool supports the satellite and HRRR Smoke analysis by highlighting a large swath of heavy and dense smoke that stretched from multiple wildfire complexes, identified by MODIS/VIIRS hot spot detection, in northern California, Oregon, Washington, Idaho, Montana, and British Columbia, Canada (**Figures 80 and 81**). The southern flank of this dense smoke plume is noted to extend across the Wasatch Front on both September 5 and September 6. Aerosol remote sensing instrumentation and satellite show elevated AOD values of 0.5-.75 on September 5 and 1-1.5 on September 6, supporting the presence of dense wildfire smoke across the Wasatch Front (**Figures 82-84**). AOD's for visible light

(wavelengths 400-700 nm) are < 0.10 are a typical clear day. In addition, elevated aerosol index layer values of 4-5, derived from satellite, were observed over the Wasatch front September 5-6 (**Figure 85**). For reference, an aerosol index value of 5 indicates heavy concentrations of biomass burning smoke located in the lower troposphere.

Figure 77 - GOES East True Color Image Sept. 4-7 - West CONUS

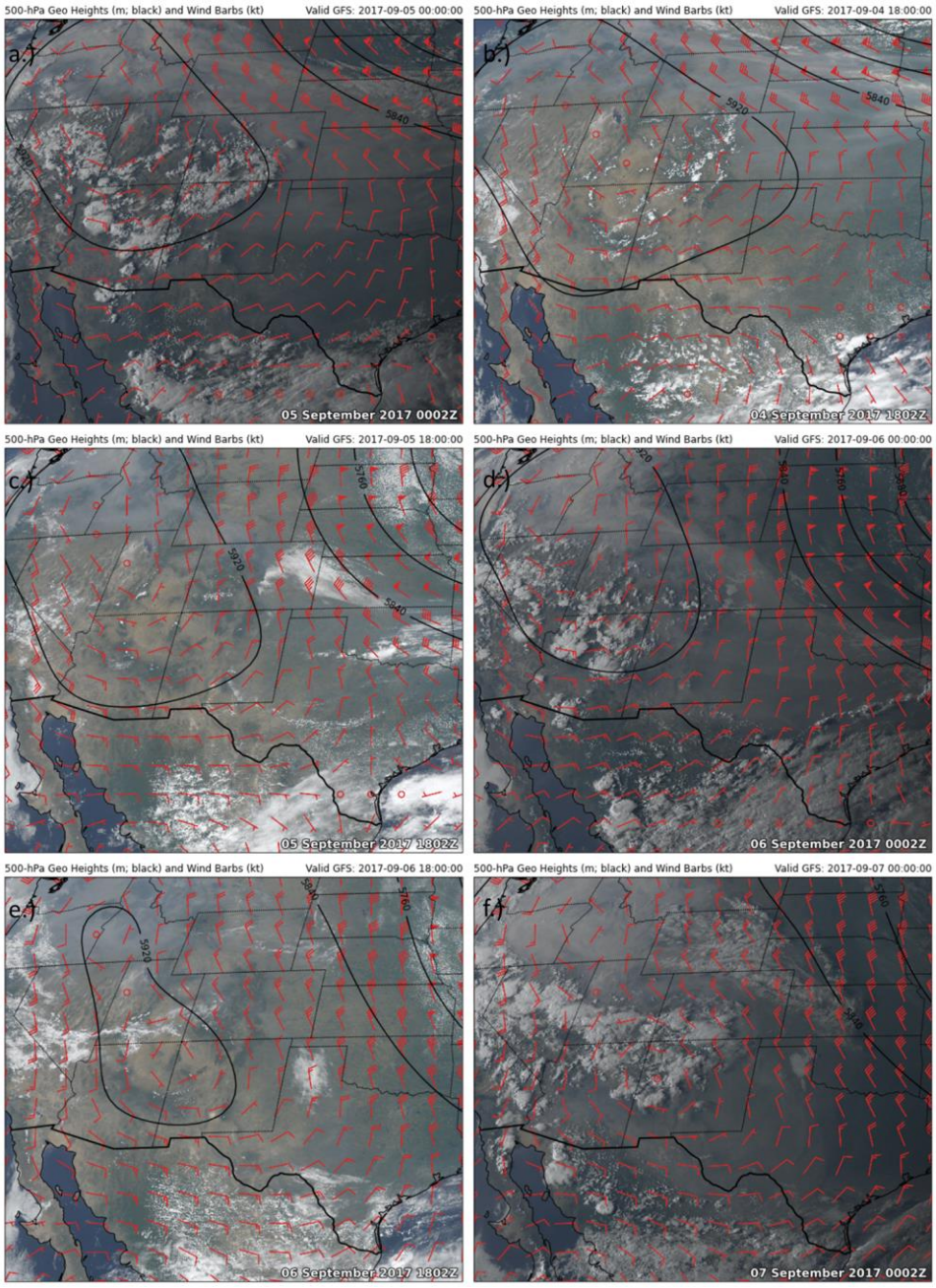

Figure 77. GOES East True Color imagery focused over the Intermountain West with GFS0p5 degree analyzed 500 mb geopotential heights and winds for **a.)** 2017-09-04 18Z, **b.)** 2017-09-05 00Z, **c.)** 2017-09-05 18Z, **d.)** 2017-09-06 00Z, **e.)** 2017-09-06 18Z, and **f.)** 2017-09-07 00Z.

Figure 78 - GOES East True Color Image Sept. 4-7 - Utah

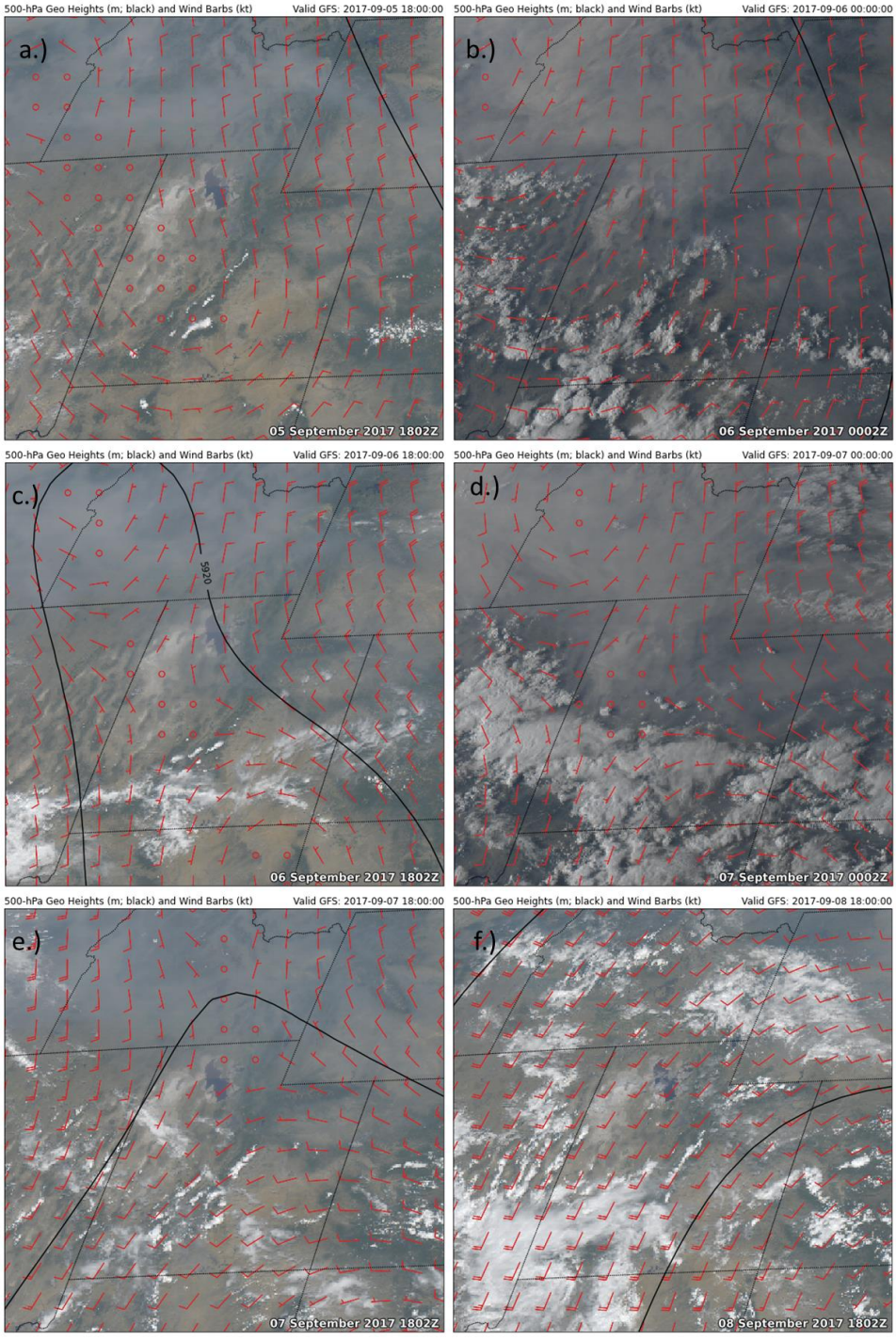

Figure 78. GOES East True Color imagery focused over Utah with GFS0p5 degree analyzed 500 mb geopotential heights and winds for **a.)** 2017-09-05 18Z, **b.)** 2017-09-06 00Z, **c.)** 2017-09-06 18Z, **d.)** 2017-09-07 00Z, **e.)** 2017-09-07 18Z, and **f.)** 2017-09-08 00Z.

Figure 79 - HRRR Smoke Near-Surface and Vertically Integrated Smoke Sept. 5-7

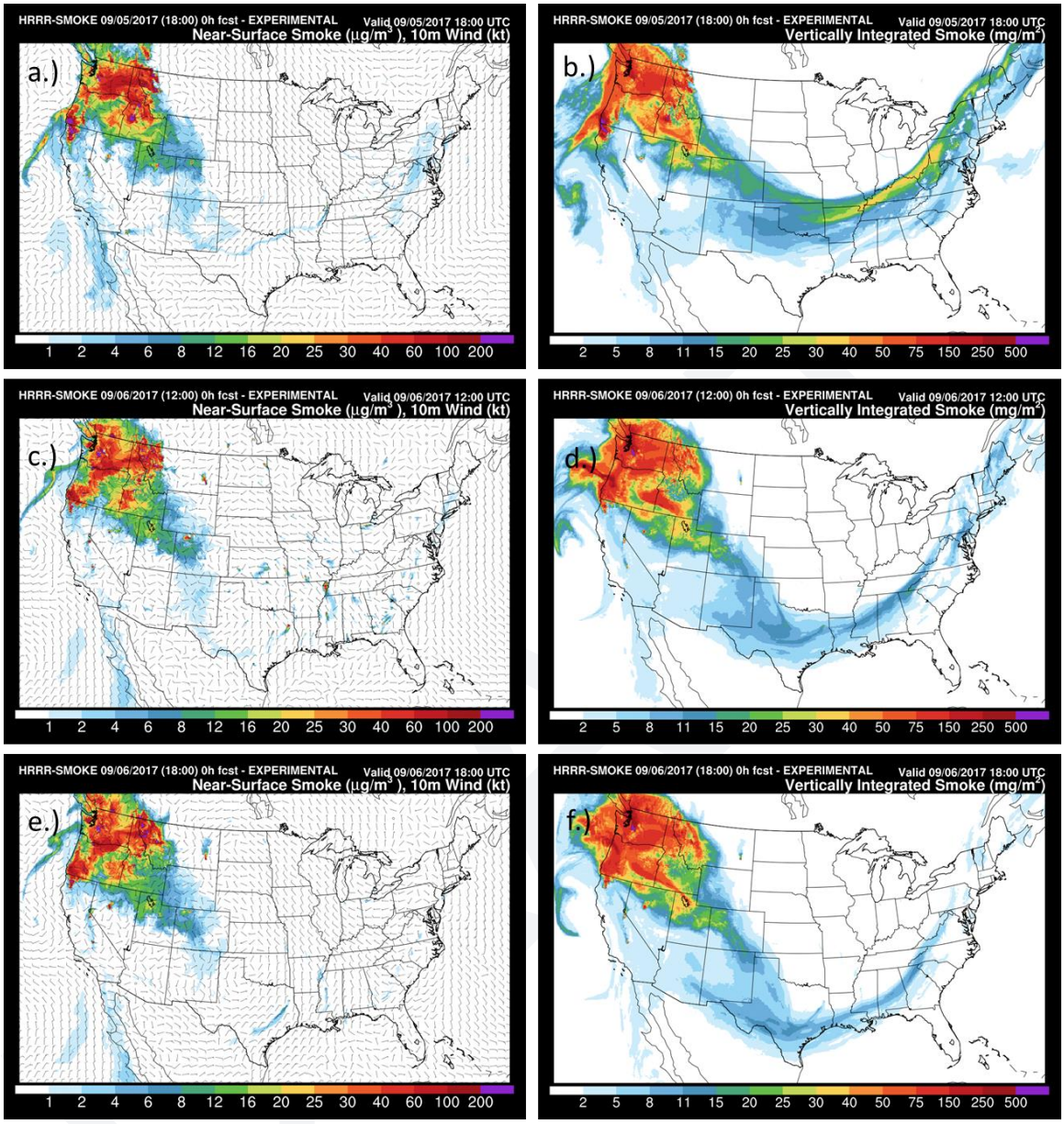

Figure 79. HRRR SMOKE analyzed near-surface smoke ($\mu g/m^3$) **a.)** 2017-09-05 18Z, **c.)** 2017-09-06 18Z, and **e.)** 2017-09-07 18Z; Vertically integrated smoke (mg/m^2) on **b.)** 2017-09-06 00Z, **d.)** 2017-09-07 00Z, and **f.)** 2017-09-08 00Z.

Figure 80 - HMS Smoke Detection Sept. 5

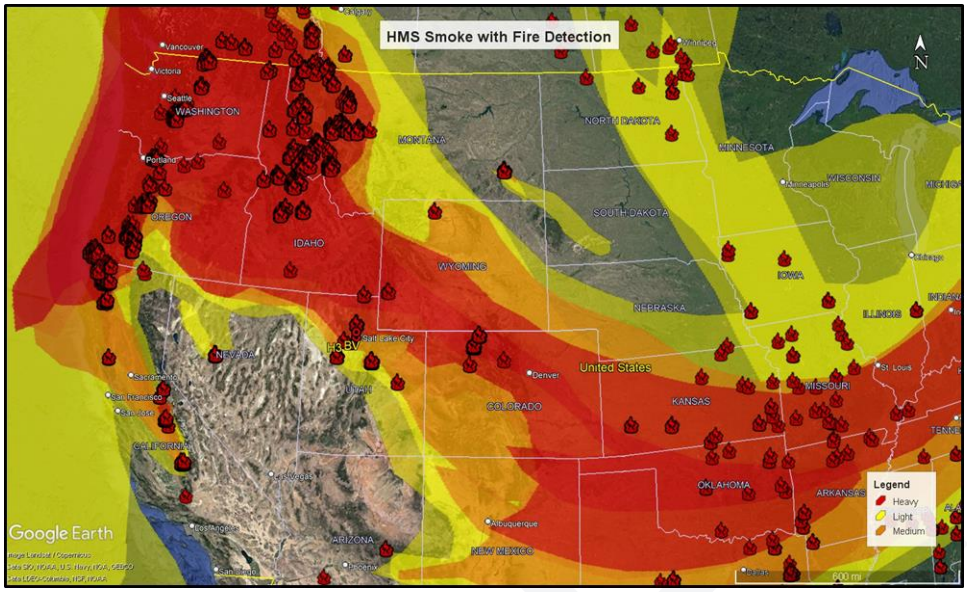

Figure 80. HMS smoke detection (yellow: light smoke, orange: moderate smoke, and red: heavy smoke) and VIIRS/MODIS active fire detections and thermal anomalies (**red flames**) on September 5, 2017. UDAQ monitors (HW, BV, and H3) are marked (**yellow filled circles**).
(Source: https://globalfires.earthengine.app/view/hms-smoke).

Figure 81 - HMS Smoke Detection Sept. 6

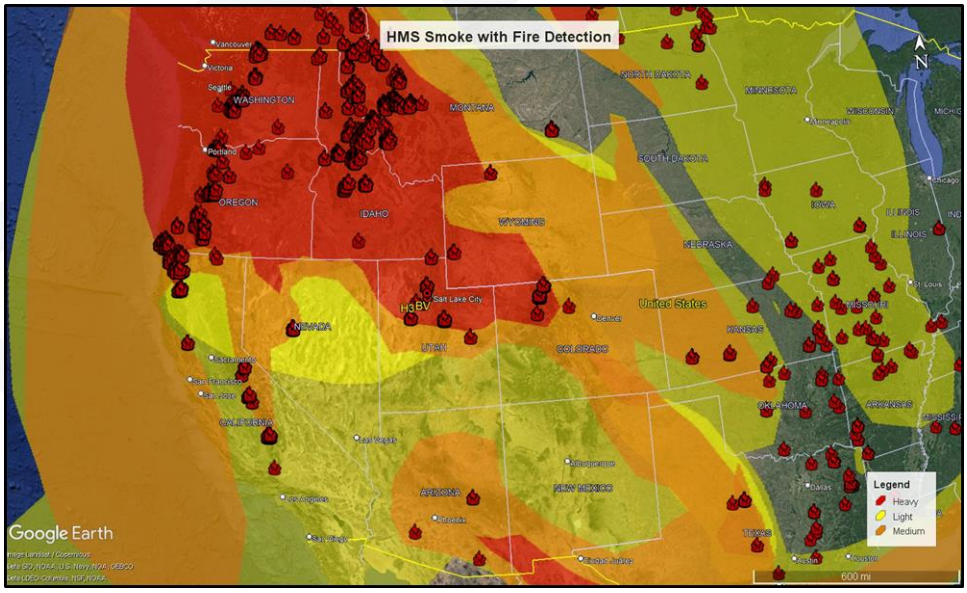

Figure 81. HMS smoke detection (yellow: light smoke, orange: moderate smoke, and red: heavy smoke) and VIIRS/MODIS active fire detections and thermal anomalies (**red flames**) on September 6, 2017. UDAQ monitors (HW, BV, and H3) are marked (**yellow filled circles**).
(Source: https://globalfires.earthengine.app/view/hms-smoke).

Figure 82 - MODIS Terra/Aqua MAIAC AOD Sept. 5

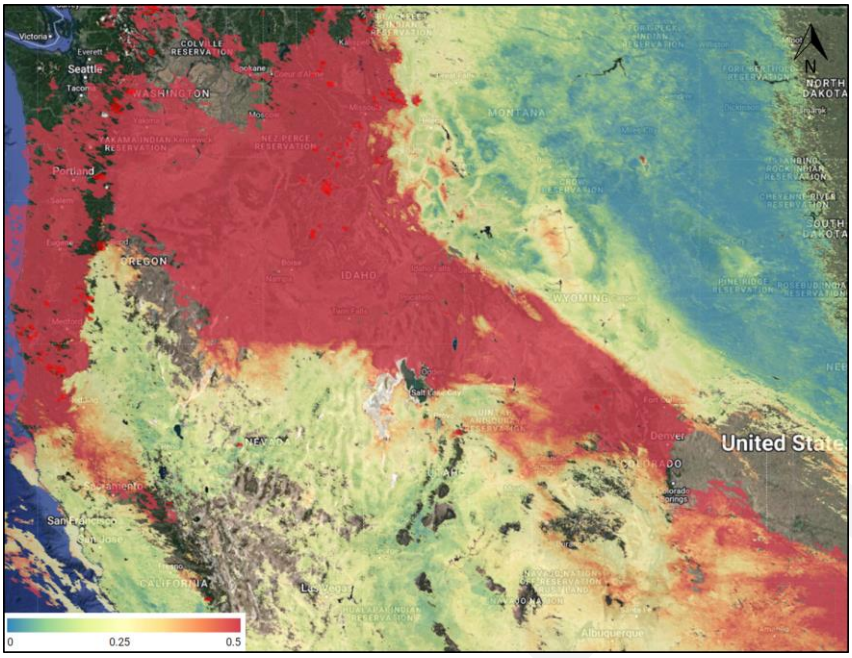

Figure 82. MODIS Terra/Aqua MAIAC Optical Depth (AOD) at 550 nm on September 5, 2017. Red markers indicate VIIRS/MODIS active fire detections and thermal anomalies (hot spot detection).
(Source: https://firms.modaps.eosdis.nasa.gov/usfs/map/)

Figure 83 - MODIS Terra/Aqua MAIAC AOD Sept. 6

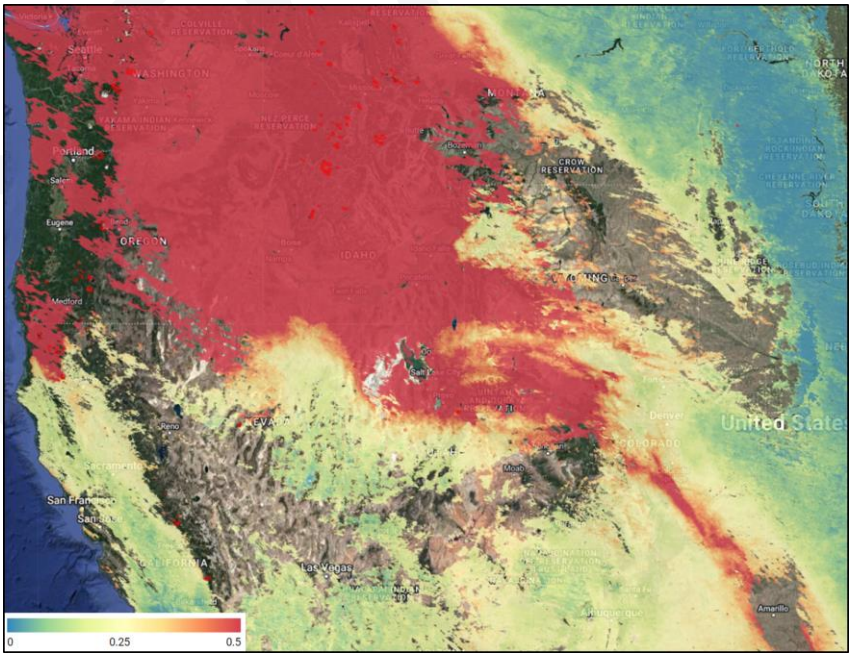

Figure 83. MODIS Terra/Aqua MAIAC Optical Depth (AOD) at 550 nm on September 6, 2017. Red markers indicate VIIRS/MODIS active fire detections and thermal anomalies (hot spot detection).
(Source: https://firms.modaps.eosdis.nasa.gov/usfs/map/)

Figure 84 - AERONET AOD Sept. 5-6

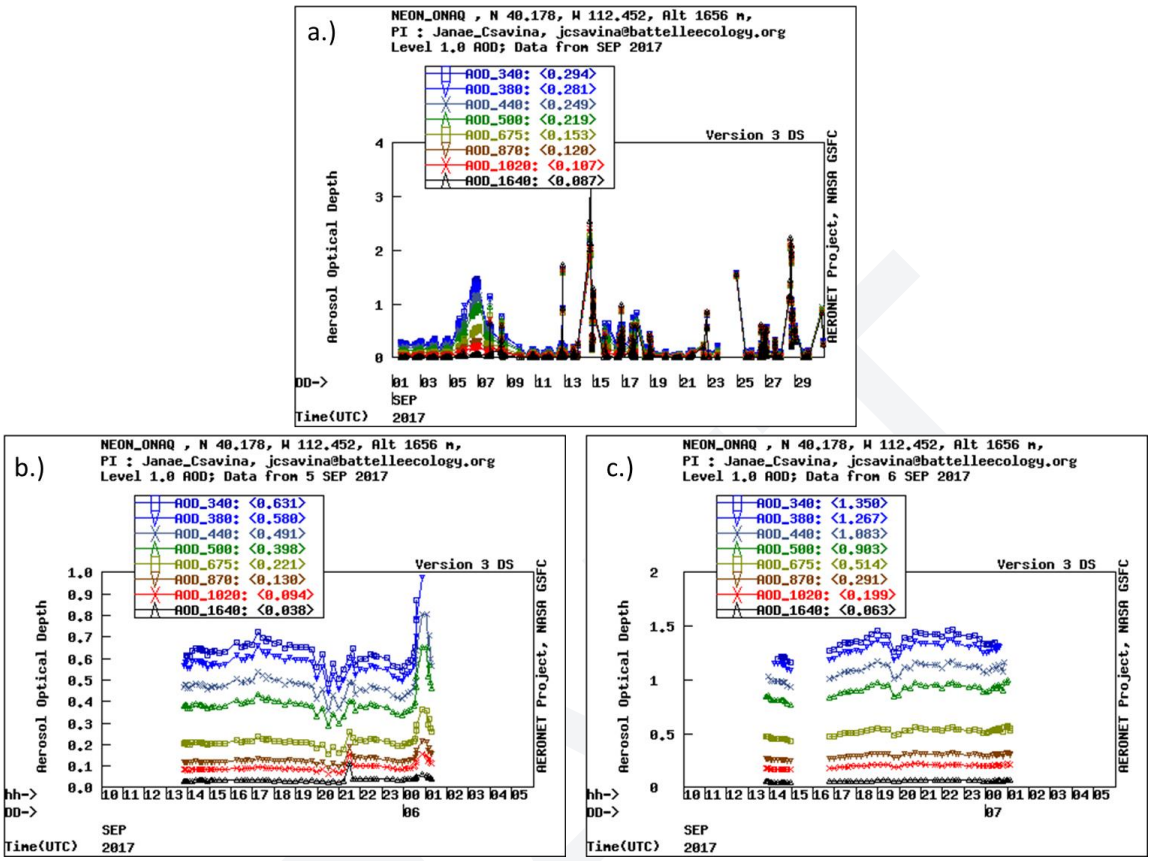

Figure 84. Time series of Aerosol Optical Depth (AOD) measured by the AERONET observation network at NEON_ONAQ site (40.17759 N, 112.45244 W) for **a.)** September 1-30, 2017, **b.)** September 5 13Z - September 6 01Z, and **c.)** September 6 13Z - September 7 01Z. (Source: https://aeronet.gsfc.nasa.gov)

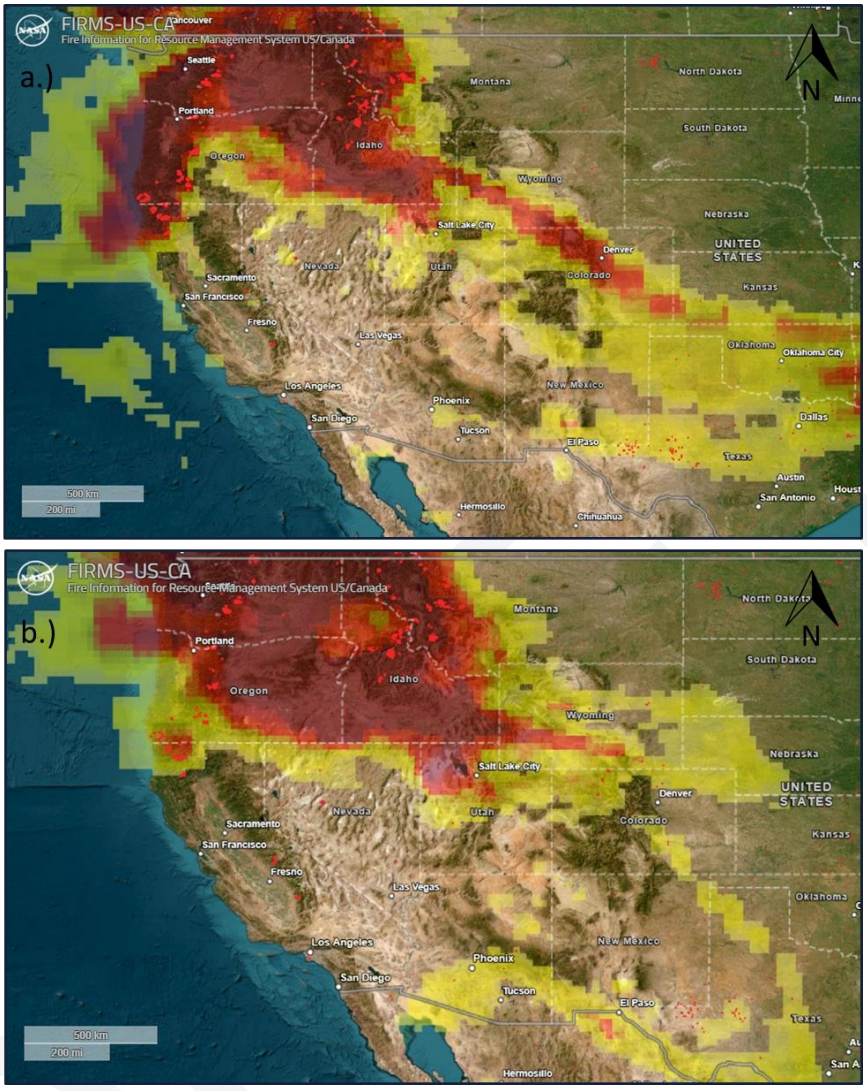

Figure 85. The OMPS Aerosol Index layer on **a.)** September 5, 2017 and **b.)** September 6, 2017. OMPS Aerosol Index layer indicates the presence of ultraviolet (UV)-absorbing particles in the air (aerosols) such as soot particles in the atmosphere; it is related to both the thickness of the aerosol layer located in the atmosphere and to the height of the layer. The Aerosol Index is a unitless range from < 0 to >= 5, where 5 indicates heavy concentrations of aerosols that are related to biomass burning smoke located in the lower troposphere (1-3 km). (Source: https://firms.modaps.eosdis.nasa.gov/usfs/map/)

In **Figures 86-89**, the analysis from GMAO's MERRA-2 shows the total column and surface mass of black and organic on September 5-6. Both black and organic carbon are produced and emitted from wildfires, which makes these emissions excellent tracers for wildfire smoke transport. The analyzed aerosol transport of black and organic carbon from MERR-2 reveals the placement and trajectory of the dense wildfire smoke plume extending from the large wildfire complexes in the PNW and northern Rockies to the southeast across the intermountain west and southern Great Plains. The aerosol transport vectors show transport that closely follows the upper level ridge circulation, with black and organic carbon transported from NW to SE over the western U.S. Elevated surface and total column black and organic

carbon concentrations were observed over the Wasatch Front on both September 5 and 6, corresponding to the heavy swath of smoke analyzed by the HMS smoke product. Black and organic carbon total column concentrations ranged from 70-90 mg/m² and 7-8 mg/m² on September 5, respectively, and >= 100 mg/m² and >=10 mg/m² on September 6, respectively (**Figure 86 and 87**). Surface mass concentrations of black and organic carbon were 3-9 μg/m³ and 72-80 μg/m³ on September 5, respectively, and 6-9 μg/m³ and >=80 μg/m³ on September 6, respectively (**Figure 88 and 89**). The extremely high levels of black and organic carbon further support the presence of very dense near-surface and elevated wildfire smoke emissions over the Wasatch Front.

Figure 86 - MERRA-2 Vertically Integrated OC Sept. 5-7

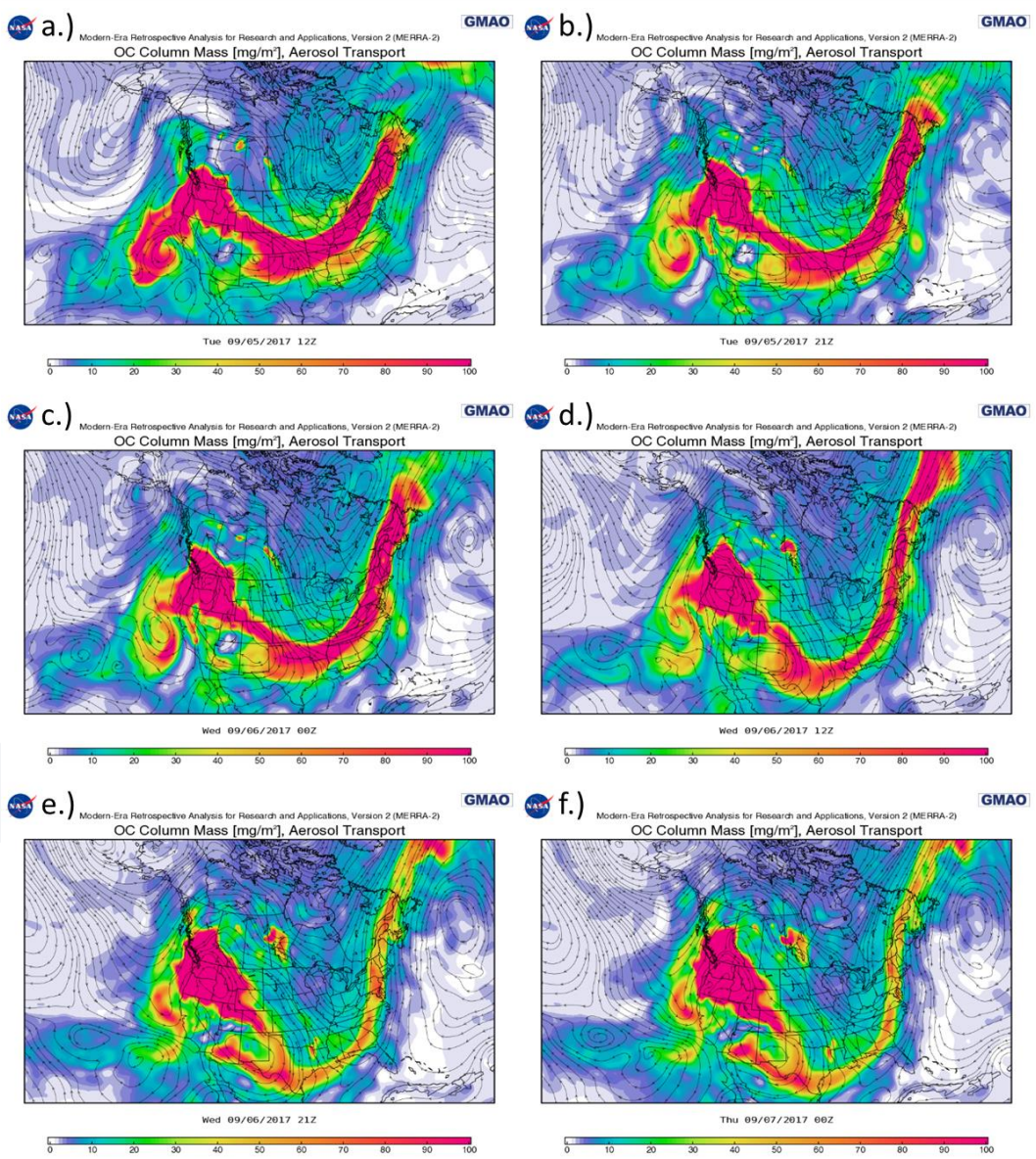

Figure 86. MERRA-2 satellite and model analyzed vertically integrated (column mass mg/m²) organic carbon (OC) with aerosol transport vectors for **a.)** 2017-09-05 12Z, **b.)** 2017-09-05 21Z, **c.)** 2017-09-06 00Z, **d.)** 2017-09-06 12Z, **e.)** 2017-09-06 21Z, and **f.)** 2017-09-07 00Z.

Figure 87 - MERRA-2 Vertically Integrated BC Sept. 5-7

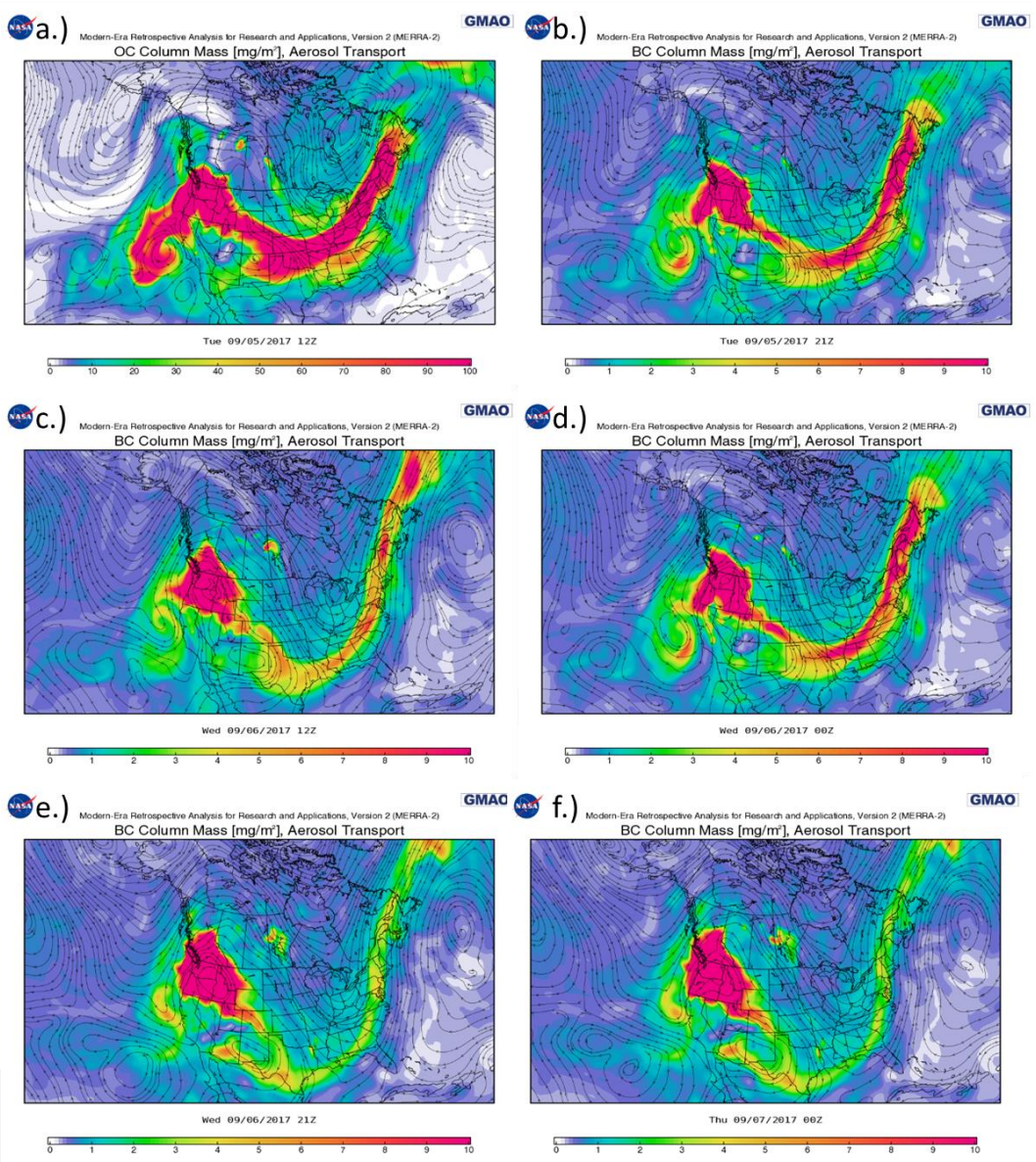

Figure 87. MERRA-2 satellite and model analyzed vertically integrated (column mass) organic carbon (OC) with aerosol transport vectors for **a.)** 2017-09-05 12Z, **b.)** 2017-09-05 21Z, **c.)** 2017-09-06 00Z, **d.)** 2017-09-06 12Z, **e.)** 2017-09-06 21Z, and **f.)** 2017-09-07 00Z.

Figure 88 - MERRA-2 Surface Mass OC Sept. 5-7

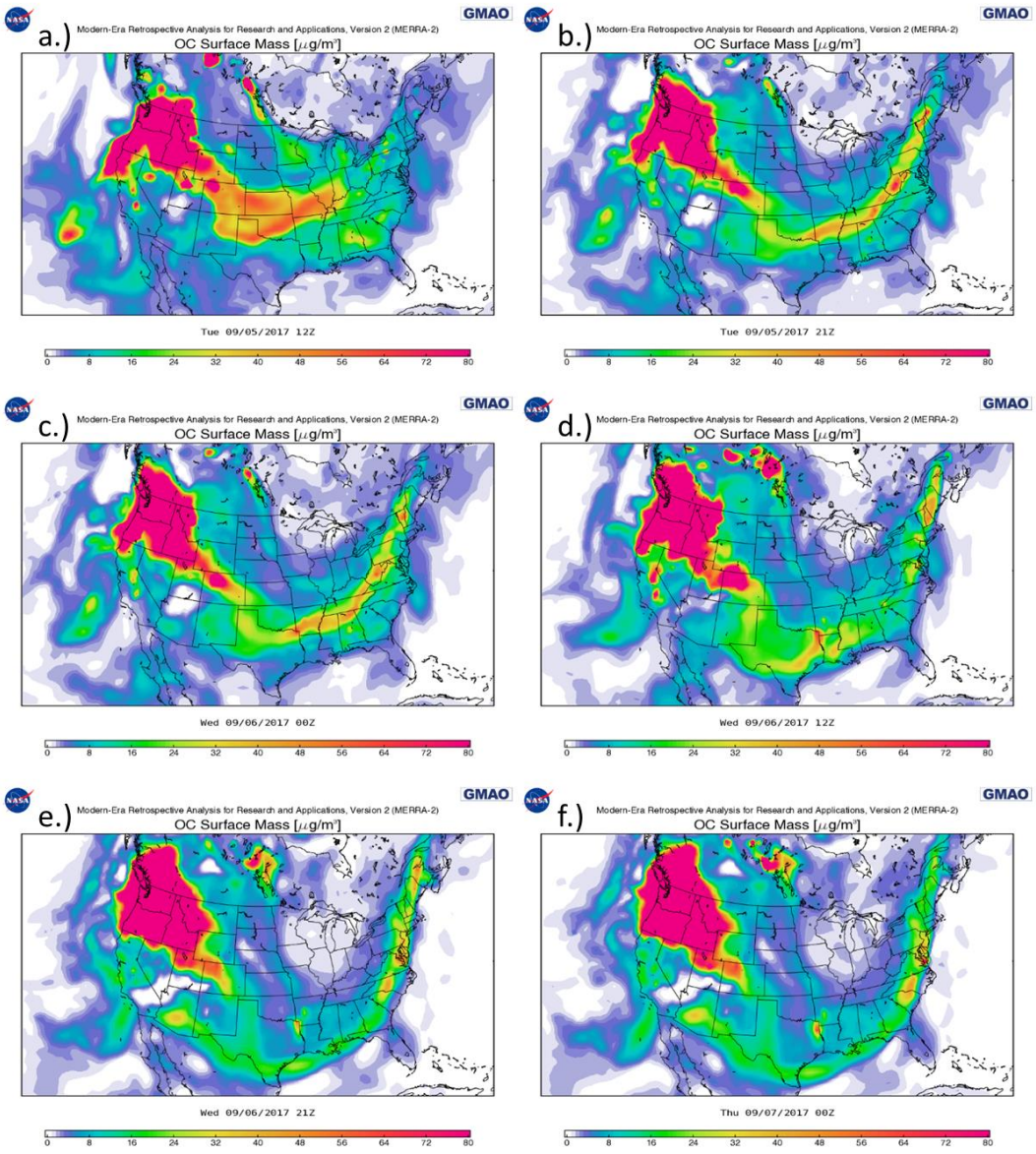

Figure 88. MERRA-2 satellite and model analyzed surface mass organic carbon (OC) for **a.)** 2017-09-05 12Z, **b.)** 2017-09-05 21Z, **c.)** 2017-09-06 00Z, **d.)** 2017-09-06 12Z, **e.)** 2017-09-06 21Z, and **f.)** 2017-09-07 00Z.

Figure 89 - MERRA-2 Surface Mass BC Sept. 5-7

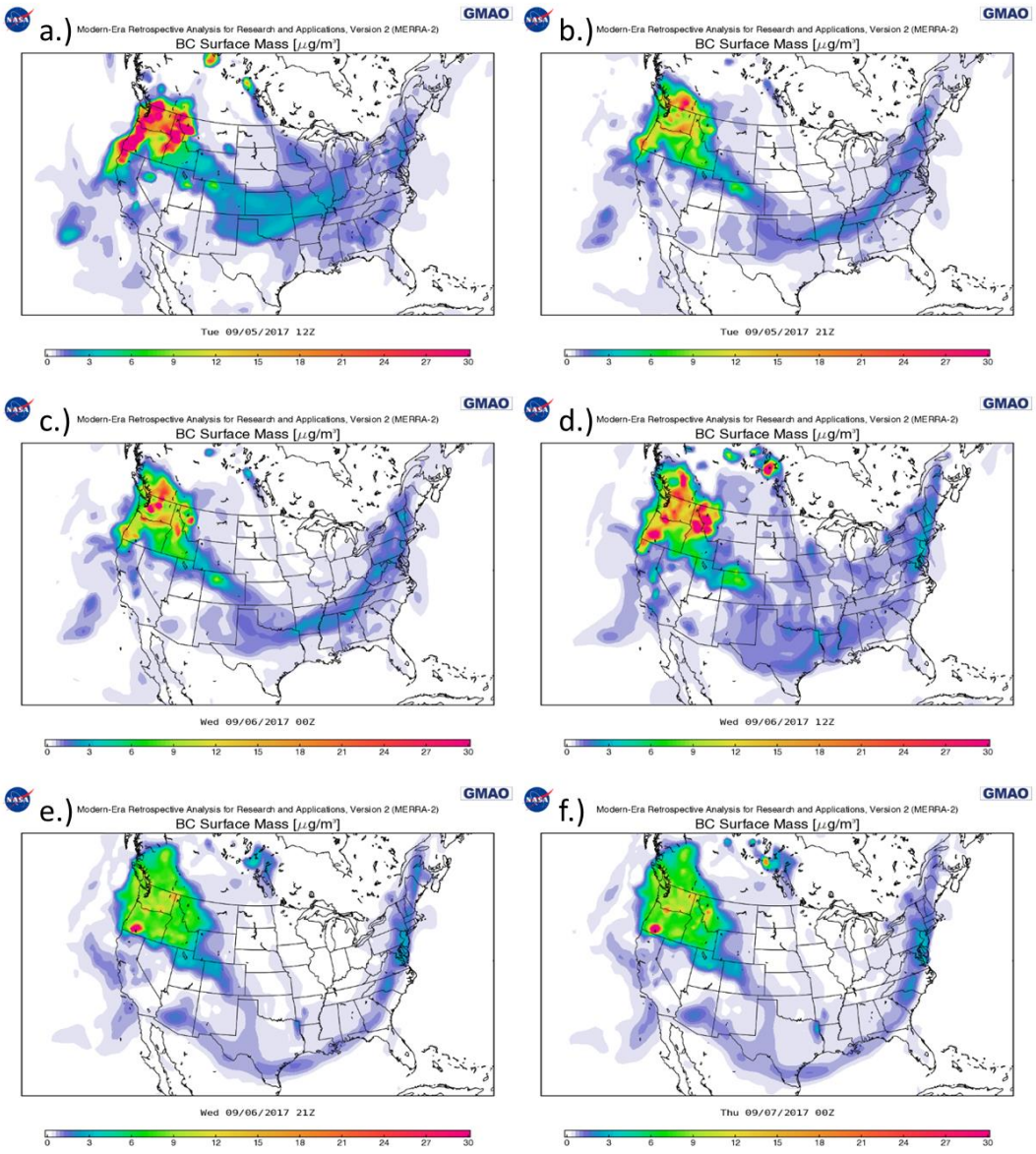

Figure 89. MERRA-2 satellite and model analyzed surface mass black carbon (BC) for **a.)** 2017-09-05 12Z, **b.)** 2017-09-05 21Z, **c.)** 2017-09-06 00Z, **d.)** 2017-09-06 12Z, **e.)** 2017-09-06 21Z, and **f.)** 2017-09-07 00Z.

We funnel our analysis down to the surface by examining captured video time-lapse of the Salt Lake Valley before, during, and after the flagged event period. The arrival of wildfire smoke, as observed from the surface, can be seen by snapshots of the Salt Lake Valley from September 4-7 (**Figure 90**). On September 4, visibility was relatively good (>= 10 statute miles). However, moving forward into September 5-6 it is evident that heavy and dense wildfire smoke had inundated the Wasatch Front (**Figure 90b and 90** on September 7 (**Figure 90d**). The decrease in wildfire smoke on September 7 in the Salt Lake Valley is exhibited in **Figure 90d**, where visibility increased to >= 10 statute miles.

Figure 90 - Camera Images Salt Lake Valley Sept. 4-7

Figure 90. Snapshots from the University of Utah-MesoWest WBBS camera (perspective: downtown facing south in the Salt Lake Valley) on **a.)** 2017-09-04, **b.)** 2017-09-05, **c.)** 2017-09-06, and **d.)** 2017-09-07.

3.3.3 Event Analysis September 5-6, 2017

Following the analysis structure from the previous event analysis sections, in this section we synthesize the meteorological and wildfire conditions analysis as it relates to trends and concentrations of observed air quality variables relevant to wildfire emissions impacting O3. This analysis is meant to provide a guide relating the presence of wildfire smoke and impact on the observed MD8A O3 exceedances during the flagged event period. Time series of wildfire tracer concentration, including PM2.5, CO, and brown carbon are given to help distinguish the impact of wildfire smoke on O3 enhancement at the monitoring sites HW, BV, and H3 (**Figures 91-95**). Furthermore, particle trajectories are computed in HYSPLIT to identify the potential source regions and transport path of wildfire smoke emissions observed at UDAQ monitors on September 5-6. The investigation of tracer trends, MD8A O3 concentrations, and parcel trajectories combined with the meteorological and wildfire spatiotemporal variability analysis provides a link between wildfire smoke transport across the Wasatch Front and high O3 concentrations. Based on this analysis, there is convincing evidence that the presence of wildfire smoke had a significant impact on the MD8A O3 exceedances on September 5-6.

A strong upper level ridge was situated across the western U.S on September 5-6, which is characteristic of a typical summer synoptic pattern and conducive to wildfire ignition and proliferation.

Meteorological analysis reveals that the mean synoptic circulation under the upper level ridge rotated clockwise, transporting a large conglomerate mass of wildfire smoke emissions from the northwest portion of the CONUS to southeast across the intermountain west. The main contributors to this accumulated mass of wildfire smoke were fire complexes located in northern California, Oregon, Washington, Idaho, Montana, and even British Columbia, Canada. We know from the wildfire smoke analysis that the smoke emitted by these sources had a residence time in the atmosphere of at least 3-4 days before making its way into Utah. Therefore, the plume can be characterized as aged. As was observed by satellite, HMS, and other wildfire smoke products, the dense plume of wildfire smoke drifted over the Wasatch Front on September 5-6. This smoke was composed of elevated and near-surface wildfire emissions, which potentially provided a reservoir of O3 precursor emission species and O3 itself from the elevated portions of the aged smoke plume. The potential transport of these reservoir species from upper levels to the surface is illustrated by the analyzed deep PBL mixed layer depths and presence of subsidence under the upper level evident in the soundings from KSLC on September 5-6. Based on this meteorological analysis, it is likely that turbulence mechanisms entrained and mixed elevated smoke emissions from the FA down through the PBL mixed layer to the near-surface. These processes had the potential to exacerbate the impact of wildfire smoke on surface O3 chemistry and enhanced concentrations.

Figure 91 - HW: MD8A and PM2.5 Sept. 3-10

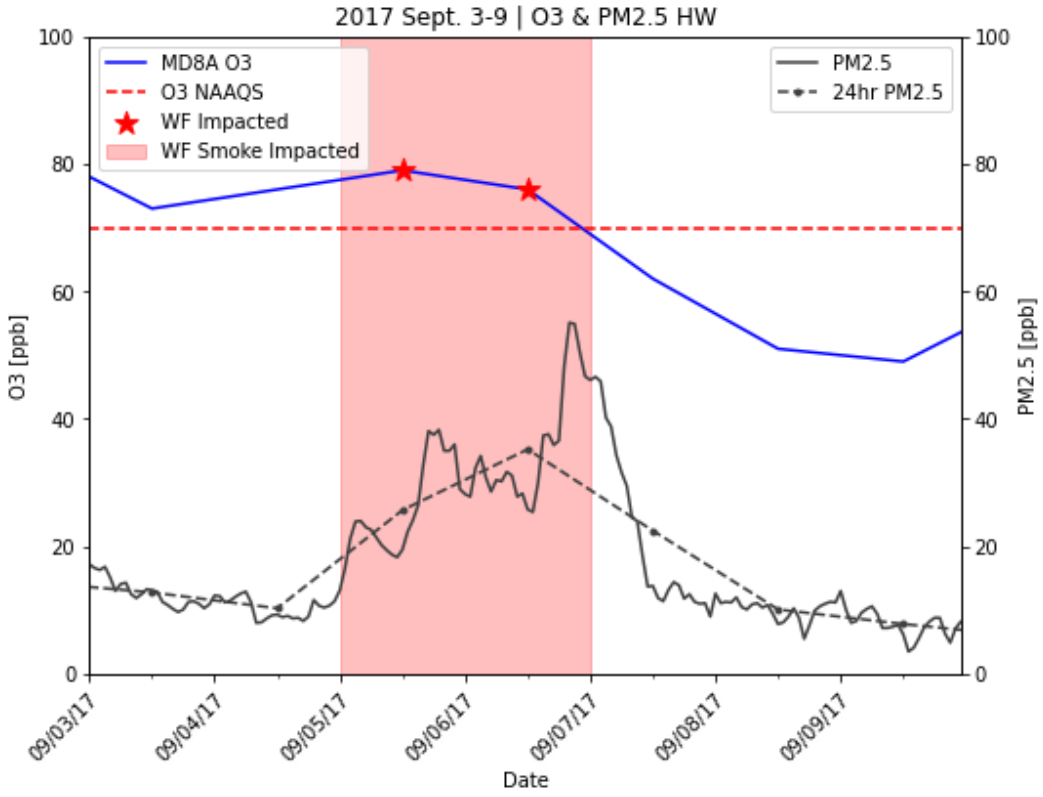

Figure 91. Observed concentrations at the HW monitor of MD8A O3 concentrations **(blue solid line)**, PM2.5 (**black solid line**), 24hr averaged PM2.5 (**dashed black line**). The 2015 MD8A O3 NAAQS is overlaid (**red dashed line**) and the red shaded area represents the event period. Red star marks the MD8A O3 value impacted by wildfire smoke.

Figure 92 - BV: MD8A and PM2.5 Sept. 3-10

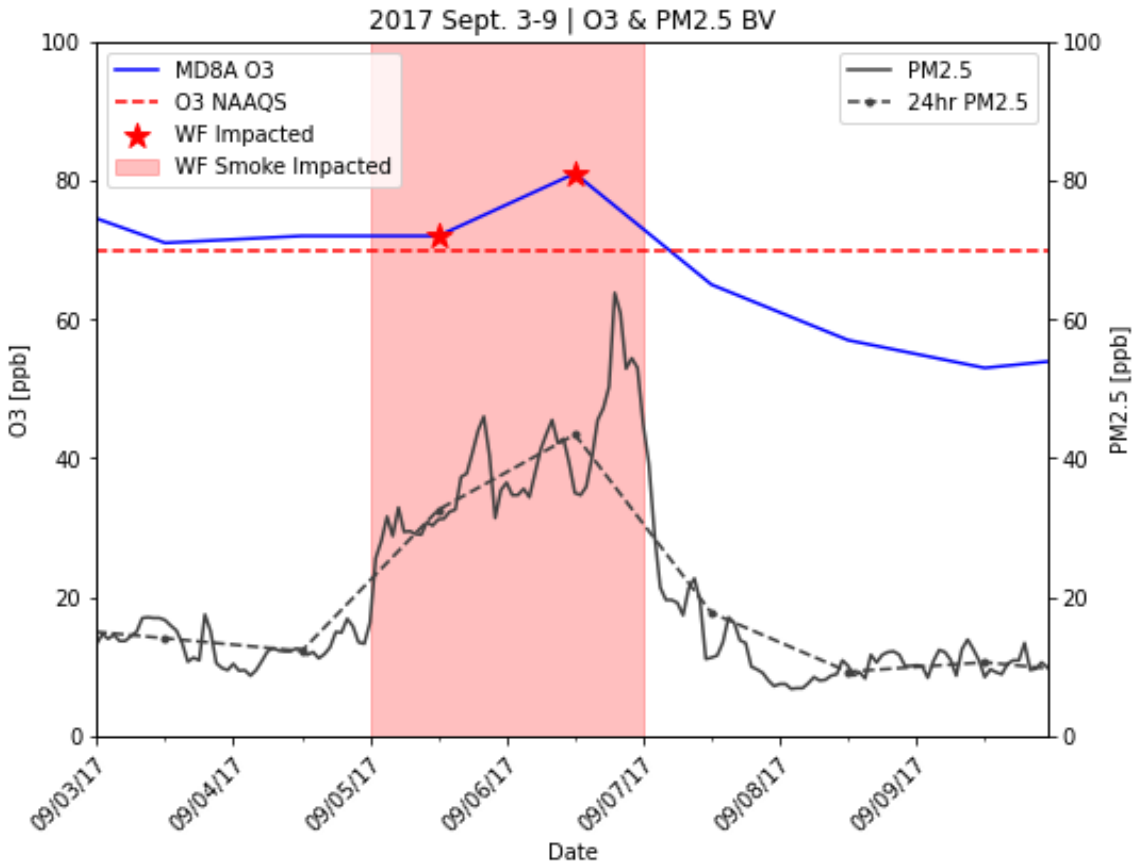

Figure 92. Observed concentrations at the BV monitor of MD8A O3 concentrations **(blue solid line)**, PM2.5 (**black solid line**), 24hr averaged PM2.5 (**dashed black line**). The 2015 MD8A O3 NAAQS is overlaid (**red dashed line**) and the red shaded area represents the event period. Red star marks the MD8A O3 value impacted by wildfire smoke.

Figure 93 - H3: MD8A and PM2.5 Sept. 3-10

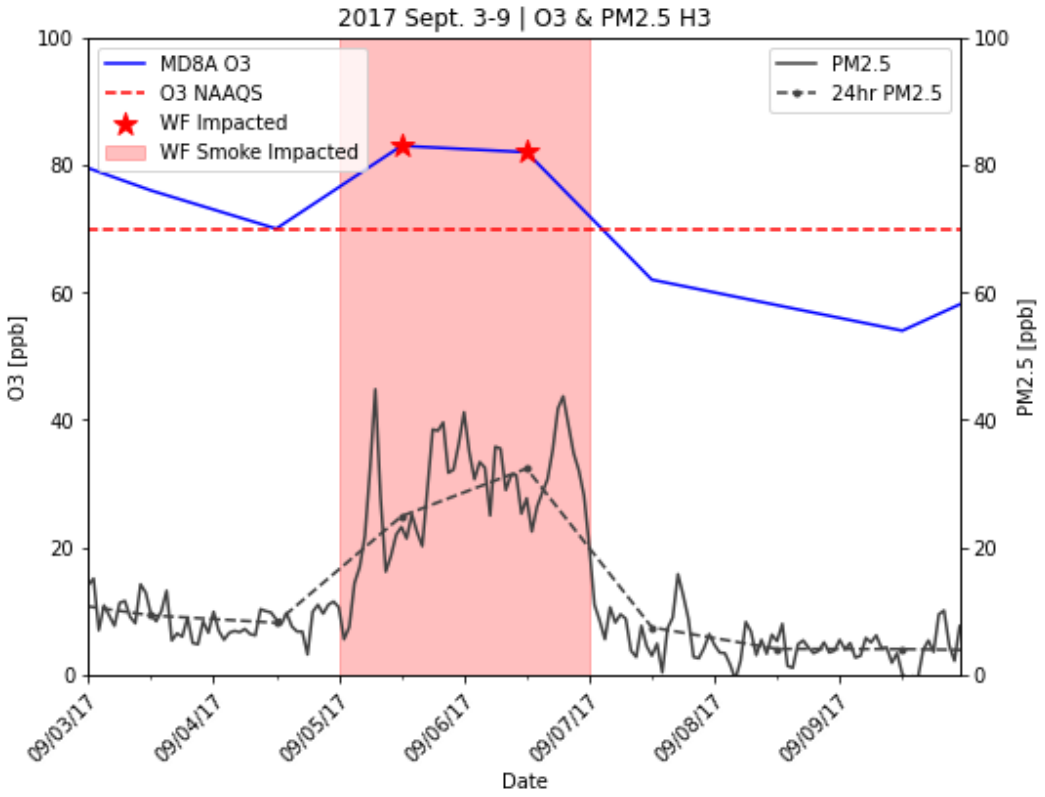

Figure 93. Observed concentrations at the H3 monitor of MD8A O3 concentrations **(blue solid line)**, PM2.5 (**black solid line**), 24hr averaged PM2.5 (**dashed black line**). The 2015 MD8A O3 NAAQS is overlaid (**red dashed line**) and the red shaded area represents the event period. Red star marks the MD8A O3 value impacted by wildfire smoke.

Figure 94 - HW: CO Sept. 3-10

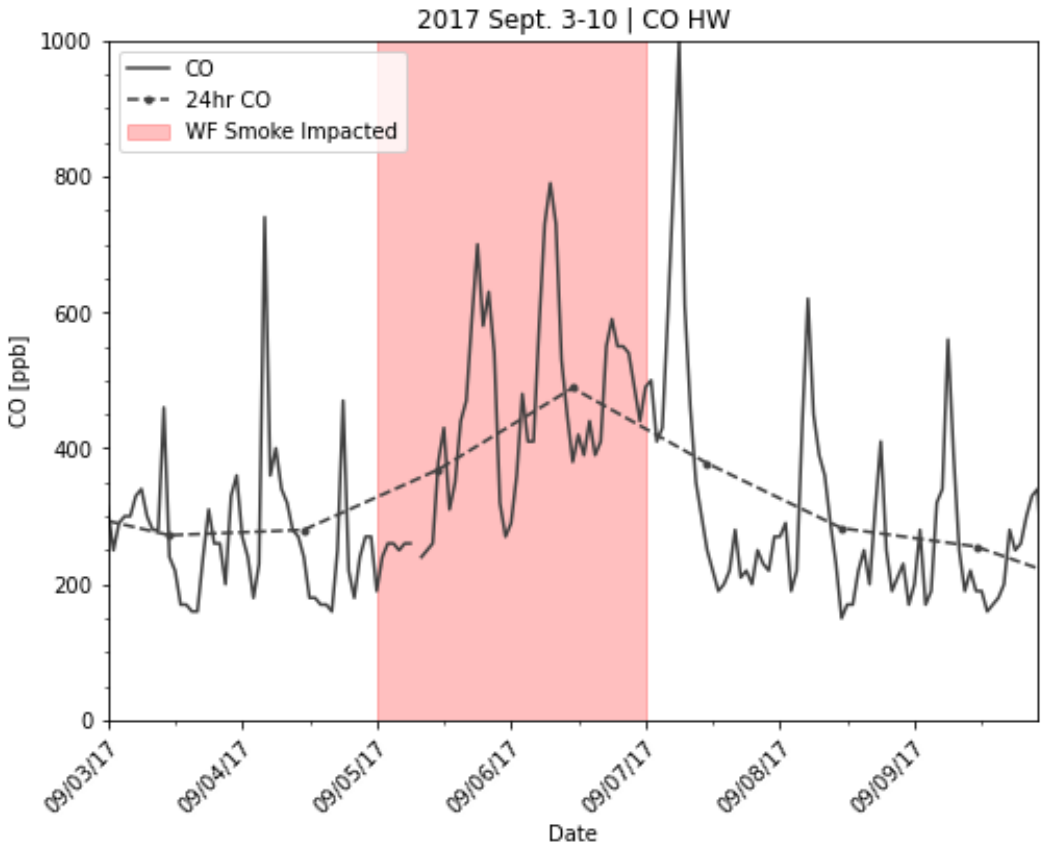

Figure 94. Observed Carbon monoxide (CO) hourly observations (ppb) from HW (**solid black line**) and 24-hour average CO (**dashed black line**). The red shaded area represents the flagged event period September 5-6.

Figure 95 - BV: Brown Carbon Sept. 3-10

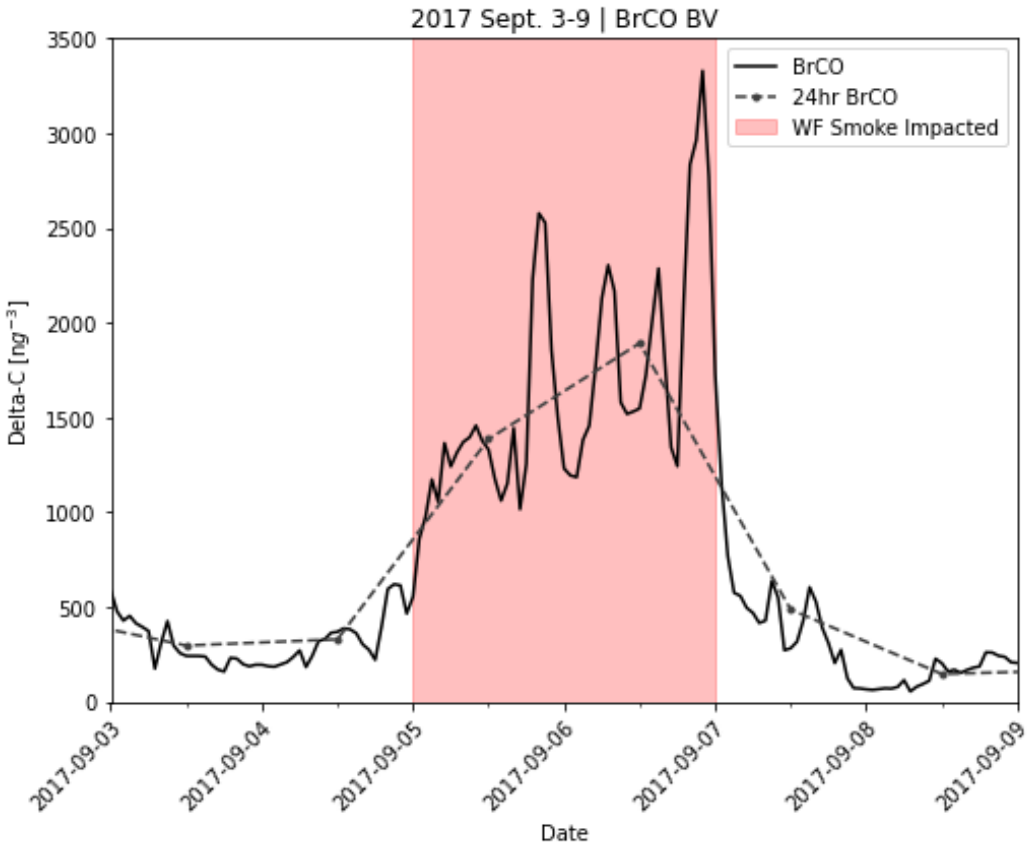

Figure 95. Brown carbon (Delta) observations (**black solid line**), 24-hour average brown carbon (**dashed black lin**e) at the BV UDAQ site September 3-9. Red shaded area represents the flagged event period September 5-6.

Ground based observations of PM2.5 are available from the HW, BV, and H3 monitors and CO and brown carbon are available from HW and BV, respectively. The time series of these observed wildfire tracers are given in **Figures 91-95**, with a focused time series of PM2.5 at the three UDAQ monitors given in **Figure 96**. At each monitoring site, there is a clear positive trend in PM2.5, CO, and brown carbon that corresponds with the arrival of the plume of wildfire smoke, as analyzed by HMS, satellite, and HRRR Smoke, on September 5 and extends through September 6. Elevated levels of PM2.5, CO, and brown carbon are noted to remain above normal background concentrations through the flagged period, peaking on September 6 when wildfire smoke was the densest. A summary of the 24hr average concentrations of these tracers and MD8A O3 is given in **Table 8**. Average background concentrations and statistics of PM2.5, CO, and brown carbon are given for respective sites in **Table 9**. All monitoring sites observed PM2.5, CO, and brown carbon above the 95th percentile for available records. Relative to the period preceding and proceeding the flagged event, the observed MD8A concentrations of O3 reveal O3 peaked on September 5-6 at the monitoring sites. This peak in O3 concentrations corresponds with the high concentrations of wildfire smoke tracers and presence of wildfire smoke. After September 6, O3 is noted to sharply decline in conjunction with a steep decrease in observed wildfire smoke tracers. From satellite and smoke products, we know that after September 6 wildfire smoke was rapidly transported away from

the Wasatch Front due to a change in the mean synoptic circulation. This shift in the mean winds is detailed in the previous section on the meteorological analysis. The concurrent positive and negative trends in both the wildfire tracers and O3 bolsters the argument that wildfire smoke helped create enhanced O3 concentrations at the monitors during the flagged period, and exhibits a clear relationship between the trend of MD8A O3 and wildfire smoke tracers.

A few other factors indicate wildfire smoke impacted O3 concentrations, including surface meteorological characteristics. On September 5 and 6, temperatures were cooler than the preceding days and had less incident solar radiation exhibited by the high values of derived ground and satellite based AOD. A thicker AOD equates to greater attenuation of solar radiation by the presence of thick wildfire smoke. The lower temperatures and decreased solar radiation should have dampened O3 production based on typical meteorological conditions conducive to O3 formation. Nevertheless, observed O3 concentrations on the flagged days were equal or higher than the observed MD8A O3 concentrations on the preceding days of September 3 and 4 (**Figures 91-93** and **Table 8**). The main contributing factor to this discrepancy in the archetypal model of O3 formation was the introduction of large amounts of wildfire smoke emissions composed of O3 precursor species. Otherwise, without the contributions from wildfire smoke O3 concentrations potentially would have been lower given the slightly cooler temperatures and significantly thick AOD.

Figure 96 - Observed PM2.5 at HW, BV, and H3 Sept. 3-10

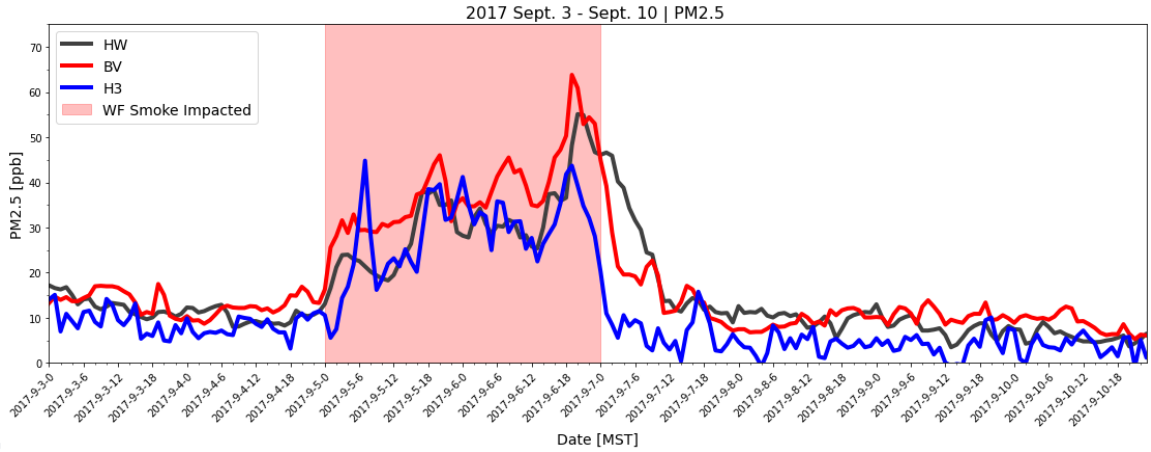

Figure 96. Hourly PM2.5 concentrations at HW, BV, and H3 for September 3-10. Red highlighted area represents the flagged wildfires smoke impacted period September 5-6.

Table 8 - 24hr MD8A, PM2.5, CO, and Brown Carbon Sept. 4-7

	HW			BV			H3	
Date	MD8A O3 (ppb)	24hr PM2.5 (ppb)	24hr CO (ppb)	MD8A O3 (ppb)	24hr PM2.5 (ppb)	24hr BrC	MD8A O3 (ppb)	24hr PM2.5 (ppb)
9/4/2017	76	10.3	280	72	12.25	328.7	70	8.2
9/5/2017	**79**	**25.6**	**368.7**	**72**	**32.6**	**1385.6**	**83**	**24.9**
9/6/2017	**76**	**35.2**	**488.75**	**81**	**43.4**	**1891.7**	**82**	**32.4**
9/7/2017	72	22.4	377.9	65	17.7	485.2	62	7.5

Table 8. MD8A O3, PM2.5, CO, and brown carbon 24hr observations (where available) from HW, BV, and H3 September 4-7.

Table 9 - HW: PM2.5 and Brown Carbon Statistics Sept. 3-8

Date	24hr PM2.5	Monthly Avg. PM2.5	95th percentile PM2.5	24hr BrC	Monthly Avg. BrC	95th percentile BrC
09-03-17	12.7	6.9	15.9	295.5	276.5	585.2
09-04-17	10.3	6.9	15.9	328.6	276.5	585.2
09-05-17	**25.6**	**6.9**	**15.9**	**1385.6**	**276.5**	**585.2**
09-06-17	**35.2**	**6.9**	**15.9**	**1891.7**	**276.5**	**585.2**
09-07-17	22.4	6.9	15.9	485.1	276.5	585.2
09-08-17	10.1	6.9	15.9	145.6	276.5	585.2

Table 9. PM2.5 and brown carbon concentration statistics at HW September 3-8.

To locate the approximate source and trajectory path of wildfire smoke emissions at UDAQ monitors on September 5-6, we conducted HYSPLIT 48hr backward ensemble trajectory analysis ending at the 1500m level above HW. The 1500m level was chosen due to the long-distance nature of wildfire smoke transport and the presence of weak synoptic forcing and relatively calm lower level winds during the flagged event periods. We utilized the HRRRv1 3km model as the meteorological input due to its higher spatial and temporal resolution, which can be advantageous in complex topography in certain situations. The ensemble trajectory approach allows trajectories to be calculated by slightly shifting the modeled meteorology in the vertical and horizontal, using the 27 ensemble members, and therefore is used as a tool to overcome possible model imprecisions. Ultimately, an ensemble approach is used to provide an average representation of the potential trajectory paths of emissions. In **Figure 97 and 98**, the HYSPLIT backward trajectories are shown for September 5 and 6 with HMS smoke fields and active wildfires overlaid. The backwards ensemble trajectory members are in fairly good agreement for both flagged episode days and indicate wildfire smoke emissions observed along the Wasatch Front originated from the numerous active wildfire complexes in the PNW, Idaho, and Montana.

Frequency 48hr backward HYSPLIT trajectory analysis was also completed to provide more detail on the "probability" that trajectories originated from certain areas (**Figure 99**). The frequency analysis uses both the HRRRv1 3km and GDAS 0.5 degree meteorological input to compare any variability in modeled source trajectory regions between higher and coarser resolution modeled meteorology, respectively. Similar to the ensemble approach, the frequency analysis exhibits a trajectory pattern where the areas with the highest probability of trajectories largely originate from the areas including the fire complexes across the PNW, Idaho, and potentially Montana. The backward trajectory paths in the ensemble and frequency analysis both correspond well to the direction of the mean circulation under the upper-level ridge described in the meteorological analysis section. This pattern substantiates that the upper level flow had a dominating impact on the transport of wildfire smoke emissions across the Wasatch Front on September 5 and 6.

Figure 97 - HYSPLIT HRRRv1 Ensemble 48hr Backward Trajectories Sept.7 00Z - Sept. 5 00Z

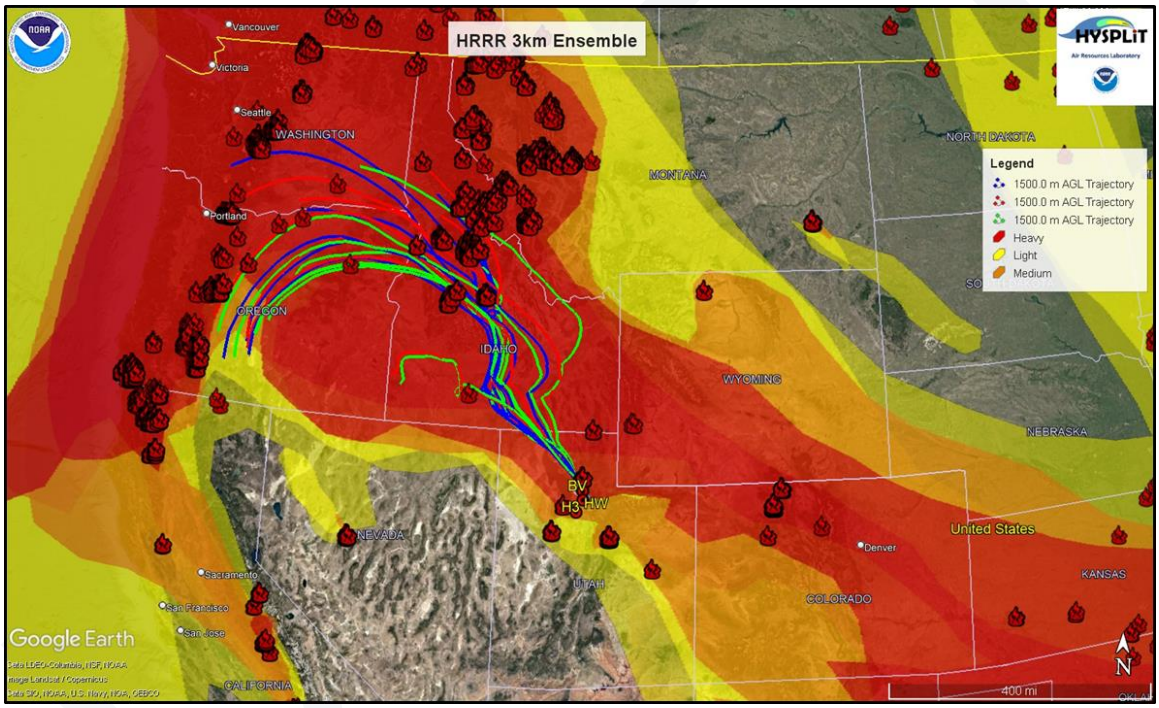

Figure 97. HYSPLIT HRRRv1 3km 27-member ensemble 48hr September 7 00Z - September 5 00Z backward trajectories ending at 1500m at the HW UDAQ monitor.

Figure 98 - HYSPLIT GDAS 0.5 Ensemble 48hr Backward Trajectories

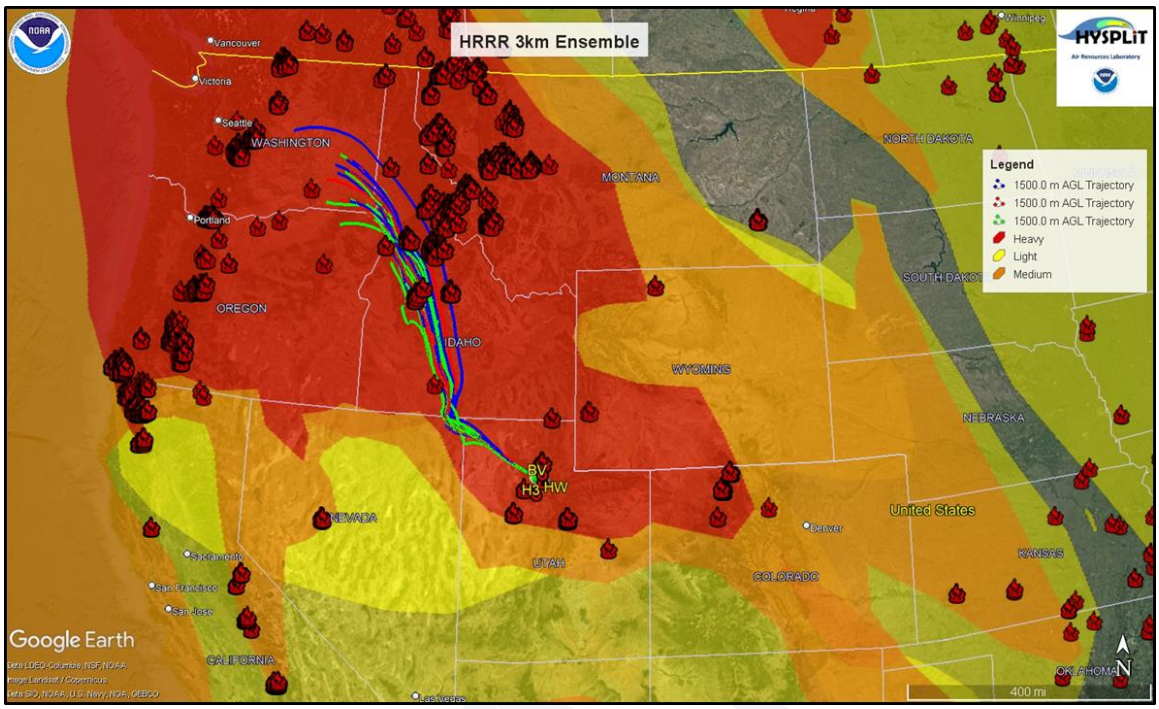

Figure 98. HYSPLIT GDAS 0.5 degree 27-member ensemble 48hr September 7 00Z - September 5 00Z backward trajectories ending at 1500m at the HW UDAQ monitor.

Figure 99 - HYSPLIT HRRRv1 and GDAS 0.5 Frequency 48hr Backward Trajectories Sept. 6 00Z - 2 06Z

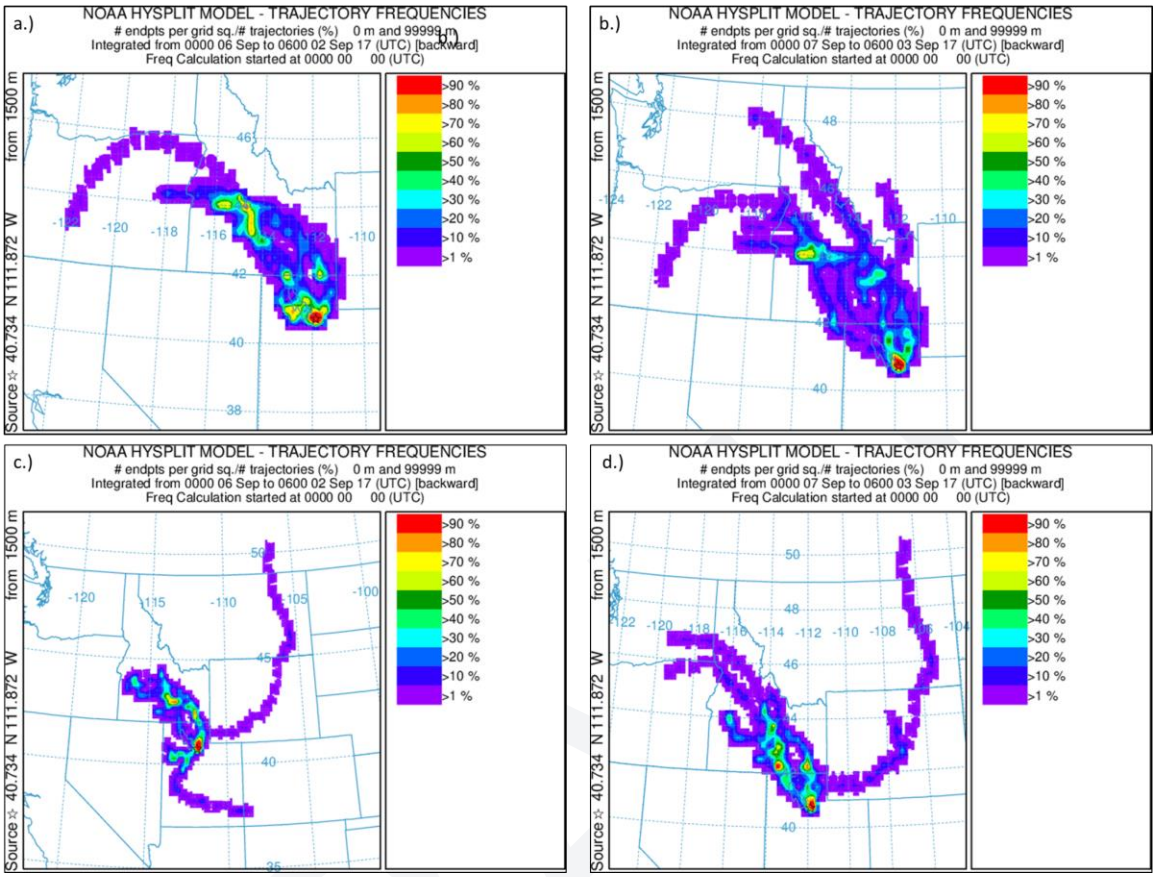

Figure 99. HYSPLIT HRRRv1 48hr backward frequency trajectory from HW for **a.)** September 6 00Z - September 2 06Z and **b.)** September 7 00Z - September 3 06Z; HYSPLIT GDAS 0.5 degree **c.)** September 6 00Z - September 2 06Z and **d.)** September 7 00Z - September 3 06Z.

4.0 Data Exclusion and Adjusted BDV

Although the flagged data from August 4, 2016, September 2, 2017, and September 5-6, 2017 potentially meets the criteria of the Exceptional Events Rule, no exceptional event documentation has been submitted on these flagged days by UDAQ for review to the EPA. This is because these flagged events were not deemed significant enough to affect the attainment/nonattainment status of the Wasatch Front nonattainment area. Therefore, no demonstration has been submitted to remove the data and the data has up until present remained in the dataset to calculate official design values. However, UDAQ has determined that the flagged event-influenced data from these days remain unrepresentative and impact the base and future year model design values for the SIP model attainment demonstration.

To counteract this potentially biased impact of event-influenced data on design value formulation, UDAQ has followed a process for excluding potentially event-influenced data when determining base design values as stated in Section 1.2. This process is described in EPA's modeling guidance, where determinations and analyses other than exceptional events are allowed when regarding mechanisms for possible monitoring data exclusion, selection, or adjustment. Specifically, monitoring data exclusion, selection, or adjustment may qualify for determinations if ambient data are not representative of base

period concentrations and have the potential to impact a determinative value in a past or projected time period. EPA acknowledges one appropriate situation when this process can be used includes the removal of air quality monitoring data when developing alternative base year and future year design values for SIP modeling in attainment demonstrations. Following these guidelines, UDAQ has flagged the four wildfire impacted events in AQS as "RT" and has readjusted design values and the baseline design value by excluding these flagged events. UDAQ has completed additional analyses by removing flagged days from the base year design value calculation to identify the impact on the baseline design and future design values as part of our modeling attainment demonstration. In the remainder of this section, we describe the adjustment of the 2017 baseline design value (BDV) by data exclusion and removal of the flagged wildfire smoke impacted O3 MD8A at the HW, BV, and H3 monitoring sites.

Table 10 - Event Period MD8A O3

Date	HW	BV	H3	Event Type	
	MD8A O3 (ppb)	MD8A O3 (ppb)	MD8A O3 (ppb)	Regional	Local
8/4/2016	81	80	83	✔	✔
9/2/2017	83	78	83	✔	✔
9/5/2017	79	72	83	✔	✔
9/6/2017	76	81	82	✔	✔

Table 10. MD8A O3 concentrations observed at HW, BV, and H3 on the four flagged wildfire impacted days. The source region of wildfire smoke is noted as regional (out of state) or local (in state).

Table 11 - 4th Max O3 Recalculation

	4th Maximum MD8A O3 Values (ppb)					
	HW		BV		H3	
	Date	MD8A O3	Date	MD8A O3	Date	MD8A O3
Old 4th Max 2016	8/1/2016	74	6/20/2016	76	6/27/2016	76
New 4th Max 2016	**8/2/2016**	**72**	**8/2/2016**	**74**	**8/1/2016**	**76**
Old 4th Max 2017	7/23/2017	81	9/2/2017	78	7/7/2017	78
New 4th Max 2017	**7/14/2017**	**79**	**7/4/2017**	**77**	**7/15/2017**	**74**

Table 11. Adjustment of the 4th maximum MD8A O3 values for HW, BV, and H3 by excluding the wildfire smoke impacted flagged data (New 4th Max).

Table 12 - Baseline Design Value Calculation with Data Excluded

Site-Specific Baseline Design Values:		**3-Year Average of 4th Max 8 Hour Average (ppb)**			**BDV** *Flagged Data* ***Included***	**BDV** *Flagged Data* ***Excluded***
Location	**County**	**2015-2017**	**2016-2018**	**2017-2019**		
Bountiful Viewmont	Davis	75	78	77	**76**	**75**
Hawthorne	Salt Lake	78	76	76	**76**	**75**
Herriman #3	Salt Lake	76	77	75	**76**	**74**

Table 12. 3-year design values and weighted 5-year BDV's for HW, BV, and H3 with and without wildfire smoke impacted flagged data removed. The adjusted BDV is shown in the far right column with flagged data excluded from the design value calculations.

The MD8A O3 concentrations at HW, BV, and H3 for the flagged event periods are given in **Table 10**. The impact of wildfire smoke and constituent emissions during these periods has been deemed consequential, and without the influx of such emissions the observed MD8A O3 concentrations may not have exceeded the NAAQS. Therefore, we exclude these MD8A O3 values from the calculation of the 4th max MD8A O3 for 2016 and 2017 at the HW, BV and H3 sites. By removing these values from the 4th max determination we compute a new 4th high MD8A O3 for each monitoring site for the years 2016 and 2017 (**Table 11**). These new 4th max MD8A O3 values are then used to derive 3-year design values, using 2017 as the baseline inventory year, for the periods 2015-2017, 2016-2018, and 2017-2019 (**Table 12**). The average of the adjusted design value periods stated above provides a revised or adjusted weighted 5-year BDV centered on the baseline inventory year of 2017. In **Table 12**, the impact of the removal of flagged data is illustrated by the comparison of the BDV constructed with and without flagged data. In general, the exclusion of wildfire impacted data reduces the BDV used for model attainment by 1-2 ppb at the three selected monitoring sites (**Table 12**).

Acknowledgment

Utah Division of Air Quality gratefully acknowledges the NOAA Air Resources Laboratory (ARL) for the provision of the HYSPLIT transport and dispersion model and/or READY website used in this publication. (https://www.ready.noaa.gov)

References

Alonso-Blanco, E., Castro, A., Calvo, A. I., Pont, V., Mallet, M., & Fraile, R. (2018). Wildfire smoke plumes transport under a subsidence inversion: Climate and health implications in a distant urban area. Science of the Total Environment, 619, 988-1002.

Colarco, P. R., Schoeberl, M. R., Doddridge, B. G., Marufu, L. T., Torres, O., & Welton, E. J. (2004). Transport of smoke from Canadian forest fires to the surface near Washington, DC: Injection height, entrainment, and optical properties. *Journal of Geophysical Research: Atmospheres*, *109*(D6).

Doran, J. C., Fast, J. D., & Horel, J. (2002). The VTMX 2000 campaign. *Bulletin of the American Meteorological Society*, *83*(4), 537-554.

Duck, T. J., Firanski, B. J., Millet, D. B., Goldstein, A. H., Allan, J., Holzinger, R., ... & van Donkelaar, A. (2007). Transport of forest fire emissions from Alaska and the Yukon Territory to Nova Scotia during summer 2004. *Journal of Geophysical Research: Atmospheres*, *112*(D10).

EPA. (January, 2017). *Revision to the Guideline on Air Quality Models: enhancements to the AERMOD dispersion modeling system and incorporation of approaches to address ozone and fine particulate matter. 40 CFR part 51, Appendix W*. EPA–HQ–OAR–2015–0310.

Office of Air Quality Planning and Standards, EPA. (April, 2019). *Additional Methods, Determinations, and Analyses to Modify Air Quality Data Beyond Exceptional Events.* Environmental Protection Agency. Air Quality Assessment Division. https://www.epa.gov/sites/default/files/201904/documents/clarification_memo_on_data_modification_methods.pdf

Horel, J., Crosman, E., Jacques, A., Blaylock, B., Arens, S., Long, A., ... & Martin, R. (2016). Summer ozone concentrations in the vicinity of the Great Salt Lake. *Atmospheric Science Letters*, *17*(9), 480-486.

Hu, X., Yu, C., Tian, D., Ruminski, M., Robertson, K., Waller, L. A., & Liu, Y. (2016). Comparison of the hazard mapping system (HMS) fire product to ground-based fire records in Georgia, USA. *Journal of Geophysical Research: Atmospheres*, *121*(6), 2901-2910.

Hung, W. T., Lu, C. H. S., Shrestha, B., Lin, H. C., Lin, C. A., Grogan, D., ... & Joseph, E. (2020). The impacts of transported wildfire smoke aerosols on surface air quality in New York State: A case study in summer 2018. *Atmospheric Environment*, *227*, 117415.

Hung, W. T., Lu, C. H. S., Alessandrini, S., Kumar, R., & Lin, C. A. (2021). The impacts of transported wildfire smoke aerosols on surface air quality in New York State: A multi-year study using machine learning. *Atmospheric Environment*, *259*, 118513.

Jaffe, D., Chand, D., Hafner, W., Westerling, A., & Spracklen, D. (2008). Influence of fires on O3 concentrations in the western US. *Environmental science & technology*, *42*(16), 5885-5891.

Lindaas, J., Farmer, D. K., Pollack, I. B., Abeleira, A., Flocke, F., Roscioli, R., ... & Fischer, E. V. (2017). Changes in ozone and precursors during two aged wildfire smoke events in the Colorado Front Range in summer 2015. *Atmospheric Chemistry and Physics*, *17*(17), 10691-10707.

Long, K. A. (2017). Analysis of Summer Ozone Concentration in the Salt Lake Valley (Doctoral dissertation, The University of Utah).

Lu, X., Zhang, L., Yue, X., Zhang, J., Jaffe, D. A., Stohl, A., ... & Shao, J. (2016). Wildfire influences on the variability and trend of summer surface ozone in the mountainous western United States. *Atmospheric Chemistry and Physics*, *16*(22), 14687-14702.

McClure, C. D., & Jaffe, D. A. (2018). Investigation of high ozone events due to wildfire smoke in an urban area. *Atmospheric Environment*, *194*, 146-157.

Miller, D. J., Sun, K., Zondlo, M. A., Kanter, D., Dubovik, O., Welton, E. J., ... & Ginoux, P. (2011). Assessing boreal forest fire smoke aerosol impacts on US air quality: A case study using multiple data sets. *Journal of Geophysical Research: Atmospheres*, *116*(D22).

Ninneman, M., & Jaffe, D. A. (2021). The impact of wildfire smoke on ozone production in an urban area: Insights from field observations and photochemical box modeling. *Atmospheric Environment*, *267*, 118764.

Pan, K., & Faloona, I. (2022). The Impacts of Wildfires on Ozone Production and Boundary Layer Dynamics in California's Central Valley. *Atmospheric Chemistry and Physics Discussions*, 1-30.

Pahlow, M., Kleissl, J., & Parlange, M. B. (2005). Atmospheric boundary-layer structure observed during a haze event due to forest-fire smoke. *Boundary-layer meteorology*, *114*, 53-70.

Reddy, P. J., & Pfister, G. G. (2016). Meteorological factors contributing to the interannual variability of midsummer surface ozone in Colorado, Utah, and other western US states. *Journal of Geophysical Research: Atmospheres*, *121*(5), 2434-2456.

Stein, A.F., Draxler, R.R, Rolph, G.D., Stunder, B.J.B., Cohen, M.D., and Ngan, F. (2015). NOAA's HYSPLIT atmospheric transport and dispersion modeling system. *Bull. Amer. Meteor. Soc., **96**, 2059-2077.*

Wu, Y., Arapi, A., Huang, J., Gross, B., & Moshary, F. (2018). Intra-continental wildfire smoke transport and impact on local air quality observed by ground-based and satellite remote sensing in New York City. *Atmospheric Environment*, *187*, 266-281.y

Wu, Y., Nehrir, A. R., Ren, X., Dickerson, R. R., Huang, J., Stratton, P. R., ... & Moshary, F. (2021). Synergistic aircraft and ground observations of transported wildfire smoke and its impact on air quality in New York City during the summer 2018 LISTOS campaign. *Science of The Total Environment*, *773*, 145030.

Xu, L., Crounse, J. D., Vasquez, K. T., Allen, H., Wennberg, P. O., Bourgeois, I., ... & Yokelson, R. J. (2021). Ozone chemistry in western US wildfire plumes. *Science Advances*, *7*(50), eabl3648.

Zumpfe, D. E., & Horel, J. D. (2007). Lake-breeze fronts in the Salt Lake Valley. *Journal of applied meteorology and climatology*, *46*(2), 196-211.